FUNCTIONAL BEARING MODEL (FBM) ANALYSIS UNDER THE DESIGN SPECTRA OF NEAR FAULT GROUND MOTIONS

TESIS

PROGRAM MAGISTER TEKNIK SIPIL
MINAT REKAYASA STRUKTUR

Ditujukan untuk memenuhi persyaratan memperoleh gelar Magister Teknik

ALFINNA MAHYA UMMATI

NIM. 156060112141001

UNIVERSITAS BRAWIJAYA

FAKULTAS TEKNIK

MALANG

2018

TESIS

FUNCTIONAL BEARING MODEL (FBM) ANALYSIS UNDER THE DESIGN SPECTRA OF NEAR FAULT GROUND MOTIONS

ALFINNA MAHYA UMMATI

NIM. 156060112141001

Telah dipertahankan di depan penguji

Pada tanggal 4 Juli 2018

Dinyatakan telah memenuhi syarat

Untuk memperoleh gelar Magister Teknik

Komisi Pembimbing,

Dosen Pembimbing I	Dosen Pembimbing II
Prof. Wang, Chung-Yue	Dr. Wisnumurti, ST.,MT.
	NIP. 19641207 199002 1 001

Malang,Juli 2018

Universitas Brawijaya

Fakultas Teknik, Jurusan Teknik Sipil

Ketua Program Magister Teknik Sipil

Ari Wibowo, ST., MT., Ph. D.

NIP. 19740619 200012 1 002

FUNCTIONAL BEARING MODEL (FBM) ANALYSIS UNDER THE DESIGN SPECTRA OF NEAR FAULT GROUND MOTIONS

Nama Mahasiswa	: Alfinna Mahya Ummati
NIM	: 156060112141001
Program Studi	: Teknik Sipil
Minat	: Rekayasa Struktur

KOMISI PEMBIMBING:

Ketua	: Prof. Wang, Chung-Yue
Anggota	: Dr. Wisnumurti

TIM DOSEN PENGUJI:

Dosen Penguji 1	: Dr. Wang, Ren-Zuo
Dosen Penguji 2	: Dr. Chuang, Ching-Chiang
Tanggal Ujian	: 04 Juli 2018
SK Penguji	:-

PERNYATAAN ORISINALITAS TESIS

Saya menyatakan dengan sebenar-benarnya bahwa sepanjang pengetahuan saya dan berdasarkan hasil penelusuran berbagai karya ilmiah, gagasan dan masalah ilmiah yang diteliti dan diulas di dalam Naskah Tesis ini adalah asli dari pemikiran saya, tidak terdapat karya ilmiah yang pernah diajukan oleh orang lain untuk memperoleh gelar akademik di suatu Perguruan Tinggi, dan tidak terdapat karya atau pendapat yang pernah ditulis atau diterbitkan oleh orang lain, kecuali yang secara tertulis dikutip dalam naskah ini dan disebutkan dalam sumber kutipan dan daftar pustaka.

Apabila ternyata di dalam naskah Tesis ini dapat dibuktikan terdapat unsur-unsur jiplakan, saya bersedia Tesis dibatalkan, serta diproses sesuai dengan peraturan perundang-undangan yang berlaku (UU No. 20 Tahun 2003, pasal 25 ayat 2 dan pasal 70).

Malang, 04 Juli 2018

(materai)

Mahasiswa,

Alfinna Mahya Ummati

NIM. 156060112141001

AUTOBIOGRAPHY

I am Alfinna Mahya Ummati, was born on October 14th, 2018, in Nganjuk city, East Java, Indonesia. Had been finished the undergraduate at Brawijaya University on 2015, then continued the master degree program with joined double degree program on master study that was held by Brawijaya University (Indonesia) and National Central University (Taiwan) during 2015-2018. Was been part of researchers on Center of Bridge and Earthquake Engineering during my study at National Central University on 2016-2018, I concerned on bridge isolation system under the earthquakes, since Taiwan and Indonesia are the countries with earthquakes prone areas, so that in the future, I expect that my research provide contributions as the matter that can be considered on failure prevention on bridge under the earthquakes. My supervisors and I developed a research from National Center of Research on Earthquake and Enginering (NCREE) Taiwan. A Fuctional Bearing Model (FBM) analysis about defining links on SAP2000 modelling based on each primary element function, in order to find out the contributions of each element on the bridge bearing isolation system that was described on this manuscript.

Taiwan, July 4th, 2018.

Alfinna Mahya Ummati

ACKNOWLEDGEMENT

My gratefulness sent to Allah SWT, my greatest spiritual wellsprings that give me blessing in every steps, and grant me knowledge from the great people that He sent. My pray belongs to Him. His kindness taught me for being kind, and always positive in every way of my thinking. And this research is impossible to finish without His favor.

Second, my gratitude aimed for my parent who never stop to support me in everything, who cherish me either in good or worst, the one who believe me I can did this without any hesitation. Who never let go of their hand to conduct me for being successful. Also for my little brother. My pray never stop for them, wishing they always be in a happiness and good healthy.

Third, I express my gratitude for the great people who teach me to be better. Professor Wang, Chung Yue as my advisor in National Central University (NCU) Taiwan. He taught me both being a good student and being a good people. Under his guidance, I learn how to do a good research and face every people that I met in Taiwan. His advice motivates me, and his high level training trained me to be a great people in the future. Overall, I regard him as my second parent in Taiwan since he always listens and give me solutions in every tough situation during my study. Then, Dr. Wang, Ren-Zuo as my co-advisor from National Center of Research on Earthquake and Engineering (NCREE) Taiwan, who trained me to do a good research and teach me how to do a good presentation. His curiosity and hardworking taught me to become unstoppable. Dr. Wisnumurti, he is my advisor from Brawijaya University and he guide me since I was on undergraduate. He introduced me with structural mechanics, and guide me patiently during my study. Dr. Wisnumurti inspire me to become a good teacher. Dr. Liu, Kuang-Yen from National Cheng-Kung University, he provides me a lot of data for my research and explained the knowledge without take any granted. His warmth heart taught me how to consider that everyone is important. Dr. Chuang, Ching-Chiang from Chung Yuan Cristian University, as my committee exam who give advices for my research.

My colleagues from Indonesian Student Association and Lab-mates from National Central University that I could not mention it one by one. Every single people is very memorable to me, my life is blessed with surrounded by the great peoples during my master study in National Central University, Taiwan.

SUMMARY

Functional Bearing Model (FBM) is an idea to represent 1 link analysis that used in common with divide it into 3 links based on each function. In this research, the rubber bearing divided into 3 elements as representation of rubber bearing system, they are: Friction element in the top of sliding interface between bearing and deck, Rubber in the middle link as a restoring element, and Frictional element in the bottom of sliding interface between bearing and column.

A shaking table size bridge proposed under the normalized peak ground acceleration under the design spectra of the near fault ground motions of Chi-Chi earthquakes TCU068, TCU102, and TCU052. In this research of FBM analysis, proof that the contribution of the rubber element and friction elements can be calculated independently.

The purposes of this research are: First, to study about the effect of variation of the friction coefficient that applied on the top surface and bottom surface of the rubber bearing system. Second, to study about determining several configuration of the friction coefficient to design a proper rubber bearing system. Third, to study about determining several configuration of the friction coefficient to design a gap between two decks in order to avoid the decks crashing when the earthquakes happen. Fourth, to study about determining several configuration of the friction coefficient to design enlargement of the column's cap beam in order to avoid the decks falling when the earthquakes happen.

Keyword: Functional Bearing Model (FBM) Analysis, Near Fault, Response Spectrum, Shaking Table Test Model, Bridge Analysis, Dynamic Analysis, Friction Coefficient, Rubber Bearing System.

RINGKASAN

Functional Bearing Model (FBM) adalah konsep penginterpretasian rubber bearing sistem yang biasanya diasumsikan sebagai satu link yang terdiri dari beberapa parameter penyusun device tersebut menjadi 3 link berdasarkan fungsi masing-masing parameter. Tiga link tersebut merupakan representasi dari Friction Element pada interface bagian atas, Rubber Element, dan Friction Element pada interface bagian bawah.

Penelitian mengenai prototip jembatan yang telah diskala menyesuaikan dengan ukuran shaking table test dibebani dengan seismic loading test dari Chi-Chi Earthquakes yang telah direkam pada stasiun gempa TCU068, TCU102, dan TCU052. Dengan konsep FBM dapat terbukti bahwa setiap komponen penyusun dari rubber bearing system dapat diketahui secara terpisah.

Tujuan dari penelitian ini yaitu: untuk mengetahui pengaruh dari variasi koefisien friksi yang diaplikasikan pada interface atas dan bawah rubber bearing system, untuk mengetahui parmeter-parameter apa saja untuk mendesain rubber bearing yang tepat untuk tipe jembatan dengan gempa tertentu, untuk mengetahui berapa jarak gap yang perlu disediakan untuk menghindari tubrukan antar deck pada saat gempa terjadi, dan terakhir untuk mengetahui ukuran dudukan jembatan yang perlu disediakan untuk menghindari slip pada jembatan pada saat gempa terjadi.

Keyword: Functional Bearing Model (FBM) Analysis, Near Fault, Response Spectrum, Shaking Table Model, Jembatan, Dinamika, Koefisien Friksi, Rubber Bearing System.

KATA PENGANTAR

Puji syukur penulis tujukan kepada Allah SWT, karena atas karunia dan izin-Nya, thesis ini dapat terselesaikan dengan baik. Serta ucapan terimakasih juga penulis sampaikan untuk kedua orang tua yang telah memberikan dukungan dalam segala hal.

Penulisan thesis ini diajukan sebagai salah satu persyaratan untuk menyelesaikan program studi magister teknik sipil Universitas Brawijaya. Penulis berharap riset ini akan bermanfaat kedepannya untuk mengembangkan teknologi pembangunan baik di Indonesia maupun mancanegara, terutama dalam bidang rekayasa struktur. Ucapan terimakasih penulis sampaikan kepada beliau yang berjasa dalam penyelesaian thesis ini:

1. Dr. Eng. Alwafi Pujiraharjo, ST., MT dan Dr. Eng. Eva Arifi, ST., MT., selaku Ketua Jurusan dan Sekretaris Jurusan Teknik Sipil Universitas Brawijaya.
2. Prof. Dien, Yong-Ming, selaku Ketua Jurusan Teknik Sipil National Central university (NCU) Taiwan.
3. Ari Wibowo, ST., MT., Ph. D., selaku Ketua Program Studi S2 Teknik Sipil Universitas Brawijaya.
4. Prof. Wang, Chung-Yue, Dr. Wang, Ren-Zuo, dan Dr. Wisnumurti, ST.,MT. sebagai dosen pembimbing dari National Central University dan Universitas Brawijaya.
5. Dr. Chuang, Ching-Chiang, sebagai dosen penguji yang telah memberikan masukan dan arahan selama penelitian.
6. Dr. Liu, Kuang-Yen, peneliti terdahulu tentang Functional Bearing Model (FBM) analysis yang telah membagikan banyak referensi dalam pengembangan metode ini.

Penulis menyadari bahwa penulisan manuskrip thesis ini pastinya jauh dari kesempurnaan. Dengan kerendahan hati, penulis memohon maaf apabila terjadi kesalahan baik dalam penulisan maupun penyampaian kata yang terdapat dalam manuskrip ini, masukan yang membangun pastinya akan membantu penulis dalam penulisan karya selanjutnya.

Taiwan, 4 Juli 2018

Alfinna Mahya Ummati

LIST OF CONTENTS

LIST OF TABLE

LIST OF FIGURE

CHAPTER I – INTRODUCTION

1.1 Background

Statistical shows that the human population in the world is continuously rising in recent years. The spread of human being in the world with increasing of their population, in large scale, it will impact on their culture and evolutionary on their capability. Nowadays, the time has passed by, the ancient place turns into a modern city. People have a great capability for altering their living such as construction, transportation, disaster prevention, and many more that related to their life that we recognize it as technology. Technology allowed people to adapt to the existing condition, as we know that there have seven continents in the world that each has different on thermal comfort, earth surface, and culture.Asia is the largest continents in the world which have about 60% of the world's population means that Asia is the most populous continents. Not only the number of people but also evolutionary of technology have been increasing rapidly, especially on construction field.

In January 1995, a 6.9 SR of Kobe earthquake occurred in Kobe City, Japan. That was one of the famous earthquakes in the world.The damage includes many death and wealth lost, about 6.5 thousand of people killed and total damage reached 200 USD. In September 1999, a 7.3 SR of Chi-Chi earthquake happened in Nantou City, Taiwan. About 2,5 thousand people killed and 11,5 thousand people injured. That was a second harm-full earthquake in Taiwan after Shinchiku-Taichu Earthquake in 1935. 5 years later, at the end of 2004 a 9.1 SR of Indian Ocean Earthquake occurred in several countries along Indian Ocean coastal side, USGS record mentionedthat was the third largest earthquake in the world after 9.5 SR of Chile Earthquake in 1960 and 9.2 SR of Alaska Earthquake in 1964.Indonesia,especially in the northern region of Sumatra is the hardest hit country then followed by Sri Lanka, India, and Thailand. The total damage was about 280 thousand of people die and 20 billion USD lost. Go ahead in Taiwan, in a midnight of February 2018, a 6.4 SR earthquake shook the northeast coastof Hualien City, at least 17 people killed and 285 people injured. Earthquake is one of the most harmful disasters that if it happens in large magnitude will increase the number of deaths of the human beings. The earthquake may be caused by volcanic and tectonics, the most deaden one is due to the tectonic earthquake.

Figure 1. 1A large building damage on its first floor due to an earthquake in Hualien City (New York Times).

Asia is known as one of the continents that have many faults, means that Asia has a variety of earth moving. As the result, almost every day the earthquake center department report there have been earthquake motions recorded in several points. Seriously disaster happens caused by the strong motion earthquake and prevents earthquake disaster on many infrastructures should be considered to minimize the damages. Based on several cases that mentioned before, it is known that Taiwan, Japan, and Indonesia include in pacific ring of fire.

Bridges is one of important construction that help many people to move from a place to another place. Related to the earthquake prevention, constructor needs to fully pay their attention to the seismic prevention instead of the bridge demand. Nowadays, technology has been developed well, there are many kinds of devices to decrease the bridge failure due to the earthquakes. Bridge isolation system is the popular prevention to protect the bridge against the seismic force. Isolation system is a good choice that chosen by constructor to help their building mitigate the earthquake effect, isolation system itself is largely developed in Asia, considering that Asia has many active faults that need to be considered.

A right bridge construction is the one that can withstand its dynamic condition even caused by the external load or seismic ground motion. *Iemura et.al* investigate that the fundamental period of the bridge vibration in the range between 0.2-1.2 sec., which is almost similar to predominant periods of an induced earthquake. Isolation system may help to elongate the fundamental period over the predominant periods. Adjusting the isolation system in a bridge, it is expected that it will reduce the energy that transmitted to the deck.

Recent, many research focused on isolation system for a bridge that crosses the fault zone. Because nowadays the existing of the faults are continuously getting larger.To overcome this situation, avoid a construction in the earthquake zone is possible, but this solution is not always a good choice for high seismicity countries such as Japan, Taiwan, and Indonesia.(P.Tsopelas&M.C.Constantinou, 1995) Contemporary techniques for seismic hazard mitigation in bridges include seismic isolation, energy dissipation and the distribution of seismic forces to elements of the substructure in accordance with their strength. Seismic Isolation System is a better way to reduce the energy of earthquake force into or approach bridge's elastic capacity, in the other way, with adjusting a Seismic Isolation System will help to reduce inelastic deformation and prevent the failure to the substructure.

Based on the research that was done byTsopelas et.al., Seismic Isolation system which have characterized by a strong restoring force have been employed in New Zealand and United States, and recently have been developed more in the most country in Asia which categorized that have high seismicity, such as Japan, Taiwan, and most region in Indonesia. In 1995, the isolated bridge was largely applied on bridge construction in United States.At that time, mostly used isolation system that consist of lead rubber bearings and the other are used sliding isolation system, considered their restoring force performance is good to compare with other. A few years later, Italian engineer developed an isolation system that consist of lubricated sliding bearings and yielding mild steel dampers, their characteristics are have large dispersion of peak displacement and development of permanent displacement.

Japan is one of the countries with outstanding on its technology of construction, after an isolation system was found and developed more, a technology named *Menshin*have been developed to protect the bridge. In *Menshin,* because of Japan is one of the country with high seismicity, they want to develop a seismic isolation system to overcome the strong earthquake with the magnitude 8 or larger.*Menshin* is a kind of bearing isolator to increase the energy dissipation capability and distribute the energy that caused by the lateral force of the ground motion to the substructure. In 2005, a combination of restoring spring and friction spring named Resilient Sliding Isolation (RSI) was introduced by Iemura et.al., because of this system combine two kinds of forces, they calculated the force that transmitted to the structure is equal with restoring force of restoring spring plus friction force at the sliding surface.

Many research related with the bearing isolation system was done before, in 1993 Constantinou et.al. conducted the experimental and analytical study of a friction pendulum system (FPS), they observe that an isolated bridge performed better than the non-isolated bridge in weak seismic excitation. On 1997 Kikuchi and Aiken proposed elastomeric seismic isolation bearings that capable of well-predicting the mechanical properties of each type of elastomeric bearing into the large strain range, the satisfying result was showed between the experimental and analysis that showed this proposed model is a good way to predict not only the peak response value but also the force-displacement relationship of the isolator and response spectra for isolated structure. In 2005, Iemura et.al. carried out a bridge shaking table test model under resilient sliding isolation (RSI) system, they put the variation of normal force on the sliding bearing due to rocking effect and vertical acceleration and found that the effect of rocking motion on variation of the normal force gets reduced with reduction in stiffness of buffers. On 2012 Lu et.al. study about the variable-frequency rocking bearing system on a bridge due to the near fault earthquake, their simulation was satisfied with the experimental result, both results showed this isolation system able to effectively suppress the excessive isolator displacement.

Several research that conducted before show that the isolation system is very important for a building to resist the loading yet the seismic excitation. This thesis research is about the development of Functional Bearing Model (FBM) analysis, in purpose to determine the behavior each response of each component of the rubber bearing. It is known that the rubber bearing generally consist of friction and restoring force, and mostly in common research a rubber bearing assumed friction and restoring force parameter instead of one multilinear plastic spring element. In 2013, Liu et.al. study about Functional Bearing Method (FBM) system of two springs as a representation of one multilinear plastic spring as mentioned before.

This chapter introduces the research overview, objectives, scope and the outline, and also explain more about the background of this research in order to show how important the Functional Bearing Method (FBM) analysis should be considered in the near future.

1.2 Research Objectives

Bridge construction that considers the earthquake resistance were carried out and considered in every bridge construction. Based on the current seismic design code of the bridge and highway bridge, the strength of the bridge support was increased to control the plastic hinge of the bridge column to dissipate the earthquake energy. Due to the evolution of the seismic design code that adds several considerations in its reinforcement due to the lack of the old version of the bridge standardized design. Shear force and moment capacity of the bridge and foundation shall be in-line with the strength of the earthquake excitation, at that time, increasing reinforcement capacity chosen as the best solution to prevent this issue. But, increasing the reinforcement capacity will not be forever give advantages, consider this method seems to need more in costing. Thus, another idea needs to find out in order to optimize the construction considering the strong earthquake without ignoring the construction cost value.

Considering rubber bearing to replace conventional bearing become another idea that come out in order to reduce the shear force and bending moment of the structure, rubber bearing give flexibility of the structure to move when the earthquake happens, this flexibility shall be reduce the shear force caused by an earthquake that transmitted into the superstructure, then automatically decreasing the energy, this concept provide similar purpose yet consider another method, concern on applying flexible bearing of course less in cost than increasing structure reinforcement. Controlling the plastic hinge to dissipate the earthquake energy and considering the relative displacement of the structural system toward the expansion joint are one of issue that need to pay more attention, the flexible bearing will allow the structure to move when the earthquake happens, and bridge falling will be the next issue that needs to prevent. Bridge falling shall not happen as long as there is sufficient length of fall-proof or provide a length movement limit, this rubber bearing concept designed to give a flexibility yet have limitation to prevent the bridge falling possibility. Rubber bearing which naturally is a flexible element and combine with the frictional element shall be a good innovation in case of reducing shear force with considering flexibility and frictional slippage phenomenon, frictional slip considered to reduce the inertial force that transmitted to the substructure, if this condition allowed to happen, the demand of seismic force design of the column and foundation will be reduced. This will be a good idea to prevent the bridge failure in an earthquake prone area, and efficiently cost due to government’s financial condition.

Functional Bearing Method (FBM) is a bearing assumption method to represent the Seismic Isolation System in structure analysis especially on a bridge.This method is done by CSI Software of SAP2000. Shorter way, this analysis was done in order to:

1. Investigate the bridge response due to the effect of variation of friction force of the rubber bearing system, in order to find out the effective value of the coefficient of friction that should be used in bridge analysis.
2. Analyze the rubber maximum deformation, to design a proper rubber bearing system using Functional Bearing Model (FBM) analysis.
3. Analyze the maximum sliding in the upper part of the rubber bearing and consider deck displacement, to design the bridge gap between one and another deck, in order to provide an enough space to avoid inter-decks crashing during the earthquake.
4. Analyze the maximum sliding in the lower part of the rubber bearing interface considering column displacement, in order to enlarge the pile cap size to provide an enough sliding space and avoid the bridge falling when the earthquake happens.
5. Analyze the bearing response in several Peak Ground Acceleration (PGA) of the Near Fault Earthquake, to observe the PGA effect in near fault subjected to the bridge model.

1.3 Research Scope and Limitation

With an eye to limitthe scope of the research to avoid widening of discussion, this research limited within:

1. The shaking table test model is the previous experimental model that own byLiu et.al. for the Functional Bearing Method (FBM) experimental test in 2013, takes place in National Center of Research on Earthquake Engineering (NCREE), Taipei, Taiwan.
2. Research analysis includes the analysis of 3 links analysis. The stiffness of its link adapts from the previous model that consider the rubber bearing's material properties and consider the experimental based of coefficient of frictions value.
3. Bridge response consists of Bearing Response, Deck Response, and Column Response.
4. The analysis was done byCSI program of SAP2000 v20.
5. Chi-Chi Earthquake 1999 on station TCU052, TCU068, and TCU102 are ground motion input as the near fault ground motiondata.
6. System analysis working on 2 Dimension, all the ground motions were input on global X direction of SAP2000 analysis.

1.4 Research Outline

In a short way, the research analysis flows on these steps:

Bridge Analysis Under the Normalized Near Fault Ground Motion of Design Spectra Analysis with General Direct Integration Method.

1. Near Fault TCU052 – 3 Links Analysis
2. Near Fault TCU068 – 3 Links Analysis
3. Near Fault TCU102 – 3 Links Analysis
4. Study about the effect of variation of the friction coefficient on the top surface friction and bottom surface friction.
5. Study about defining parameter to design a proper rubber bearing to avoid the bearing failure.
6. Study about defining parameter to design an enough gap of two decks to prevent the decks crashing.
7. Study about defining parameter to design an enough size of the column's cap beam in order to avoid the bridge falling possibility.

CHAPTER II – LITERATURE REVIEW

2.1 Introduction

In this chapter present a short literature review of bridge construction, include the overview of bridge nomenclature especially for bridge isolation system. This section also provides a detailed look at the various elements that compose a bridge superstructure. Substructure of the bridge that deals with three major components on it, abutments, piers, and bearings, also will explain more. The research about Functional Bearing Method (FBM) is the analysis of the variation of the spring assumption and its running on dynamic analysis, in order to discuss about the theoretical background, in this chapter also explain short literature review about the structural dynamic of the bridge model.

2.2 Highway Bridge Structure

Highway bridge structure is one of the most integral components in any transportation network. Highway bridge commonly consist of a slab-on-stringer configuration crossing relatively short span lengths. The girders have a role as a resting place of a deck and usually the typical of bridge girder is use to decide the bridge category. The following type of bridge girders commonly are: Steel rolled section or plate girders, Prestressed concrete beams, and Timber beams. Highway design mostly concerned for the overpass and underpass alignment and geometry, and for the highway bridge itself is an overpass construction with the structural design consist of superstructure and substructure elements.

The superstructure comprises all the components of a bridge above the support. Generally, superstructure in a bridge consist of: wearing surface, deck, primary members, and secondary members. And for substructure components consist of: abutments, piers, bearings, pedestals, back-wall, wing-wall, footing, and piles. This research will be focused on superstructure and the bearing.

Type of superstructure that define the bridge can be based on a variety of factors ranging from maintenance consideration to personal preference. Specially, some of the commonly used criteria in selecting the type of superstructure to be used are: material function and availability, construction cost, speed of construction and constructability, design complexity, maintenance cost and life expectancy, environmental concerns, and aesthetics.

Superstructure's type also would change due to the bridge span lengths. Each type of superstructure has span limitations beyond which it will become uneconomical.

Superstructure generally varied by several parameters, one of them is support type. Nowadays, support systems have been developed as seismic isolations to overcome the large earthquake to reduce the energy that received by the structure. Seismic isolation system is one of good solution to prevent the large earthquake. It will be suitable to apply in many structures that build in high seismicity country like Japan and Taiwan. Mostly, support system that was developed become isolation system have different techniques of resisting from conventional seismic resistance (L-Y. Lu et al., 2012).

2.3 Earthquake Ground Motion

An earthquake is an impact of ground shaking caused by an energy that suddenly released in lithosphere layer, (Dowrick, 1987). Earthquake may cause by either tectonic or volcanic activity, yet the earthquake due to volcanic process only happen in specific area near the prone area and the time can be predicted in real time prediction, the damage due to this earthquake can be prevent well. An earthquake due to tectonic activity will be risky, so that the damage prevention technology extensively developed to reduce the harmful effect, especially for human beings. The energy produced due to some interaction between the crust and the earth's inner layer. Releasing energy itself involve the fracture of the surface along the plane which passes through the hypocenter. Largely of the shallower earthquake, this surface plane known as a fault.

The strength of the earthquake known in two definitions, they are intensity and magnitude. Intensity is the strength of ground shaking at any given place, and magnitude is accumulation strength of the existing ground motion. Intensity is a severity measuring of the earthquake at the certain place, intensity measured by Mercalli (MM). Yet, magnitude use to measure the size of an earthquake, associated with the energy release which is area independent, magnitude measured by Seismogram (M).

The seismic wave divide into four main types, there are:

1. Body waves: seismic waves that travel pass through inside the earth, body waves divided into two class of waves based on the wave's properties:
   a. P-Waves, vibration particle move parallel with the direction of seismic waves. Also known as primary wave, longitudinal or pressure wave.

b. S-Waves, vibration particle that move perpendicularly through the seismic wave direction. S-waves also known as shear waves, secondary waves, or transverse wave.

2. Surface waves: different with body waves, surface waves are seismic waves pass through along the surface earth or the outer layer near the surface. Surface waves divided into two classes in general:

a. Love waves: vibration particle on horizontal axis which is perpendicular with the seismic waves direction.

b. Rayleigh waves: vibration particle on vertical axis which is parallel with the seismic waves direction.

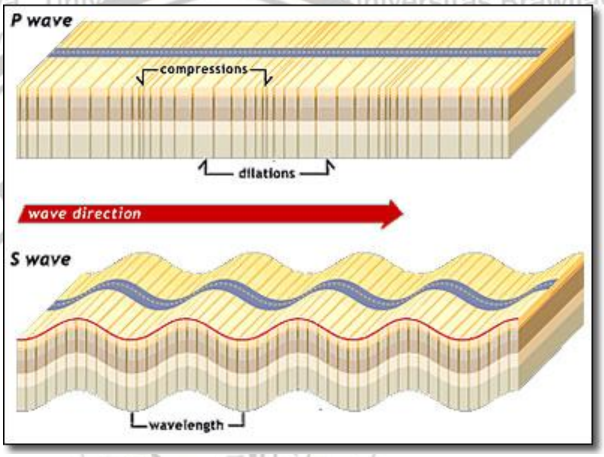

Figure 2. 1P-wave and S-wave of body wave (SMS Tsunami Warning)

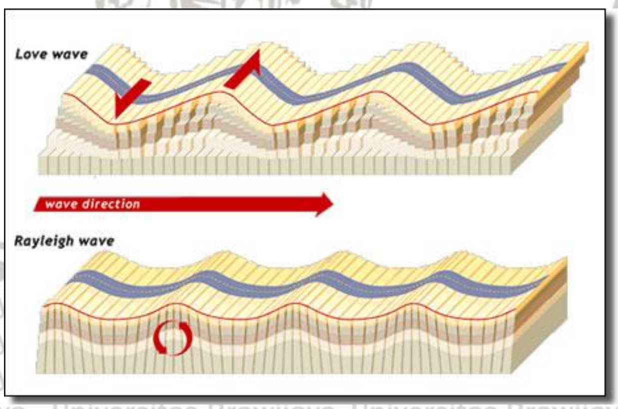

Figure 2. 2 Love wave and Rayleigh wave of surface wave (SMS Tsunami Warning)

2.3.1 Near Fault Earthquake

Earthquakes are essentially vibrations of the earth's crust caused by subterranean ground faults. They occur several times a day in various part of the world, although only a few in a year are sufficient magnitude to cause significant damage to buildings. Major earthquakes occur most frequently in particular areas of the earth's surface that called zones of high probability. However, it is theoretically possible to have a major earthquake anywhere on the earth at some time, (Ambrose, J. &Vergun, D., 1995).

A major earthquake is usually rather in short in duration, often lasting only a few seconds and seldom more than a minute or so. During the general earthquakes, there are usually one or more major peaks of magnitude of motion. These peaks represent the maximum effect of the quake. Although the intensity of the quake is measured in terms of the energy release at the location of the ground fault, the critical effect on a given structure is determined by the ground movements at the location of the structure. The extent of these movements is affected mostly by the distance of the structure from the epicenter, but they are also influenced by the geological conditions directly beneath the structure and by the nature of the entire earth mass between the epicenter and the structure, (Ambrose, J. &Vergun, D., 1995).

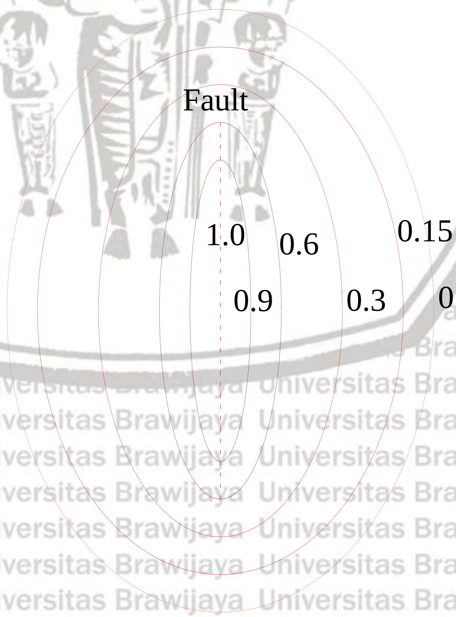

Figure 2. 3 Idealized contour lines of intensity of ground shaking, normalized to unit epicenterintensity, (Dowrick, D., 1987)

Figure 2.3 shows an idealized distribution of intensity of the ground shaking in relation to near vertical fault rupture, such as discussed for Californian earthquakes by Housner. The traditional attenuation relationships are made to fit the mean of the data about a point source, and hence represent all the intensity contours as circle with attenuation being the same in all directions. The attenuations of near field data earthquakes allow for the effect of the line source by relating peak ground motion to distance to the fault trace, implying a contour pattern consisting of a series of straight lines parallel and equal in length to the fault trace with the ends joined by semicircles, (Dowrick, D., 1987).

The symmetry about the fault trace (i.e. where the fault breaks the ground surface) of the contours in figure 2.3 clearly depends on the slope of the fault rupture surface, and an asymmetrical pattern, at least about the fault trace, could be expected from under-thrust faults of the main fault types, (Dowrick, D., 1987).

A common issue that comes up in the earthquakes studies is the estimation of grounf motions at particular locations for engineering analyses. The dense strong motion recordings from the Chi-Chi earthquake allow a direct measurement of how much ground motions can change as a function of the distance away from the nearest strong motion recording. The standard deviation pf the natural log of the ratio of the ground motions for sites on similar soil conditions are estimated as a function of separation distance, (ASCE, 2000).

2.3.2 Earthquake Response in Linear System

Equation 2.1 govern the motion of a linear single degree of freedom system subjected to ground acceleration:

$$\ddot{u} + 2\zeta\omega_n\dot{u} + {\omega_n}^2 u = -\ddot{u}_g(t) \qquad \textit{Eq. 2. 1}$$

It is clear that for a given $\ddot{u}_g(t)$ the deformation response u(t) of the system depends only on the natural frequency ω_n or natural period T_n of the system and its damping ratio ζ, writing formally, $u \equiv u(t, T_n, \zeta)$. Thus any two system having the same values of T_n and ζ will have the same deformation response u(t) even though one system may be more massive than the other or one may be stiffer than the other, (Chopra, A., 2013).

It is observed that the system with more damping respond less than lightly damped system, because the natural period of the three systems is the same, their responses display a similarity in the time required to complete a vibration cycle and in the times the maxima and minima occur. Once the deformation response history u(t) has been evaluated by the dynamic analysis of the structure, the internal forces can be determined by static analysis of the structure at each time instant, one of them is based on the equivalent static force f_s, (Chopra, A., 2013).

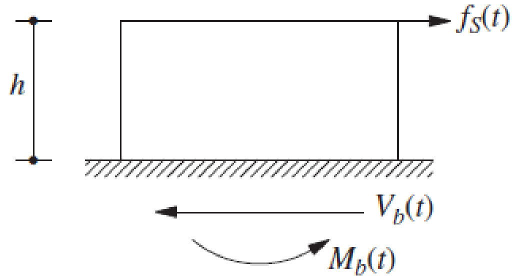

Figure 2. 4 Equivalent static force, (Chopra, A., 2013).

$$f_s(t) = m\omega_n{}^2 u(t) = mA(t) \quad \text{Eq. 2. 2}$$

$$A(t) = \omega_n{}^2 u(t) \quad \text{Eq. 2. 3}$$

$$V_b(t) = f_s(t) \quad \text{Eq. 2. 4}$$

$$M_b(t) = hf_s(t) \quad \text{Eq. 2. 5}$$

$$V_b(t) = mA(t) \quad \text{Eq. 2. 6}$$

$$M_b(t) = hV_b(t) \quad \text{Eq. 2. 7}$$

Where $f_s(t)$ is the equivalent static lateral force, m is mass, ω_n is the natural frequency, A(t) is pseudo acceleration response, $V_b(t)$ is the base shear, $M_b(t)$ is the base overturning moment, and h is the structures height.

(Chopra, A., 2013)

2.3.3 Earthquake Response in Non-Linear System

The governing equation for an inelastic system is written bellow:

$$m\ddot{u} + c\dot{u} + f_s(u) = -m\ddot{u}_g(t) \quad \text{Eq. 2. 8}$$

Divided by m:

$$\ddot{u} + 2\zeta\omega_n\dot{u} + \omega_n{}^2 u_y \tilde{f}_s(u) = -\ddot{u}_g(t) \quad \text{Eq. 2. 9}$$

Where:

$$\omega_n = \sqrt{\frac{k}{m}} \quad \text{Eq. 2. 10}$$

$$\zeta = \frac{c}{2m\omega_n}$$ *Eq. 2. 11*

$$\tilde{f}_s(u) = \frac{f_s(u)}{f_y}$$ *Eq. 2. 12*

$$a_y = \frac{f_y}{m}$$ *Eq. 2. 13*

For a given $\ddot{u}_g(t)$ considering the ductility factor μ as the parameter of inelastic system, define:

$$\mu(t) \equiv \frac{u(t)}{u_y}$$ *Eq. 2. 14*

Take the consideration that $u(t) = u_y.\mu(t), \dot{u}(t) = u_y.\dot{\mu}(t), \ddot{u}(t) = u_y.\ddot{\mu}(t)$, and $\bar{f}_y = {}^{u_y}/_{u_0}$ if the equation 2.9 divided by u_y, then the equation will be:

$$\ddot{\mu} + 2\zeta\omega_n\dot{\mu} + \omega_n{}^2\tilde{f}_s(\mu) = -\omega_n{}^2\frac{\ddot{u}_g(t)}{a_y}$$ *Eq. 2. 15*

Where $f_s(u)$ is the resisting force for an elastoplastic system, and $\tilde{f}_s(u)$ describes the force-deformation relation in partially dimensionless form, u_y is yield deformation, and a_y interpreted as the acceleration of the mass necessary to produce the yield force f_y.

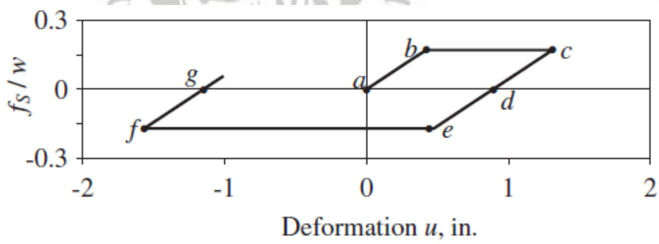

Figure 2. 5 Force-deformation relation (Chopra, A., 2013)

Figure 2.5 shows the force-deformation relation in elastoplastic system. Starting on point a when u and f_s are both zero. At this point the system is linearly elastic and remains so until point b. when the deformation reaches the yield deformation for the first time, identified as b, yielding begins. From b to c the system is yielding, the force is constant at f_y, and the system is on plastic branch b-c of the force-deformation relation. At c, a local maximum of deformation, the velocity is zero, and the deformation begin to reverse, the system begins to unload elastically along c-d and is not yielding during this time. Unloading continues until point d when the resisting force reach zero. Then the system begins to deform and load in the opposite direction and this continues until point f, f_s=-f_y during this time span and the system is moving along the plastic branch e-f. At f local minimum for deformation, the velocity is zero, and the deformation begin to reverse, the system begins to reload elastically along f-g and is not yielding during this time. Reloading brings the resisting force in the system to zero at g, and it continues along this elastic branch until the resisting force reach $+f_y$, (Chopra, A., 2013).

2.4 Isolation System

Bridge is one of the most important part of a highway which its failure will be seriously affected road link network system. Recently, seismic isolation related to the bridge support system have been largely developed in many countries with high seismicity. T. Taghikhany et al. in 2005, mention that isolation system helps a bridge to dissipate the energy also overcome the large earthquake with elongating the fundamental period beyond the base motion's predominant period. This concept also applied on long-period system of conventional isolation system. L-Y. Lu et al., describe that isolation layer was implemented on the seismic isolation in conventional method by applied a soft isolation layer under the protected structure. Undesirable large displacement that caused by long period is the side effect of applying a seismic isolation system, long period happened in line with increasing on noise and vibration. Time flies and many research about seismic isolation system have been largely developed to reduce the side effect of seismic isolation system. In Japan, an outstanding seismic isolation technology called *menshin* was introduced, this system stayed still have elongation in its fundamental period but this system may increase the energy dissipation capability and decrease the lateral force that transmitted to the substructure.

After many research were done about seismic isolation system in conventional seismic resistance, that was confirmed that conventional isolation system may reduce the excessive displacement due to near fault earthquake, but with elongation in fundamental period may cause oversized in isolator design, fundamental frequency may decrease and increase the possibility of pounding effect. Several literatures categorized the isolation system's variable into three categories: active, semi-active, and passive. Conventional system mostly as active and semi-active control, means that isolation system come from additional device that adjusted to overcome the adaptive force. Different with conventional system, isolation system that developed nowadays mostly categorized as passive control that mean the isolation device is part of the bridge itself, so that this system considered in case of serve a better performance for a whole structure, (L-Y. Lu et al., 2012).

Seismic isolation system is one of a good choice to reduce the bridge failure, such due to vehicle load, wind, earthquake, etc. Isolation system will control the bridge response and keep the response stay under the limit. This idea in order to prevent the bridge failure such as bridge falling when the earthquake happen with provide safety enough gap distance. Especially for earthquake, the ground motion contributes some kinetic energy toward the building structures, and the subject related to the ground motion are to control the location and damage level caused by this kinetic energy, engineers in nowadays must be consider to protect the building structure with reduce the kinetic energy of the earthquake toward the building in order to prevent the failure that may cause by. There are many ways related with it, the kinetic energy must be limited using energy decreasing device on the foundation level, then famously called base isolation system. The other way, energy dissipating device will dissipate the energy excess caused by kinetic energy of an earthquake, (Dowrick, 1987). This two concept became an idea to make a flexible bearing as an energy dissipating device to limit the kinetic energy of the ground motion. Flexible bearing in a structure especially in a bridge give many advantages for the structure itself, flexible bearing capable to protect the bridge from temperature changing that caused by either natural climate or machinery, while the damping energy contribute the energy dissipating capability to absorb the excess kinetic energy caused by vehicle, wind, or earthquake.

Isolation system also give a contribution in elongating the fundamental period beyond the predominant period, (Iemura, et. al., 2005). Fundamental period of a structure cannot be closed with dominant period of the earthquake, otherwise the resonance shall occur in this condition. With adjusting seismic isolation system, the structure will be more flexible to move in line with the earthquake motion, and bridge failure caused by resonance shall be avoided.

2.4.1 Rubber Bearing

Rubber bearings is one type of flexible bearing, it is a conventional bearing that had been used in 1951 in London, specifically in the Royal Festival Hall, need to carefully notice that at that time this building had been a place for the concert hall that sometimes caused sensitive vibration. Rubber bearings seems give the good contribution to prevent the building failure, until in 1985 a hundred building built under rubber bearing technology. In 1970, rubber bearings verified the requirements of non-linear analysis capability and rubber bearing finally acquired a patent as advantageous flexible bearing technology, (Dowrick, 1987).Rubber bearing is the conventional bearing that extensively used in around the world.

Practically, rubber bearing consist of layers of rubber and steel that placed intermittently each other, with top and bottom side have a steel plate containing PTFE layer as friction element that provide a friction behavior in a rubber bearing.

2.4.2 Functional Bearing Model (FBM)

The main concept of isolation system is to limit the continuity between two elements in contact, with the purpose is to limit the motion that happen in both interface in the direction of its discontinuity so that it shall not be all transmitted toward the structure. Discontinuity means the interface layer between two elements which has shear force low resistance compared with overall structure, the shear force may cause by horizontal seismic motion. This discontinuity part is the right point to place the isolation system. Low capability to resist the shear force in discontinuity part may cause the large amount of the shear force, with putting an isolation system at this point, isolation system itself will absorb the excess energy caused by the large

Figure 2. 6 Natural rubber bearing (Taghikhani, et.al., 2005)

Figure 2. 7 Rubber bearing mechanism

amount of the shear force, then the shear force that transmitted to the superstructure shall be reduced.

In 2005, Taghikhany developed a High Pressure Shoe (HiPS) of a rubber bearing which was contain PTFE (Poly Tetra Fluoro Ethylene) as a friction sliding surfaces that represented infinitely thin sliding surface through the rubber bearing in a few centimeters of thick. Friction layer that combine with the rubber bearing provide as controlling system of bearing deformation which occur in discontinuity point. PTFE layer may become the friction substance that mostly used to provide a friction, collaborated with the rubber bearing that provide flexibility in a bearing system.

In 2013 Liu et.al. developed the functional bearing system that assume the springs analysis and divide as each function. This reasonable concept is the main idea of this research. Many study about rubber bearing as the isolation system assumed as a single spring that contain rubber stiffness and friction as one spring element that placed in discontinuity part, in another way, Liu develop his simulation of rubber bearing in shaking table test model as two springs, one spring in the top side represent the friction element and another spring represent the rubber itself, he assumed that sliding only happened in the interface between rubber and deck.

Functional support system concept has been carried out and continuously developed in Republic of China. The definition of the functional bearing method associated with the rubber bearing as a bridge support system under the strong motion earthquake ground motion will produce the sliding friction mechanism in order to dissipate the seismic energy and consider the rubber maximum deformation as an initial value of sliding displacement, and put the maximum value of friction element as a maximum sliding displacement. This idea proposed in order to minimize the damage of large amount of seismic energy that transmitted from sub structure toward superstructure, either in a bridge or building, also to prevent the bridge falling due to an earthquake. Functional bearing system provide the contribution data of rubber and friction separately, then each behavior and the dominant contributor of the failure shall be find out using this concept.

2.5 Structural Optimization

2.5.1 Earthquake Response and Design Spectrum Analysis

A plot of the peak value of a response quantity as a function of the natural vibration period T_n of the system, or a related parameter such as circular frequency ω_n or cyclic frequency f_n, is called the response spectrum for that quantity. Each such plot id for SDF system having a fixed damping ratio ζ, and several such plots for different values of ζ are included to cover the range of damping values encountered in actual structures whether the peak response is plotted against f_n or T_n is a matter of personal reference. A variety of response spectra can be defined depending on the response quantity that is plotted. Consider the following peak responses:

$$u_0(T_n, \zeta) \equiv max_t|u(t, T_n, \zeta)| \quad \textit{Eq. 2. 16}$$

$$\dot{u}_0(T_n, \zeta) \equiv max_t|\dot{u}(t, T_n, \zeta)| \quad \textit{Eq. 2. 17}$$

$$\ddot{u}_0^t(T_n, \zeta) \equiv max_t|\ddot{u}^t(t, T_n, \zeta)| \quad \textit{Eq. 2. 18}$$

The deformation response spectrum is a plot of u_0 against T_n for fixed ζ. A similar plot for $\dot{u}_0$ is the relative velocity response spectrum, and $\ddot{u}_0^t$ is the accelerations response spectrum, (Chopra, A., 2013).

The deformation spectrum provides all the information necessary to compute the peak values of deformation $D \equiv u_0$ and internal force. Where E_{s0} is the relationship between strain energy and kinetic energy, consider a quantity of peak deformation before, then the pseudo velocity response spectrum calculated by:

$$V = \omega_n D = \frac{2\pi}{T_n} D \quad \textit{Eq. 2. 19}$$

$$E_{s0} = \frac{k{u_o}^2}{2} = \frac{kD^2}{2} = \frac{k(\frac{V}{\omega_n})^2}{2} = \frac{mV^2}{2} \quad \textit{Eq. 2. 20}$$

And pseudo acceleration A and base shear V_{b0}calculated by:

$$A = {\omega_n}^2 D = \left(\frac{2\pi}{T_n}\right)^2 D \quad \textit{Eq. 2. 21}$$

$$V_{b0} = f_{s0} = mA = \frac{A}{g} w \quad \textit{Eq. 2. 22}$$

The response spectrum for a given ground motion component $\ddot{u}_g(t)$ can be developed by implementation of these following steps:

1. Numerically define the ground motion acceleration $\ddot{u}_g(t)$. Typically, the ground motion ordinates are defines in every time step Δt.
2. Select the natural vibration period T_n and damping ratio ζ of a system.

3. Compute the deformation response u(t) of the system due to the ground motion $\ddot{u}_g(t)$ by any of the numerical methods.
4. Determine u_0, the peak value of u(t).
5. The spectral ordinates are $D = u_0$, $V = (2\pi/T_n)D$, $A = (2\pi/T_n)^2 D$.
6. Repeat steps 2 to 5 for a range of T_n and ζ values covering all possible systems of engineering interest.

Figure 2.8 will be an example of the combination D-V-A response spectrum for El-Centro Ground motion with damping ratio 2%.(Chopra, A., 2013)

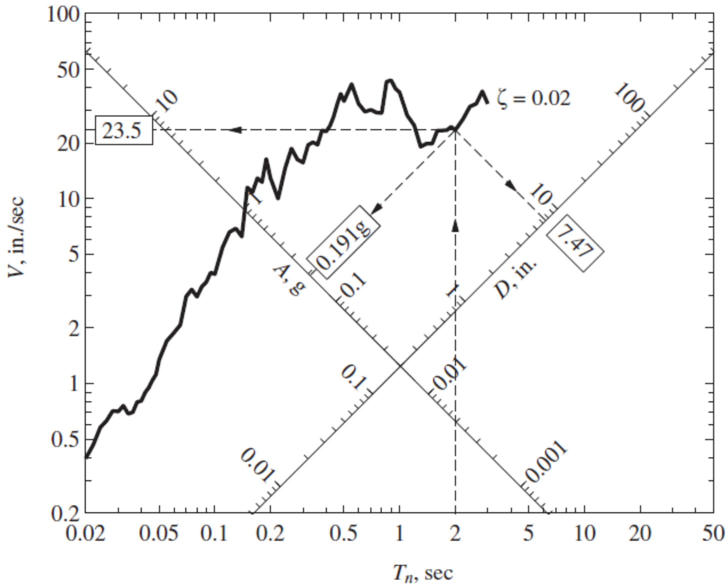

Figure 2. 8 Combined D-V-A response spectrum for El-Centro ground motion ζ=2%, (Chopra, A., 2013).

2.5.2 Numerical Evaluation

N. M. Newmark developed a family of time stepping methods based on this equations:

$$\dot{u}_{i+1} = \dot{u}_i + [(1-\gamma)\Delta t]\ddot{u}_i + (\gamma \Delta t)\ddot{u}_{i+1} \quad \textit{Eq. 2. 23}$$

$$u_{i+1} = u_i + (\Delta t)\dot{u}_i + [(0.5-\beta)(\Delta t)^2]\ddot{u}_i + [\beta(\Delta t)^2]\ddot{u}_{i+1} \quad \textit{Eq. 2. 24}$$

The parameter γ and β define the variation of acceleration over a time step and determine the stability and accuracy characteristics of the method. Typical selection for $\gamma = 0.5$ and $1/6 \le \beta \le 1/4$ is satisfactory from all point of view, including that of accuracy. If u_{i+1}, $\dot{u}_{i+1}$, and $\ddot{u}_{i+1}$ are provided as the bases for computing, then the equation of motions will be:

$$m\ddot{u}_{i+1} + c\dot{u}_{i+1} + ku_{i+1} = p_{i+1} \quad \textit{Eq. 2. 25}$$

$$u_{i+1} = \frac{\gamma}{\beta\Delta t}(u_{i+1} - u_i) + \left(1 - \frac{\gamma}{\beta}\right)\dot{u}_i + \Delta t\left(1 - \frac{\gamma}{2\beta}\right)\ddot{u}_i \qquad \textit{Eq. 2. 26}$$

If it assume $\hat{k}$ and $\hat{p}_{i+1}$ is:

$$\hat{k}u_{i+1} = \hat{p}u_{i+1} \qquad \textit{Eq. 2. 27}$$

$$\hat{k} = k + \frac{\gamma}{\beta\Delta t}c + \frac{1}{\beta(\Delta t)^2}m \qquad \textit{Eq. 2. 28}$$

$$\hat{p}_{i+1} = p_{i+1} + \left[\frac{\gamma}{\beta\Delta t}c + \frac{1}{\beta(\Delta t)^2}m\right]u_i + \left[\frac{1}{\beta\Delta t}m + \left(\frac{\gamma}{\beta} - 1\right)c\right]\dot{u}_i + \left[\left(\frac{1}{2\beta} - 1\right)m + \Delta t\left(\frac{\gamma}{2\beta} - 1\right)c\right]\ddot{u}_i \qquad \textit{Eq. 2. 29}$$

Displacement and acceleration at time i+1 is computed from:

$$u_{i+1} = \frac{\hat{p}_{i+1}}{\hat{k}} \qquad \textit{Eq. 2. 30}$$

$$\ddot{u}_{i+1} = \frac{p_{i+1} - c\dot{u}_{i+1} - ku_{i+1}}{m} \qquad \textit{Eq. 2. 31}$$

(Chopra, A., 2013).

2.6 Software Simulation

This research was done by software simulation of CSI SAP2000 version of 20. SAP2000 is a structural program for analysis and civil structures design categorized as stand-alone finite element based. It offers an intuitive, yet powerful user interface with many tools to aid in the quick and accurate construction of the models, along with the sophisticated analytical techniques needed to do the most complex projects.

SAP2000 is object based, meaning that the models are created using members that represent the physical reality. A beam with multiple members framing into it is created as a single object, just as it exists in the real world, and the meshing needed to ensure that connectivity exists with the other members is handled internally by the program. Result for analysis and design are reported for the overall object, and not for each sub-element that makes up the object, providing information that is both easier to interpret and more consistent with the physical structure.

CHAPTER III – FUNDAMENTAL THEORY AND METHODOLOGY ANALYSIS

3.1 Functional Bearing Model (FBM)

The objectives of this research is to design a flexible bearing yet consider the frictional slippage phenomenon. Combining rubber bearing with friction layer at the top and the bottom side of interface is the basic model of the bearing rubber subject in this research, as describe in Figure 3.1.

Figure 3. 1 Rubber and friction element in flexible bearing.

Functional Bearing Model (FBM) is an idea to represent 1 link analysis that used in common with divide it into 3 links based on each function. Most of the bearing analysis in a structure especially for bridge under the earthquake have assume to combine the restoring and frictional capability into 1 link assumption, it does not mean this idea is incorrect analysis, but 1 link assumption provide rough data of link behavior, so that the displacement result is the final displacement of collaboration work between rubber and friction element. In FBM system, this 1 link assumption represented into several links based on each constituent element. In this research, the rubber bearing consist of 3 elements as shown in Figure 3.1 as representation of rubber bearing system, the links are: Friction element in the top of sliding interface between bearing and deck, Rubber element in the middle part as a restoring element, and Frictional element in the bottom of sliding interface between bearing and column. Then, with FBM concept this bearing analysis built on 3 links analysis as shown in figure 3.2.

Figure 3.2 show three links that will be use as FBM representation in this research, considering the column displacement in each element's displacement, it is define U_c directly as displacement in the bottom side of the bottom friction link, U_3 as the displacement of the upper side of the bottom friction link which is same with the displacement in bottom side of the rubber link, U_2 as the displacement of the upper side of the rubber bearing which is as a same displacement as the bottom side of top friction link, and U_1 is the displacement in the upper side of top friction element, all of displacement function analyze in each reference time.

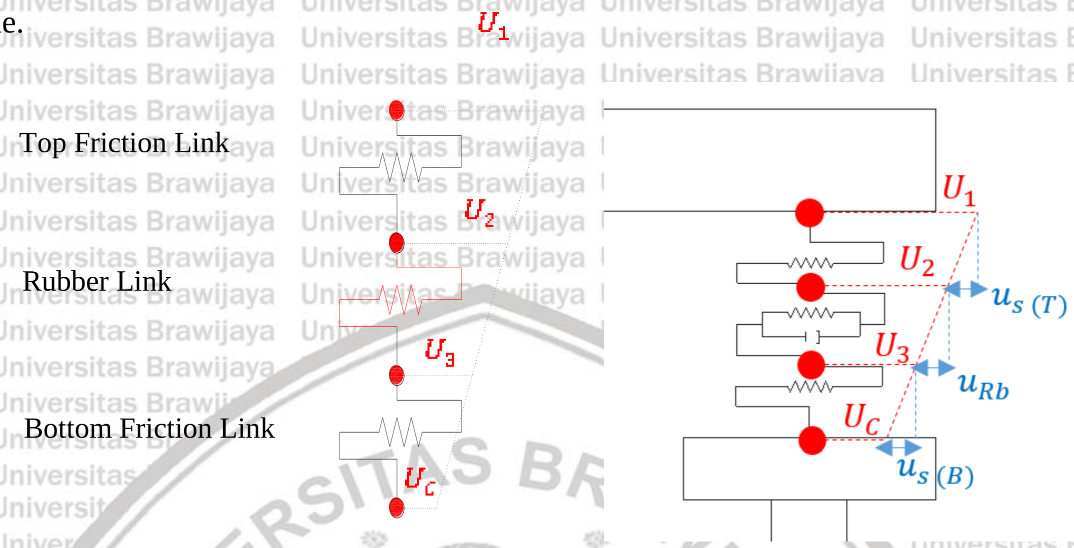

Figure 3. 2 Three links analysis in Functional Bearing Model (FBM) concept.

3.2 State Space Analysis Process

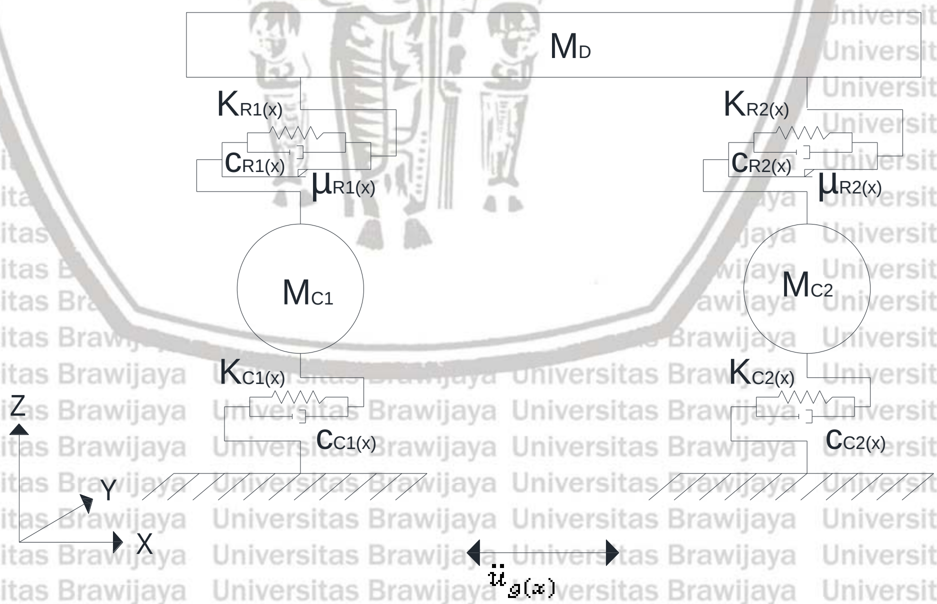

Figure 3. 3 Bridge MDOF system single spring assumption

Figure 3.3 is Bridge MDOF system in common analysis, when the rubber bearing assume as 1 spring that including rubber stiffness, coefficient of friction, and damping coefficient in one bearing system. Applying 3 links analysis as representation of the rubber bearing system in a bridge modeling give the meaning that sliding allowed in the top and in the bottom side of sliding interface, details shown in figure 3.4. In application of FBM system, the bearing allowed to have a movement both in bottom side and top side of its interface related with the deck and the column, the bearing only placed between column and deck without anchored. Large size of the cap beam need to design in order to prevent the bridge falling related with this issues, second reason is enough gap distance need to provide also in order to prevent the inter-deck crashing. Therefore, both bridge deck with the functional support and bridge column with functional support have a friction interface with coefficient of friction $\mu$and describe the sliding displacement u, and other parameter that explained in the next sub chapter.

Considering the earthquake excitation means that the external force is considered in this model, when the inertial force of the deck is less than the maximum friction force in the sliding interface, the deck's motion dominated by the elastic behavior of the functional support (sticking state). And if the inertial force beyond the maximum of the friction force on the sliding interface, then the deck will be sliding (sliding state). This behavior affected by the friction in the sliding interface point. Therefore, analyzing under the dynamic analysis, the states are divided into two states condition, sticking state and sliding state, (Liu, 2013).

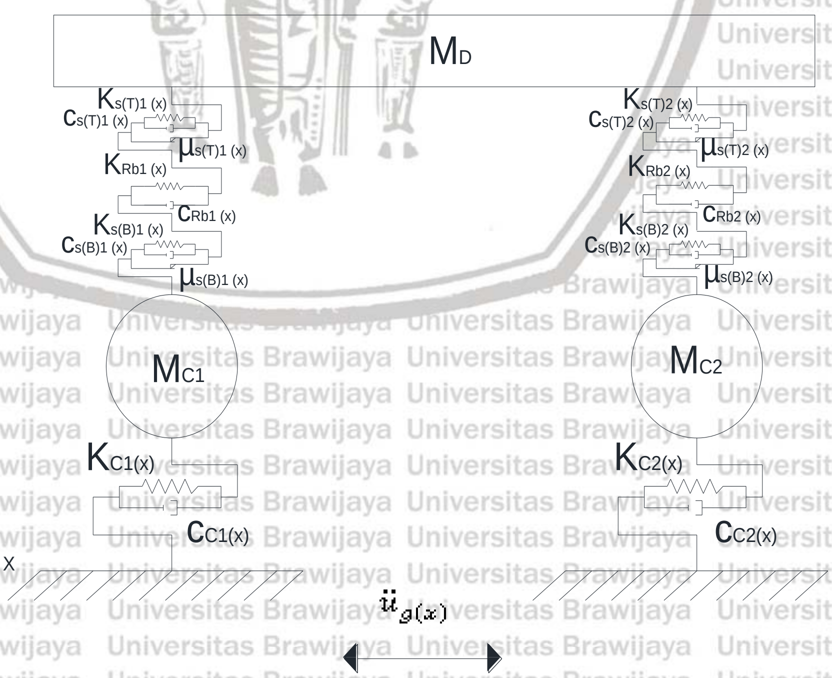

Figure 3. 4 Bridge MDOF system in three springs assumption

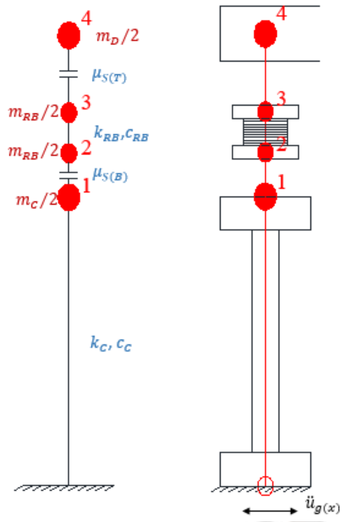

Figure 3. 5 Bridge lumped mass distribution

If the bridge model assumes as a lumped mass system that shown by figure 3.5. then the dynamic modelling of the system will be:

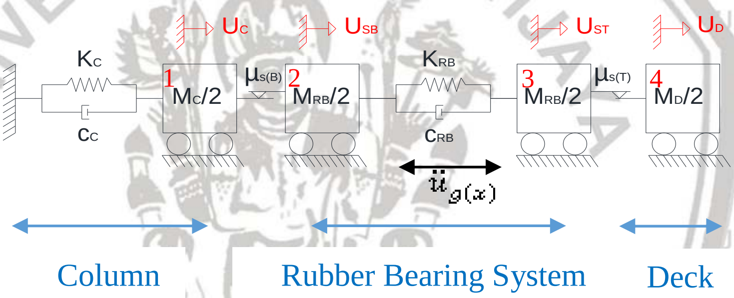

Figure 3. 6 Sticking state MDOF simplified model

Four degree of freedoms proposed in order to represent the dynamic model of the bridge. Assume that mass of the column divide into two point in the top and bottom of a frame, the bottom part of a frame, each column mass value is $^{m_c}/_2$, in the bottom part should be in the fixed, whereas mass in fix end is equal with zero, then for the lumped mass number 1 there are column mass $^{m_c}/_2$, column stiffness k_c and column damping c_c. Next, the total rubber mass divided into two part of the rubber bearing system, and each part will be lumped mass number 2 and 3, $^{m_{RB}}/_2$. There is surface friction that connect lumped mass number 1 and 2, named bottom friction surface. Because of there is nothing anchor for the bearing, then the bearing system allowed to give a movement in this part. Thus, $^{m_c}/_2$ of the column and $^{m_{RB}}/_2$ of the bottom rubber bearing connected by μ_{SB}. Rubber bearing system divided in to two part in the top (lumped mass number 3) and bottom (lumped mass number 2) side.

Rubber bearing defined as an elastic element with low stiffness of k_{RB} and the rubber damping of c_{RB}. These elements connect lumped mass number 2 and 3.The last, deck assume as rigid body that the mass transmitted to the both column, each column received $^{m_D}/_2$ as the lumped mass number 4. Deck and rubber bearing system connected by the surface friction, then the lumped mass number 3 and 4 are connected by μ_{ST}.

Take a force balance of figure 3.6, then four degree of freedoms matrix of motion determined bellow:

$$\begin{bmatrix} -{}^{m_c}/_2 & 0 & 0 & 0 \\ 0 & -{}^{m_{RB}}/_2 & 0 & 0 \\ 0 & 0 & -{}^{m_{RB}}/_2 & 0 \\ 0 & 0 & 0 & -{}^{m_D}/_2 \end{bmatrix} \begin{bmatrix} \ddot{u}_c \\ \ddot{u}_{SB} \\ \ddot{u}_{ST} \\ \ddot{u}_D \end{bmatrix} + \begin{bmatrix} -c_C & 0 & 0 & 0 \\ 0 & -c_{RB} & c_{RB} & 0 \\ 0 & c_{RB} & -c_{RB} & 0 \\ 0 & 0 & 0 & 0 \end{bmatrix} \begin{bmatrix} \dot{u}_c \\ \dot{u}_{SB} \\ \dot{u}_{ST} \\ \dot{u}_D \end{bmatrix} + \begin{bmatrix} -k_C & 0 & 0 & 0 \\ 0 & -k_{RB} & k_{RB} & 0 \\ 0 & k_{RB} & -k_{RB} & 0 \\ 0 & 0 & 0 & 0 \end{bmatrix} \begin{bmatrix} u_C \\ u_{SB} \\ u_{ST} \\ u_D \end{bmatrix} = \begin{bmatrix} {}^{m_c}/_2 \\ {}^{m_{RB}}/_2 \\ {}^{m_{RB}}/_2 \\ {}^{m_D}/_2 \end{bmatrix} \ddot{u}_g + \begin{bmatrix} \mu_{SB} \\ -\mu_{SB} \\ \mu_{ST} \\ -\mu_{ST} \end{bmatrix}$$

From this matrix of motion, the equations of motion of each element can be calculated as follows:

$$-{}^{m_c}/_2\, \ddot{u}_c - c_c \dot{u}_c - k_c u_c = {}^{m_c}/_2\, \ddot{u}_g + \mu_{SB} N_D \qquad \textit{eq. 3. 1}$$

$$-{}^{m_{RB}}/_2\, \ddot{u}_{SB} + c_{RB}(\dot{u}_{ST} - \dot{u}_{SB}) + k_{RB}(u_{ST} - u_{SB}) = {}^{m_{RB}}/_2\, \ddot{u}_g - \mu_{SB} N_D \qquad \textit{eq. 3. 2}$$

$$-{}^{m_{RB}}/_2\, \ddot{u}_{ST} - c_{RB}(\dot{u}_{ST} - \dot{u}_{SB}) - k_{RB}(u_{ST} - u_{SB}) = {}^{m_{RB}}/_2\, \ddot{u}_g + \mu_{ST} N_D \qquad \textit{eq. 3. 3}$$

$$-{}^{m_D}/_2\, \ddot{u}_D = {}^{m_D}/_2\, \ddot{u}_g - \mu_{ST} N_D \qquad \textit{eq. 3. 4}$$

Determining the equation of motion of the shear force in the bottom interface (FSB):

$$FSB = c_{RB}(\dot{u}_{ST} - \dot{u}_{SB}) + k_{RB}(u_{ST} - u_{SB}) \qquad \textit{eq. 3. 5}$$

And the equation of the shear force in the top interface (FST):

$$FST = -c_{RB}(\dot{u}_{ST} - \dot{u}_{SB}) - k_{RB}(u_{ST} - u_{SB}) \qquad \textit{eq. 3. 6}$$

Then, these two equations of FST and FSB will be an important parameter to determine the state condition in the top and bottom sliding in the interface. As reminder, top sliding interface is the sliding in the interface between rubber bearing system and deck, and bottom sliding interface is the sliding in the interface between rubber bearing system and column.

3.2.1 Sticking State

Generally, sticking state happen if the system fulfills these two requirements. First, there is no sliding in the top of the sliding interface, its happen when the inertial force of the deck is less than the friction force of the top sliding interface. Second, there is no sliding in the bottom of the sliding interface, and its happen when the shears force of the column is less than the friction force of the bottom interface. Only pure deformation of the rubber happens in the sticking state condition and the system keep on elastic.

Dynamic model of the bridge while sticking state condition is like general dynamic modeling as shown in figure 3.6. In sticking state condition, a whole system working in unity and there is no sliding in both interface. If the friction force due to the external force in sticking state FS_{stick} is static friction coefficient $\mu_{(s)}$ multiplied with normal force of the deck N_D :

$$FS_{stick} = \mu_{(s)} N_D \qquad \text{eq. 3.7}$$

Then, sticking state happen with two requirements:

Requirement 1:

Bottom interface: No Sliding

$$FSB < \mu_{SB(S)} . N_D \qquad \text{eq. 3.8}$$

Requirement 2:

Top interface: No Sliding

$$FST < \mu_{ST(S)} . N_D \qquad \text{eq. 3.9}$$

Furthermore, the deck and column on sticking state condition is working in coherency, from this unit matrix then the equation of motion in this state space can be derived, if FSB is the friction force in the bottom interface and FST is the friction force in the top interface, with fulfilling both requirement of equation 3.8 and 3.9 then the system is defined on sticking state condition.

3.2.2 Sliding State

Related with the sticking state requirements as in equation 3.8 and 3.9, if the components in the left side is greater than or equal with the component in the right side, the static coefficient of friction turn into kinetic coefficient of friction, sticking state will be over then the sliding will happen. In sliding state condition, the system lose its coherency and the deck worked independently with the column but its affected each other by the force in the sliding interface.

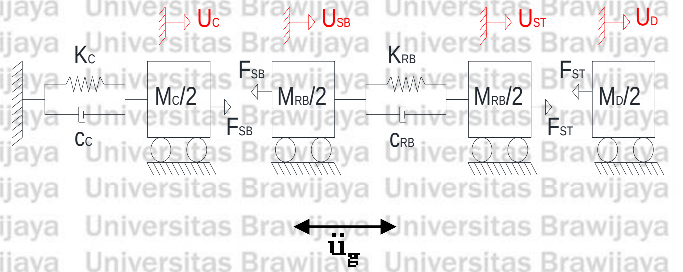

Figure 3. 7 Sliding State Dynamic Model

Since the system in sliding state working independently based on which sliding part that happen on a system, then the dynamic model of the bridge will be divided into several part consider on where the sliding state happen. And the number of the degree of freedom also based on the sliding state conditions. There are three conditions in sliding state condition:

Condition 1: Sliding in the top interface only.

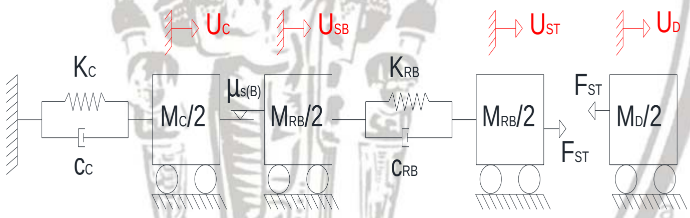

Figure 3. 8 Sliding in the top interface only

Sliding state in the top interface only happen if the system follows these two requirements:

Requirement 1:

Bottom interface: No Sliding

$FSB < \mu_{SB(S)} . N_D$ *eq. 3. 10*

Requirement 2:

Top interface: Sliding

$If, FST \geq \mu_{ST(S)} . N_D$ *eq. 3. 11*

Then, $FST = \mu_{ST(k)} . N_D$ *eq. 3. 12*

Condition 2: Sliding in the bottom interface only.

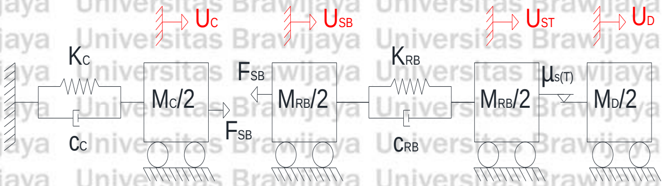

Figure 3. 9 Sliding in the bottom interface only

Sliding state in the bottom interface of the rubber bearing system shall occur when the system fulfills these two requirements:

Requirement 1:

Bottom interface: Sliding

If, $FSB \geq \mu_{SB(S)}.N_D$ *eq. 3. 13*

Then, $FSB = \mu_{SB(k)}.N_D$ *eq. 3. 14*

Requirement 2:

Top interface: No Sliding

$FST < \mu_{ST(S)}.N_D$ *eq. 3. 15*

Condition 3: Sliding in both top and bottom interface.

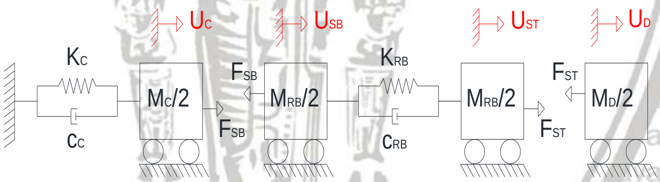

Figure 3. 10 Sliding in both interface

Sliding will happen in top and bottom interface of the rubber bearing system, if the system fulfills these two requirements:

Requirement 1:

Bottom interface: Sliding

If, $FSB \geq \mu_{SB(S)}.N_D$ *eq. 3. 16*

Then, $FSB = \mu_{SB(k)}.N_D$ *eq. 3. 17*

Requirement 2:

Top interface: Sliding

If, $FST \geq \mu_{ST(S)}.N_D$ *eq. 3. 18*

Then, $FST = \mu_{ST(k)}.N_D$ *eq. 3. 19*

3.3 Fundamental Theory

3.3.1 Free Body Diagram

A whole bridge that consist of rigid deck, rubber bearing system, column, and fixed foundation was proposed as a target model of the analysis. Assume the bridge deck as a rigid body, its mean that the deformation curvature shall not be happen in the system. And columns that provide small displacement and should be considered in the rubber bearing behavior made each component in bridge model will be influenced each other.

All of the motion come from the ground due to the earthquake ground motion, then the energy transferred from substructure toward superstructure. Reducing earthquake energy is the main purpose to prevent the bridge failure. Applying flexible rubber bearing system famously known as one of many ways to reduce the transferred energy due to its energy dissipating capability. In his research, Liu compared the support hysteresis loop with the acceleration history of the deck and observed that the bearings produce slippage when the deck acceleration reach an extreme value. Which means that slippage happen in plastic area due to non-linear capability of the rubber bearing system to absorb the energy excess.

In this analysis, general force equilibrium explained as free body diagram in figure 3.11. But each force component in this free body diagram are dependent with the dominant force that working on the structure, which means that the force direction can be changed in its opposite if the dominant force is changing.

Mention that N is the normal force of the deck that received by the column. This free body diagram prevails when the inertial force of the deck is the dominant force than the bearing’s shear force. While in sticking state condition, the system goes in right direction and the motion only pure deformation without sliding. But if another possibility that shears force become the dominants one due to the source energy comes from the substructure, the deck will move in left side than the force equilibrium turn in the opposite direction. The system has possibility to behave in several conditions, and these conditions explained in the next sub chapter.

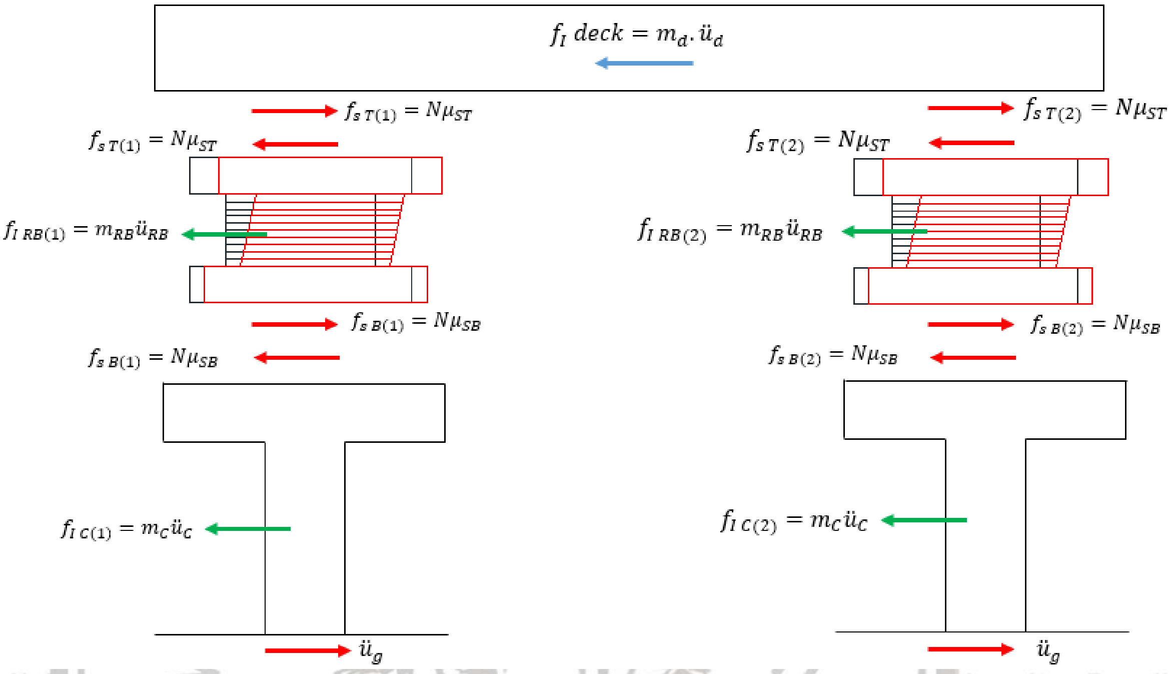

Figure 3. 11 Free Body Diagram

3.3.2 Conditions

Due to there is no constrain to limit the structural movement, all possibility condition need to be considered. Totally there are 16 conditions that may be happen in the structure both loaded under Near Fault and Far Fault earthquake, these 16 conditions mention as in table 3.1.

Table 3.1 shows the motion possibility that will happen on a structure during the earthquake loading. The deck assumed as a solid caused the deck movement close to rigid body motion, so that either curvature or deck rotation did not happen. This rigid body motion gave some contribution for the motion in both left and right side column, this rigid deck caused both column accept same force and move in a unity.

As displacement comparison of case A2 which configured on different value of coefficient of friction on the top and the bottom interface, under the near fault of Chi-Chi earthquake 600 gal and far fault of El-Centro earthquake 600 gal, due to the same of section and material properties of the column, the shear force shall be transferred equally toward both column, thus when the earthquake happen, column 1 and column 2 behave in the same state condition, then this phenomenon categorized the bridge model as a regular bridge.

Table 3. 1 Possibility conditions

Near Fault	Column 1	Top Interface	No Sliding	Sliding	No Sliding	Sliding
		Bottom Interface	No Sliding	No Sliding	Sliding	Sliding
	Column 2	Top Interface	No Sliding	Sliding	No Sliding	Sliding
		Bottom Interface	No Sliding	No Sliding	Sliding	Sliding
Far Fault	Column 1	Top Interface	No Sliding	Sliding	No Sliding	Sliding
		Bottom Interface	No Sliding	No Sliding	Sliding	Sliding
	Column 2	Top Interface	No Sliding	Sliding	No Sliding	Sliding
		Bottom Interface	No Sliding	No Sliding	Sliding	Sliding

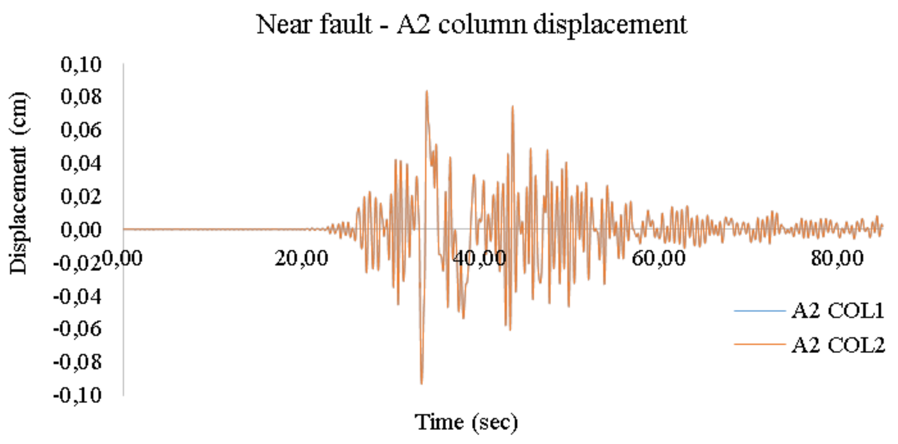

Figure 3. 12 Near fault 600 gal – case A2 column displacement

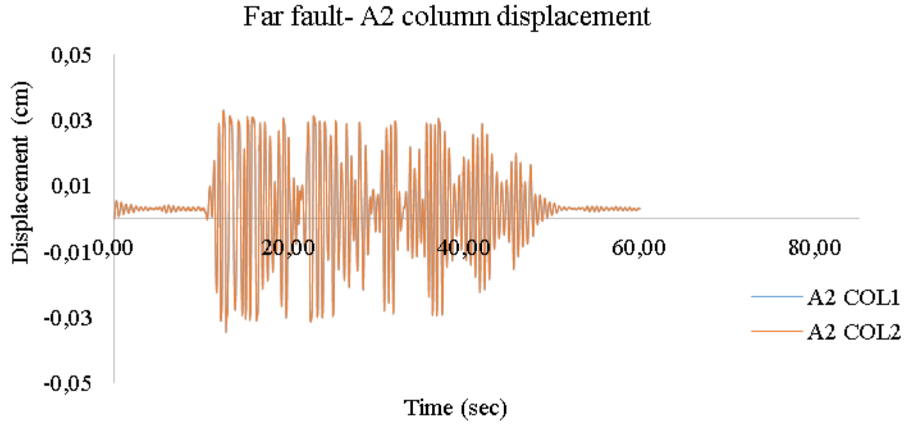

Figure 3. 13 Far fault 600 gal – case A2 column displacement

As mention in the sub chapter 3.2, there are two state condition that possibly happen, they are sticking state and sliding state. Since there are two interface (top interface and bottom interface) considered in the system, sticking and sliding may happen either in one interface or both interface together. There is no slippage in sticking state condition due to the motion only provided by the rubber deformation.

In the top interface, sticking state limited by $FST < \mu_{ST(S)}.N_D$ and sticking state in the bottominterface limited by $FSB < \mu_{SB(S)}.N_D$, simply means that in the top interface, sticking state happen when the friction force of the top interface of the system is less than the friction force due to the top surface roughness. Meanwhile, in the bottom interface, the shear force in the bottom surface of the system should be less than the friction force of the bottom surface roughness. This is the requirement of the sticking state condition.

At the time when the equation in the left side of the sticking state requirement is equal or greater than the equation in the right side, for the top sliding interface $FST \geq \mu_{ST(S)}.N_D$ and the bottom sliding interface $FSB \geq \mu_{SB(S)}.N_D$ the state will be turn into sliding state condition. Sliding might happen either in the top interface only or both interface, as long as which one interface that reached the sliding state requirement first.

Related with the force balance in figure 3.10, shear force occurs because of the element interconnection, and since each element set free to give a motion, then displacement in each element should be paid more concern, details on figure 3.11. In the other hand, due to the same behavior of the left and right side column, same state condition may occur in both columns, and due to there are two part of the sliding interface under far fault and near fault earthquake ground motion, as the number of conditions might occur in the system:

Near Fault Earthquake

Condition 1:

- Column 1: Top surface sticking state$FST < \mu_{ST(S)}.N_D$

  Bottom surface sticking state $FSB < \mu_{SB(S)}.N_D$
- Column 2: Top surface sticking state $FST < \mu_{ST(S)}.N_D$

  Bottom surface sticking state $FSB < \mu_{SB(S)}.N_D$

Condition 2:

- Column 1: Top surface sticking state $FST < \mu_{ST(S)}.N_D$

Bottom surface sliding state $FSB = \mu_{SB(K)} . N_D$

- Column 2: Top surface sticking state $FST < \mu_{ST(S)} . N_D$

  Bottom surface sliding state $FSB = \mu_{SB(K)} . N_D$

Condition 3:

- Column 1: Top surface sliding state $FST = \mu_{ST(K)} . N_D$

  Bottom surface sticking state $FSB < \mu_{SB(S)} . N_D$

- Column 2: Top surface sliding state $FST = \mu_{ST(K)} . N_D$

  Bottom surface sticking state $FSB < \mu_{SB(S)} . N_D$

Condition 4:

- Column 1: Top surface sliding state $FST = \mu_{ST(K)} . N_D$

  Bottom surface sliding state $FSB = \mu_{SB(K)} . N_D$

- Column 2: Top surface sliding state $FST = \mu_{ST(K)} . N_D$

  Bottom surface sliding state $FSB = \mu_{SB(K)} . N_D$

Far Fault Earthquake

Condition 1:

- Column 1: Top surface sticking state$FST < \mu_{ST(S)} . N_D$

  Bottom surface sticking state $FSB < \mu_{SB(S)} . N_D$

- Column 2: Top surface sticking state $FST < \mu_{ST(S)} . N_D$

  Bottom surface sticking state $FSB < \mu_{SB(S)} . N_D$

Condition 2:

- Column 1: Top surface sticking state $FST < \mu_{ST(S)} . N_D$

  Bottom surface sliding state $FSB = \mu_{SB(K)} . N_D$

- Column 2: Top surface sticking state $FST < \mu_{ST(S)} . N_D$

  Bottom surface sliding state $FSB = \mu_{SB(K)} . N_D$

Condition 3:

- Column 1: Top surface sliding state $FST = \mu_{ST(K)} . N_D$

  Bottom surface sticking state $FSB < \mu_{SB(S)} . N_D$

- Column 2: Top surface sliding state $FST = \mu_{ST(K)} . N_D$

Bottom surface sticking state $\mathrm{FSB} < \mu_{SB(S)}.N_D$

Condition 4:

- Column 1: Top surface sliding state $\mathrm{FST} = \mu_{ST(K)}.N_D$

  Bottom surface sliding state $\mathrm{FSB} = \mu_{SB(K)}.N_D$

- Column 2: Top surface sliding state $\mathrm{FST} = \mu_{ST(K)}.N_D$

  Bottom surface sliding state $\mathrm{FSB} = \mu_{SB(K)}.N_D$

3.3.3 Sliding Mechanism

Sliding mechanism explain about the bridge motion path. Structure allowed to give a motion in line with the earthquake excitation in order to reduce the shear force and prevent the failure. Figure 3.13 show the bridge motion, start from the original position, because of the main loading come from the ground, the earthquake energy transmitted to the foundations then columns, columns will start the motion first then the energy from the columns transmitted to the most flexible element, rubber will deform to absorb some energy and if the rubber capacity reach the limit, the energy will be transferred into the top and the bottom side of the rubber bearing, if the surface roughness of the sliding interface provide the friction force larger than the existing shear force, this friction element able to dissipate the excess energy without any slippage. In the opposite, if the existing shear force over than friction force of the surface roughness, then the sliding shall occur to prevent the bearing failure.

Next consideration toward the sliding displacement in top and bottom side of the rubber bearing system. Inertial force of the deck and friction force from the top surface contribute the slippage in the sliding interface between deck and rubber bearing system, meanwhile friction force from the top surface that reduced by the rubber bearing inertial force and friction force from the bottom surface contribute the slippage in the sliding interface between rubber bearing system and column. Look backward on previous free body diagram, force balance of each element shall provide its own displacement function, details show on figure 3.11.

The deck motion provide u_D, friction force in the top sliding interface ($f_{s(T)}$) provide $u_{s(T)}$, pure deformation (u_{Rb}) from rubber bearing itself, and effect of friction force from the top sliding interface that reduced by rubber bearing inertial force ($f_{s(T)} - f_{I\ RB}$) produced bottom sliding displacement $u_{s(B)}$. These three displacement shall be main discussion in this

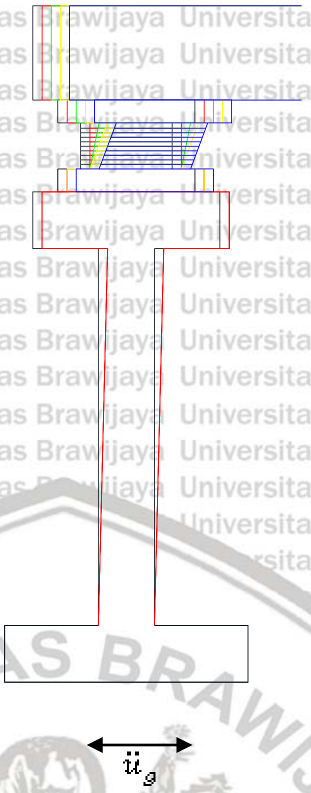

Figure 3. 14 Motion path

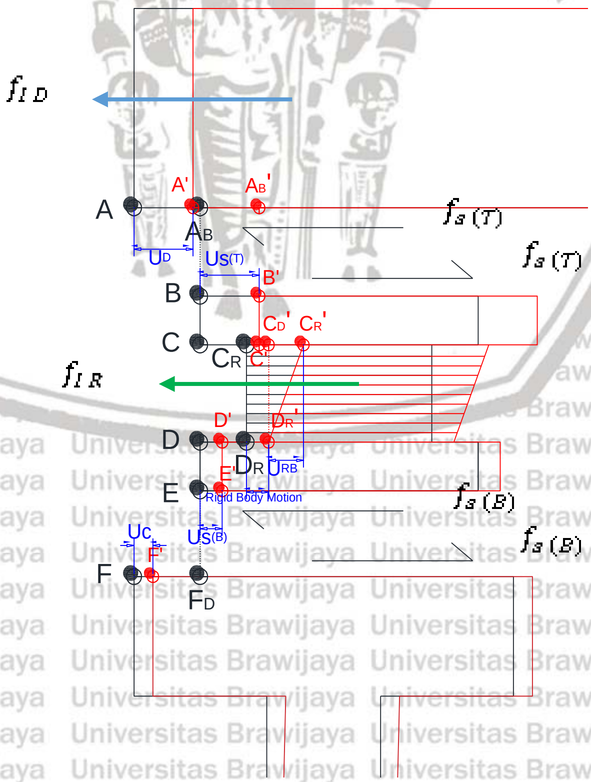

Figure 3. 15 Displacement point

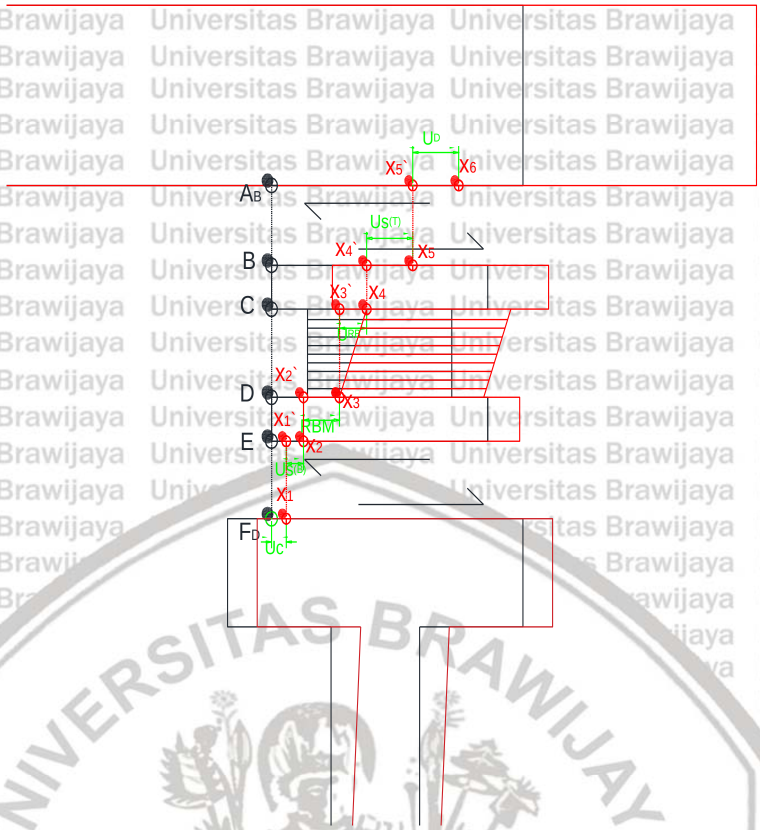

Figure 3. 16 Displacement path of point x

Table 3. 2 Sliding bar

Original point	Sliding distance	Displacement point
A_B	u_D	X_6
B	$u_{s(T)}$	X_5
C	u_{Rb}	X_4
D	RBM	X_3
E	$u_{s(B)}$	X_2
F_D	u_c	X_1

Note:

u_D : Deck displacement

$u_{s(T)}$: Top sliding displacement

u_{RB} : Rubber deformation

RBM : Rigid body motion

$u_{s(B)}$: Bottom sliding displacement

u_c : Column displacement

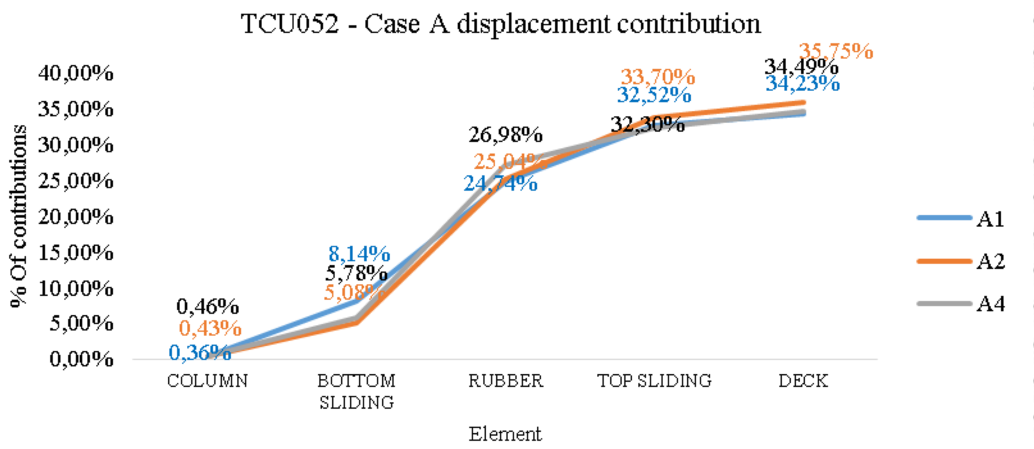

Figure 3. 17 Near fault 600 gal case A displacement contribution

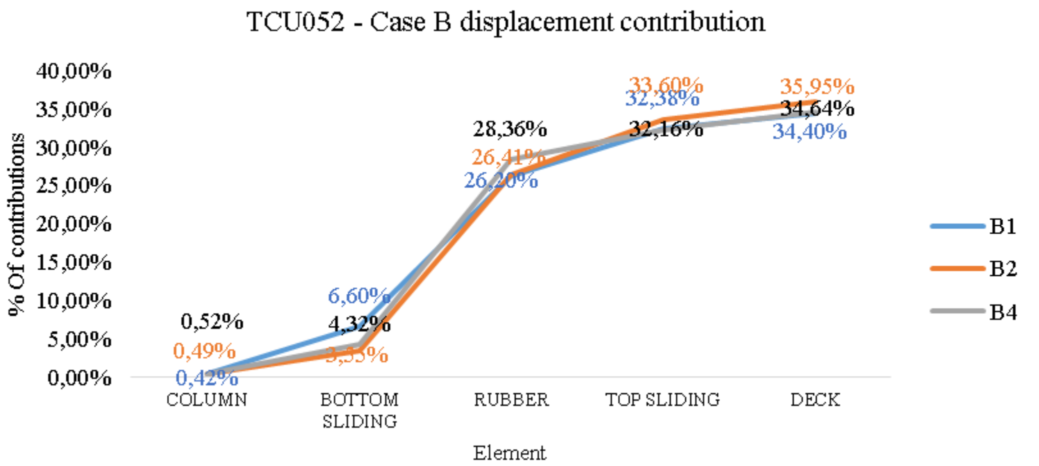

Figure 3. 18 Near fault 600 gal case B displacement contribution

analysis remembering sliding distance is the important consideration to prevent the bridge falling possibility.

Generally, each element in the bridge model will be displaced independently each other as describe in figure 3.15. Yet, the main loading excitation comes from the ground and transferred to the successor structure, and the bridge motion is in a unity, in fact, displacement of an element is contributed by the displacement of preceding elements. It shows in figure 3.16, if a point considered in each element and uniformly in the same position for all elements, start from point F_D in the cap beam that will move to x_1 due to column displacement, then x_1' is x_1 position in the bottom rigid body of the rubber bearing system that will move to x_2 because of the sliding in the bottom interface, continuously happen until point x_5' that move to x_6 due to deck displacement. Each position of the red point in figure 3.2 shows displacement path of point x due to the displacement capability of each element, point x_n take some contribution from point x_{n-1} means that the final displacement is contributed from the total each element's displacement. This explanation proven in figure 3.17 and figure 3.18.

3.4 Research Flowchart

Research flowchart bellow may show the research step that start from determining the purpose until taking research conclusion, this flowchart will become simply yet important in order to understand the path of this analysis.

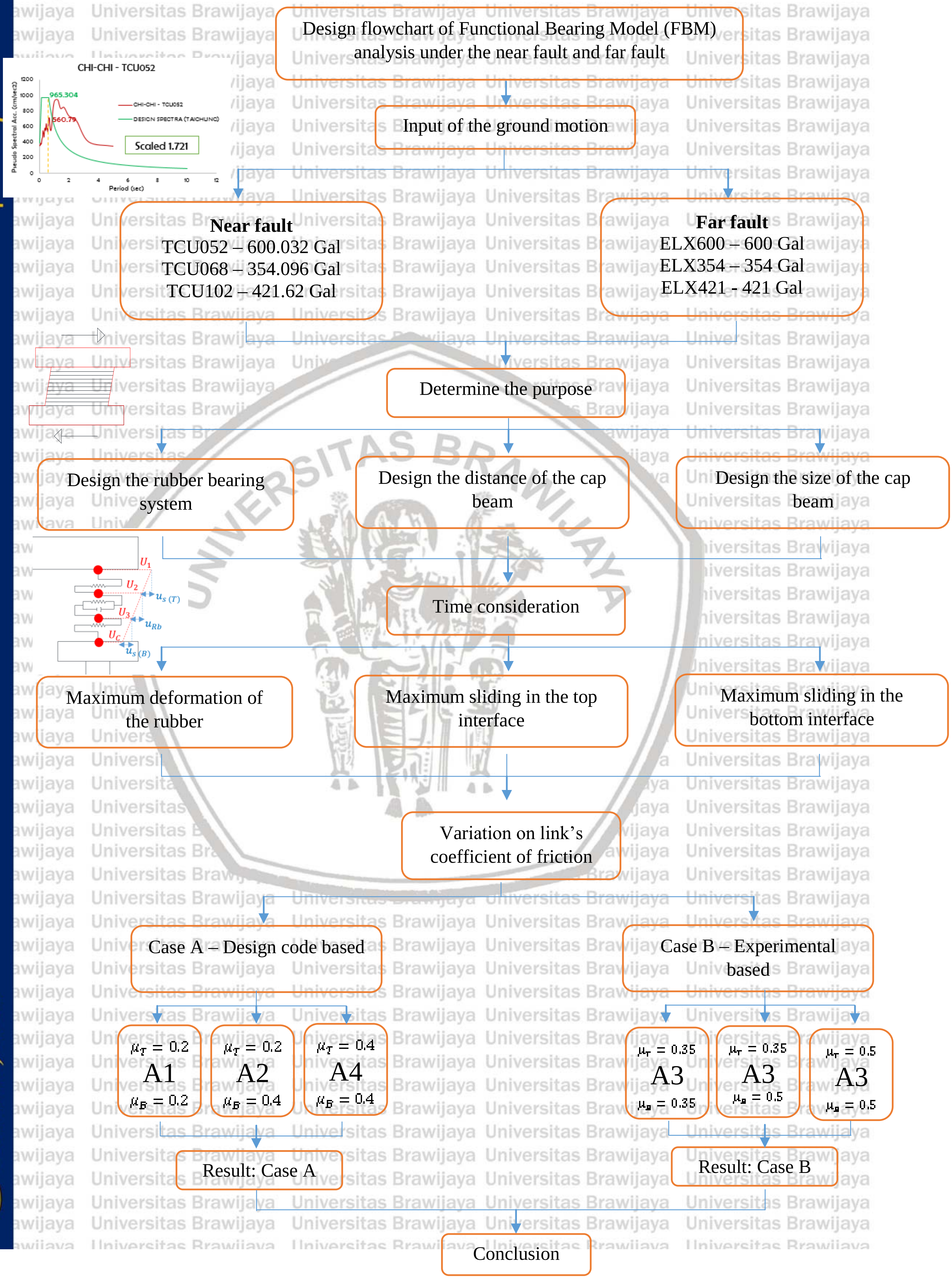
Design flowchart of Functional Bearing Model (FBM) analysis under the near fault and far fault
CHI-CHI - TCU052
965.304
560.79
CHI-CHI - TCU052
DESIGN SPECTRA (TAICHUNG)
Scaled 1.721
Pseudo Spectral Acc. (cm/sec2)
Period (sec)
Input of the ground motion
Near fault
TCU052 – 600.032 Gal
TCU068 – 354.096 Gal
TCU102 – 421.62 Gal
Far fault
ELX600 – 600 Gal
ELX354 – 354 Gal
ELX421 - 421 Gal
Determine the purpose
Design the rubber bearing system
Design the distance of the cap beam
Design the size of the cap beam
U_1
U_2
U_3
U_C
$u_{s(T)}$
u_{Rb}
$u_{s(B)}$
Time consideration
Maximum deformation of the rubber
Maximum sliding in the top interface
Maximum sliding in the bottom interface
Variation on link's coefficient of friction
Case A – Design code based
Case B – Experimental based
$\mu_T = 0.2$ A1 $\mu_B = 0.2$
$\mu_T = 0.2$ A2 $\mu_B = 0.4$
$\mu_T = 0.4$ A4 $\mu_B = 0.4$
$\mu_T = 0.35$ A3 $\mu_B = 0.35$
$\mu_T = 0.35$ A3 $\mu_B = 0.5$
$\mu_T = 0.5$ A3 $\mu_B = 0.5$
Result: Case A
Result: Case B
Conclusion

3.5 Modelling

3.5.1 Bridge Model

Prototype of bridge model was proposed in an experimental test using shaking table to analyze the bridge behavior under strong motion earthquake. Bridge model is scaled model that proposed by Liu on 2013 for the experimental test that was done in National Center of Research on Earthquake Engineering (NCREE), Taipei city.

The bridge model is a single span bridge that consist of the superstructure, support system, and the substructure. For the supper structure, consist of reinforced concrete deck and additional load as vehicle load. Support system is the rubber bearing system that consist of rubber bearing and friction layer in the top surface interconnection between rubber bearing and deck. And substructure consist of the cap beam, column, and foundation.

Figure 3.19 shows the real appearance of the bridge shaking table test model that was done by Liu in 2013. This research develops Liu's bridge model to analyze the condition when the top and bottom surface interconnection of rubber bearing system are considered as friction surface. Near fault of Chi-Chi earthquake and far fault of El-Centro earthquake is considered as the earthquake loading, in a reason since this both ground motion have special characteristic of strong motion.

Adapted from Liu's experimental model, numerical analysis using CSI software of SAP2000 is proposed in order to study more about Functional Bearing Model (FBM) in more advance condition. Liu study about Functional Bearing Model (FBM) with assume the bearing system in two links since the lower part of the rubber bearing system is locked with the cap beam, the first link represents the frictional element in the upper part of the rubber bearing system and the second link represents the rubber element itself. More advance, this research is study about Functional Bearing Model (FBM) with assume that the bearing has frictional surface in the upper part and lower part of the bearing system. Thus, its assume that the rubber bearing system into 3 links analysis. The first link represents the frictional element of the surface interconnection in the upper part of the rubber bearing system with the deck, named Top friction link. The second link represent the rubber element itself that make sure this rubber link is more flexible than others, named Rubber link. The third link represent the frictional element of the surface interconnection in the lower part of the rubber bearing system with the cap beam, named Bottom frictional link. Furthermore, with the same material and section properties as Liu's previous model, yet different assumption to define the rubber bearing system, a SAP2000 model was proposed as shown in figure 3.20.

Figure 3. 19 Single span bridge experimental model of Liu's in 2013.

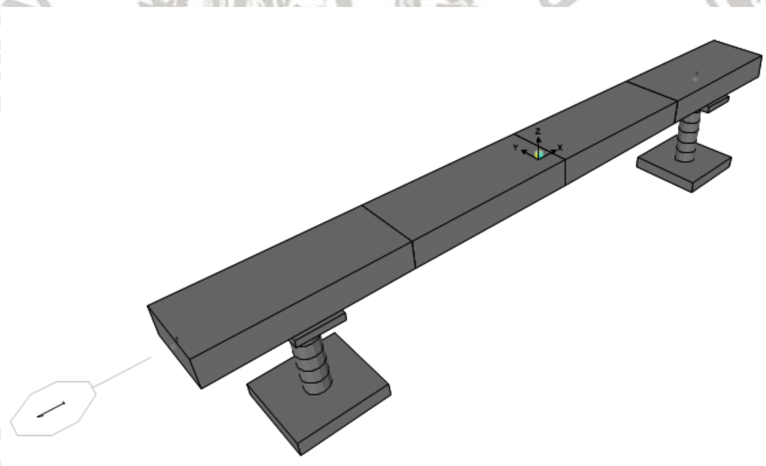

Figure 3. 20 Bridge model of SAP2000 for 3 links assumption of the Functional Bearing Model (FBM) Analysis

3.5.2 Material and Section Properties

About 500x50x20 cm of the deck dimension that overall made by reinforced concrete slab with design compressive strength is 6.87 KN/cm^2. 18 mass blocks also configured as additional mass, thus the overall weight of superstructure is about 57.68 KN. As depicted in figure 3.18, bridge model that dominated by steel as the material was proposed to analysis the dynamic behavior under the near fault of Chi-Chi Earthquake and far fault of El-Centro earthquake. In the previous analysis, Liu study about rubber bearing system that consider about bearing's top surface only as a sliding surface and in the bottom of the rubber bearing was fixed with the column. The size of the rubber bearing pad is 7.5x5.0x2.5 cm and 3 sheets of thin steel layer were put inside. For the substructure, cap beam was made from the rectangular solid steel with the dimension about 30x51 cm, columns are made by hollow steel A36 with the diameter of 16.9 cm and thickness of 0.67 cm, and the foundations are made from A36 steel blocks size 60x60 cm. All this information is follow the experimental model of Liu's in 2013.

In this analysis, a SAP2000 analysis is proposed to analyze the bridge experimental model under different case and condition. A simulation bridge model as shown in figure 3.19 was built that consist of three main structure: superstructure, rubber bearing system, and substructure. A solid frame was built to construct the bridge model, superstructure that consist of deck mass and additional loading that calculated together assumed as four segmental frame with its material density and sectional properties about 500x50x20 cm. Rubber bearing system that defined as 3 links system, a multilinear plastic link defined to assume top friction link and bottom friction link, meanwhile linear link defined to assume rubber link itself, link's properties shall explain further in the next sub chapter. Substructure that consist of the cap beams, columns, and foundations are construct as solid frame that overall are define with steel materials. Cap beam build as a single frame of steel with the cross section about 30x51 cm and 5 cm of the thickness. Columns with 60 cm of its height and defined as hollow steel column that divided into 6 segments to keep the convergence and stability result, 16.9 cm of the diameter and 0.67 cm of the column thickness. And footing or foundation that defined as single frame with steel as the material properties have dimension 60x60cm and thickness is 10 cm. All part in left and right side of the substructure have same parameter both in material and section properties, also its assumed that both column placed on the same site condition, thus, this bridge model categorized as regular bridge model.

3.5.3 Comparison Proposed Model with Previous Experimental Model

Former model proposed by Liu, et. al. in their experimental test on 2013. They studied about functional bearing system and divided rubber bearing system into 2 spring analysis. They assumed that the bottom side of rubber bearing system was anchored with the column, so that the prohibit the movement in the bottom side of the rubber bearing system. The sliding only allowed in the top side of the rubber bearing system, thus their functional system consistof two links, they are rubber link and top friction link (interconnection between bearing and deck).

SAP2000 model that proposed in this research followed all the former model that proposed by Liu, et. al., in 2013. About the section and material properties construct precisely similar with the previous model, yet the system analysis is totally different. Take the expectation that this proposed Functional Bearing Model (FBM) analysis shall provide the result in another conditions from the previous model. Proposed FBM analysis of three links assumptions, study about when there is no anchoring in the bottom side of the rubber bearing system. That is means the rubber bearing system placed over the seating of the cap beam, and the deck placed over the rubber bearing system. In this condition, the sliding motion shall occur both in the top and bottom side of the rubber bearing system. Meanwhile, the sliding motion influenced by the friction, then three links analysis created to assume each constituent element of the rubber bearing system. Proposed FBM analysis divide the rubber bearing system into three links analysis, they are: Top friction link (interface deck-bearing system), rubber link (rubber bearing system), bottom friction link (interface bearing system-column).

To make sure that the proposed SAP2000 model is in correct. SAP2000 simulation was done to compare the proposed SAP2000 model and the experimental test result. Under El-Centro earthquake 50 gal of the peak ground acceleration, the comparison result of deck acceleration and deck displacement between proposed SAP2000 model and the experimental test shown in figure 3.21 and 3.22.

This comparison result was done in order to make sure that the bridge model that use in this research is precisely similar with the previous experimental model. There is no significant different in both result of deck acceleration and deck displacement. Thus, the bridge model that built on SAP2000 can be analyze using Functional Bearing Model (FBM) analysis on three links assumptions.

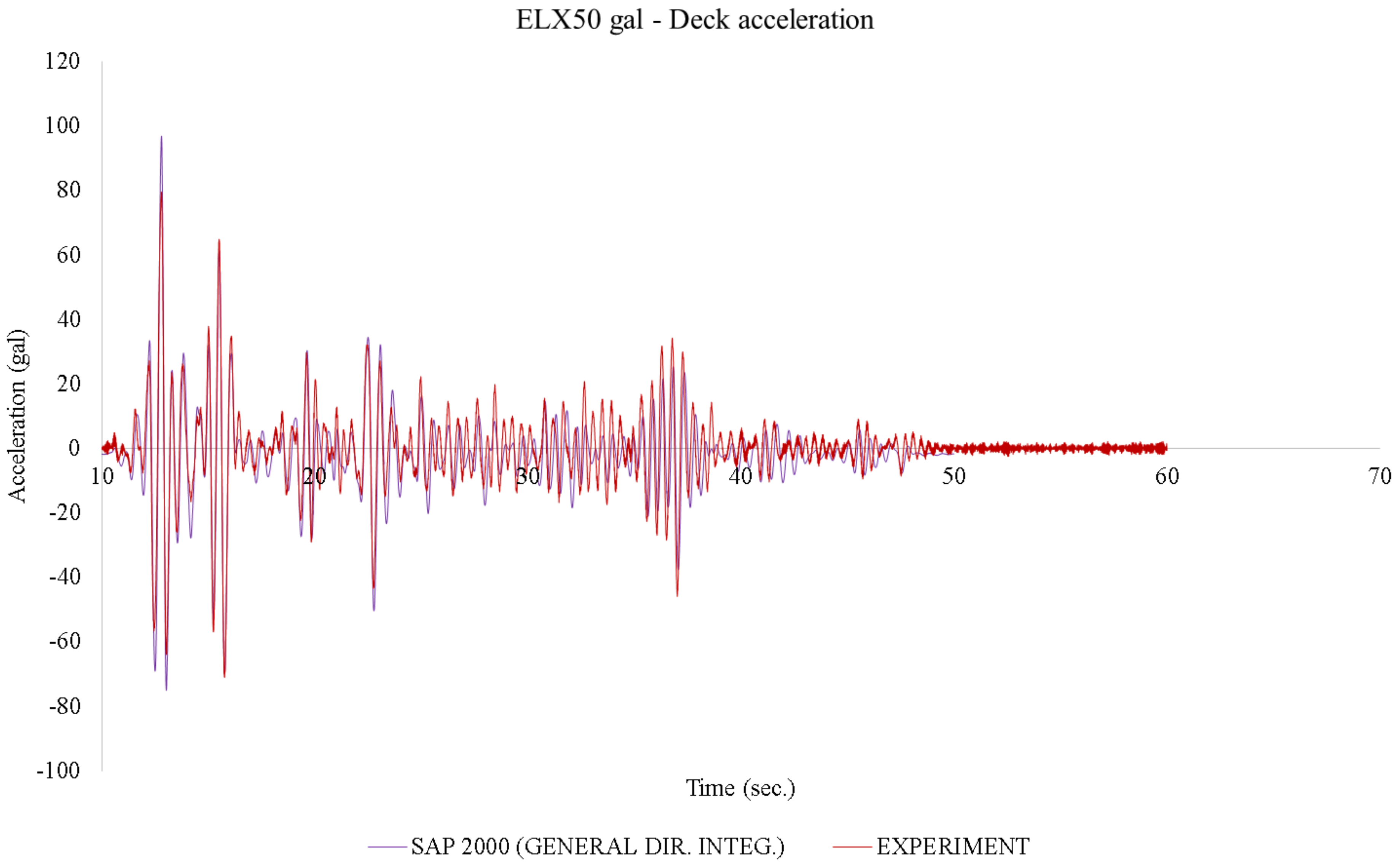
ELX50 gal - Deck acceleration
120
100
80
60
40
20
0
-20
-40
-60
-80
-100
Acceleration (gal)
10
20
30
40
50
60
70
Time (sec.)
SAP 2000 (GENERAL DIR. INTEG.)
EXPERIMENT

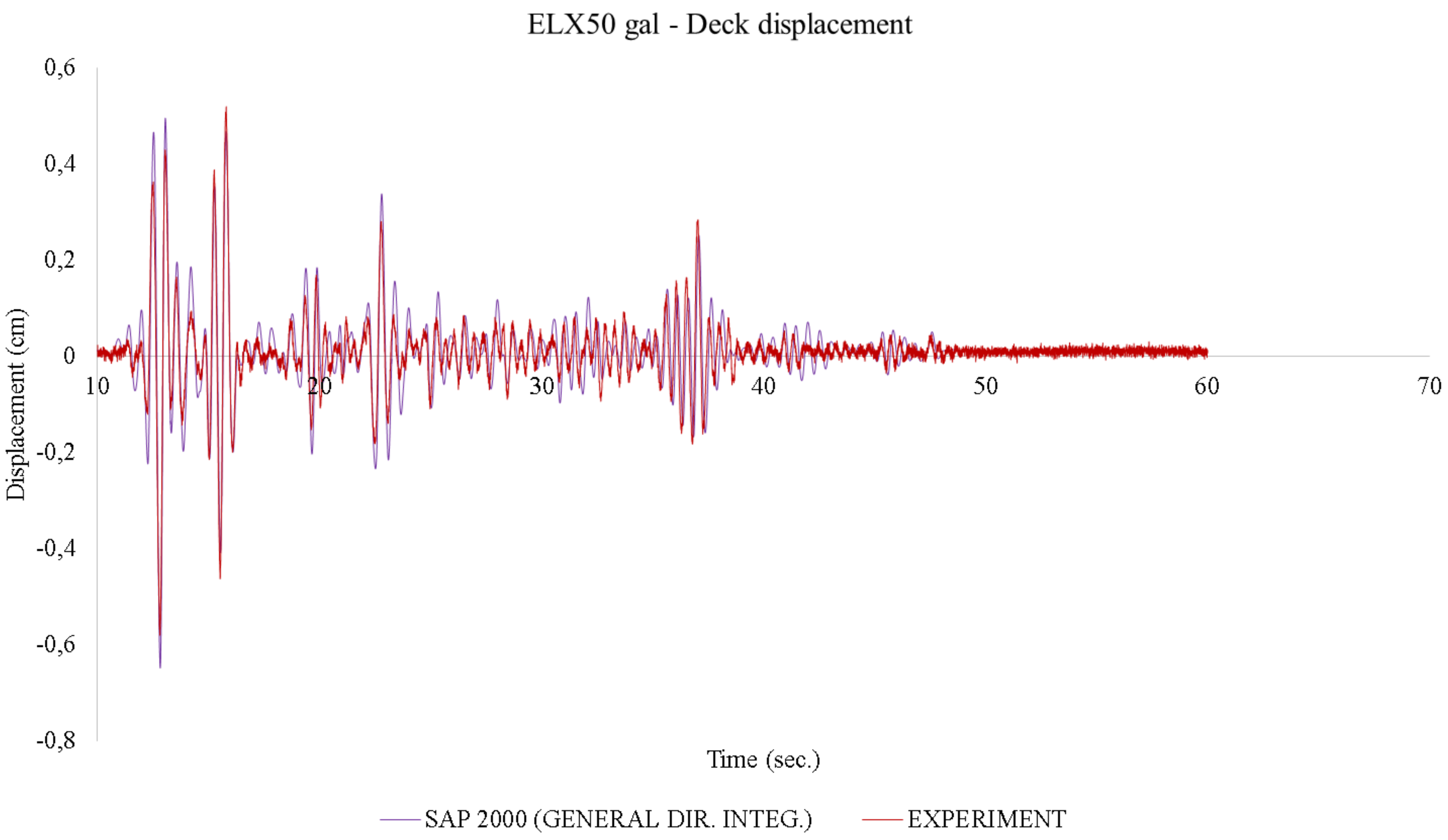

Figure 3. 22 Deck displacement of proposed model and experimental test

3.5.4 Resonance Possibility

Resonance happen when the fundamental period of the structure nearly closed with predominant periods of the earthquake. As the principal concept of considering isolation system in a bridge that mentioned by Iemura, et. al., 2005, that the isolation system helps in

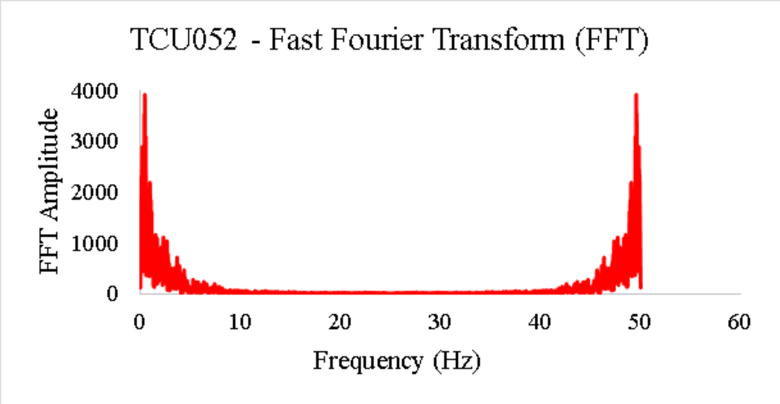

(a)

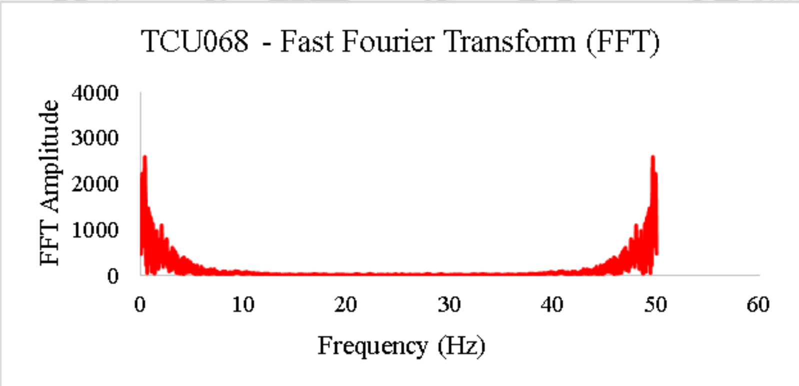

(b)

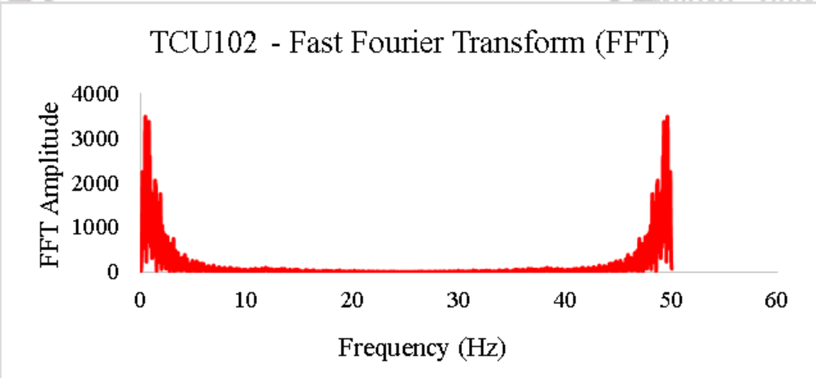

(c)

Figure 3. 23 Near Fault – Fast Fourier Transform (FFT) of (a). TCU052 (600 gal), (b). TCU068 (354 gal), (c). TCU102 (421 gal)

elongating the fundamental period of the bridge beyond the predominant periods of base motion. Due to there are two considerable periods that need to calculate carefully in order to avoid the resonance, here the structural frequency and earthquake frequency were calculated using Fast Fourier Transform (FFT) to make sure the resonance is not happen.

Figure 3.23 are the Fourier transform of the near fault earthquake as the loading system. It has been known that the structural natural frequency of the bridge is 1.857 sec. From the FFT analysis of the ground acceleration of the earthquake input, the seismicfrequency can be calculated. Then it can be found that the seismic frequency of TCU052 is 0.452 Hz, TCU068 is 0.378 Hz, and TCU102 is 0.415 Hz. It can be make sure that the resonance will not happen in this analysis, since the structural frequency of the bridge and the seismic frequency is far from close.

3.6 Earthquake Input

Chi-Chi earthquakes that happen in Taiwan on 1999 were considered as the near fault earthquake and El-Centro earthquake known as Imperial Valley earthquake that happen in Southern California in 1940 considered as the far fault earthquake. Furthermore, the main discussion is about the near fault earthquake analysis, then the far fault earthquake analysis considered only as the comparison result for the near fault earthquake analysis. These two ground motions have their own special characteristic and have been chosen due to their special behavior of the strong motion earthquakes. Three magnitude of Chi-Chi earthquake were normalized based on the design spectra analysis that will explain more in the next sub-chapter. Simplicity, 354 Gal, 421 Gal, and 600 Gal of ground motion PGA was considered in the analysis for both near and far fault earthquake ground motion.

3.6.1 Near Fault Earthquake

In the middle of the night about 1:47 am local time on September 21, 1999 there was large magnitude of earthquake in central western Taiwan, a severe earthquake that famously called Chi-Chi earthquake occur and caused thousand building collapsed, deaths, and about 20 billion USD of the total economic lost. Beside thousand building collapsed, another infrastructure such like power system, communication, water and wastewater system, gas system, railroads, dams, and tanks damaged due to Chi-Chi earthquake that happen in near Nantou City, Taiwan.

Based on tectonic map of Taiwan region that showed in figure 3.24, the collision of the Philippine sea plate into the Asian plate controlling the tectonics behavior of Taiwan, thus

Taiwan is categorized as part of the Ryukyu-Taiwan-Philippine arc system. Chilungpu fault is known as a major thrust fault in western of Taiwan, then Chi-Chi earthquake happened due to the rupture of Chilungpu fault as describe on figure 3.25 that the red line is the major fault of Chilungpu, and the epicenter of Chi-Chi earthquake occur on star point, its prove that Chi-Chi earthquake happen due to the activity of Chilungpu fault.

Taiwan government of Central Weather Bureau (CWB) predict that the epicenter of Chi-Chi earthquake was on Nantou City, and in hypocenter predict on 7 km of depth under the surface ground, because of this reason Chi-Chi earthquake is categorized as severe earthquake that estimated by the moment magnitude about M_w=7.7. Issue comes up toward engineering analysis about earthquake studies to consider about the estimation of ground motion in the particular location related with building construction, analysis about Chi-Chi earthquake related with the strong motion density measure about how much ground motion contribution can change as a function of the distance away from the nearest strong motion recording, (ASCE, 2000).

Three recorded strong motion of Chi-Chi earthquake proposed in this analysis to study about the dynamic analysis of the bridge model under the near fault earthquake as shown in 3.26 until figure 3.28, there are TCU052, TCU068, and TCU102. These three ground motion have each characteristic since this ground motion recorded in different locatio of the earthquake. ASCE in the textbook of lifeline performance of Chi-Chi earthquake 1999 that edited by Anshel et.al mentioned that TCU068 was located at the northern end of the rupture and have large velocity pulses due to the permanent movement of the fault (fling step) and were not due to rupture directivity effects such in Northridge earthquake in 1994 and Kobe earthquake in 1995.

special characteristic that showed in TCU102 need to be studied more, in case of there are two peak in this ground motion that made the structure under TCU102 is more sensitive in its peak ground acceleration (PGA). TCU052, TCU068, and TCU102 ground motions chosen due to their special characteristic of the Chi-Chi earthquake as near fault earthquake that happen, and some of them have large velocity pulses due to the fling attenuate faster with increasing distance to the fault than do large velocity pulses due to directivity effects.

special characteristic that showed in TCU102 need to be studied more, in case of there are two peak in this ground motion that made the structure under TCU102 is more sensitive in its peak ground acceleration (PGA). TCU052, TCU068, and TCU102 ground motions

chosen due to their special characteristic of the Chi-Chi earthquake as near fault earthquake that happen, and some of them have large velocity pulses due to the fling attenuate faster with increasing distance to the fault than do large velocity pulses due to directivity effects.

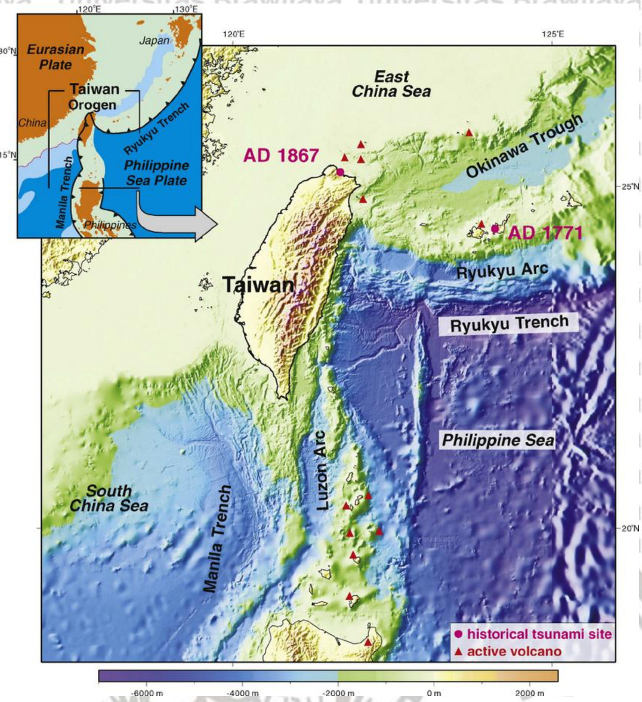

Figure 3. 24 Tectonic map of Taiwan, Taiwan lies on Ryukyu trench and Manila trench (www.researchgate.net)

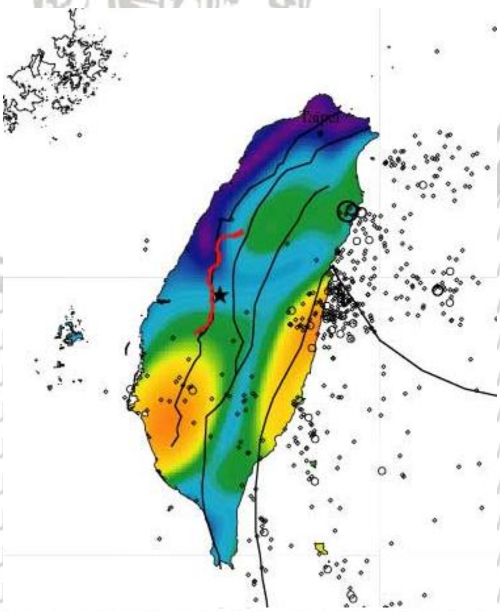

Figure 3. 25 Major fault in Taiwan, (www.eri.u-tokyo.ac.jp)

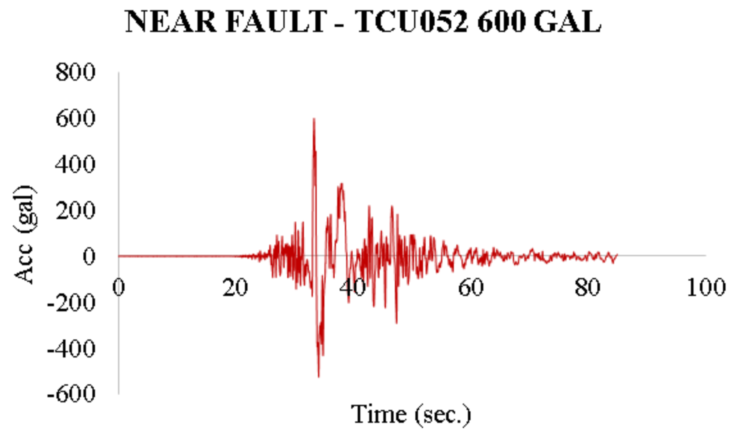

Figure 3. 26 Near fault TCU052 with peak ground acceleration 600.032 gal

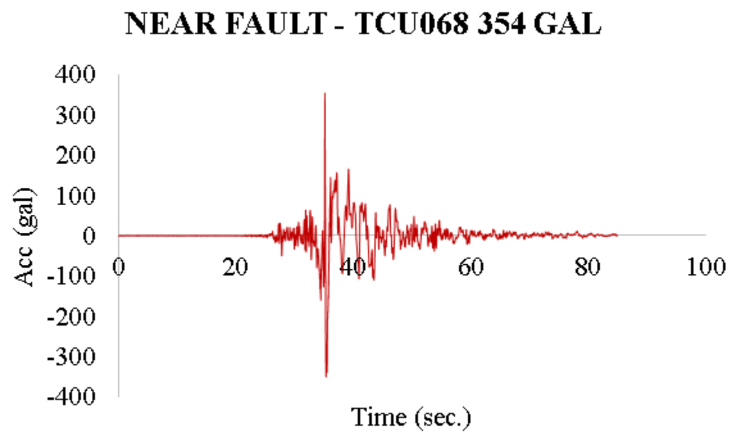

Figure 3. 27 Near fault TCU068 with peak ground acceleration 354.096 gal

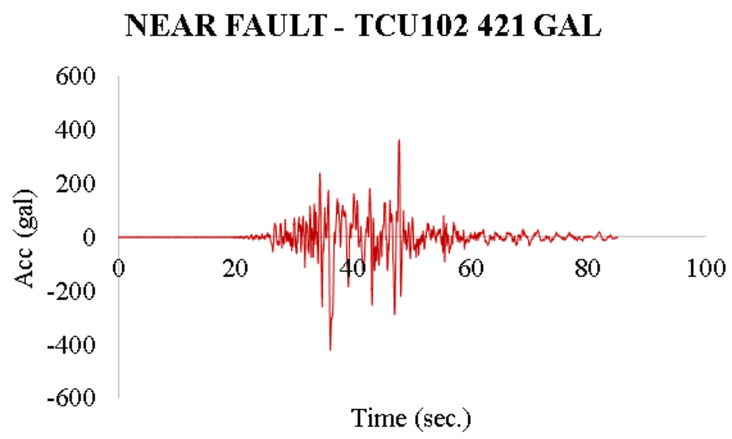

Figure 3. 28 Near fault TCU068 with peak ground acceleration 421.62 gal

TCU052, TCU068, and TCU102 were recorded in the same time yet different location. Based on ground motion pattern, TCU052 is the basic pattern of Chi-Chi earthquake, meanwhile TCU068 and TCU102 are special characteristic of Chi-Chi And x

3.6.2 Far Fault Earthquake

El-Centro ground motion was chosen as far fault earthquake. Far fault is minor analysis as comparing result of near fault analysis to find out the difference of bridge response especially for rubber bearing system behavior under near fault and far fault. Even though its acknowledge that the large velocity pulses in near fault are more localized to the near fault region than the previous research of directivity effect.

El-Centro earthquake that usually known as imperial valley occurred on 1940 in southern California, famously used in many research about dynamic activity of a structure since El-Centro earthquake is special characteristic of strong motion earthquake. Since far fault earthquake analyzed as comparison data, there are three normalized El-Centro ground motion ELX354, ELX421, and ELX600 that have same PGAs same as near fault earthquake. Figure 3.22 until figure 3.24 show far fault of El-Centro earthquake.

3.6.3 Design Spectra Analysis

Earthquake as a ground shaking is one of consideration in analyzing the response of structure since this is one of the most important application of the structural dynamic theory. Determining the peak response of system considering the site construction and the existing soil condition as part of response spectrum concept is the most important to determine the

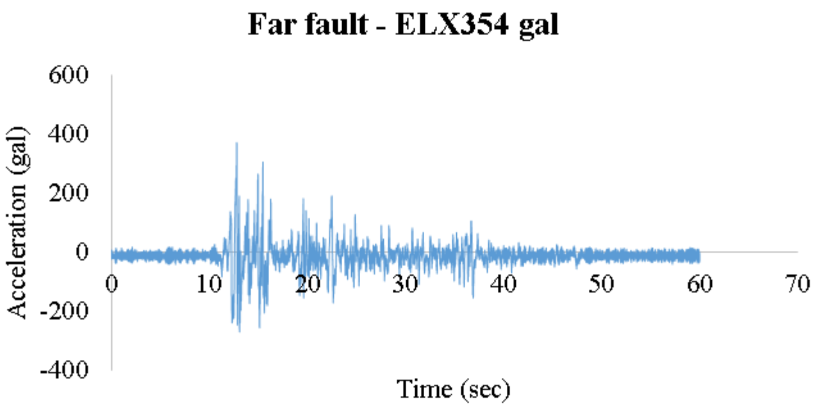

Figure 3. 29 Far fault of ELX354 with peak ground acceleration 354 gal

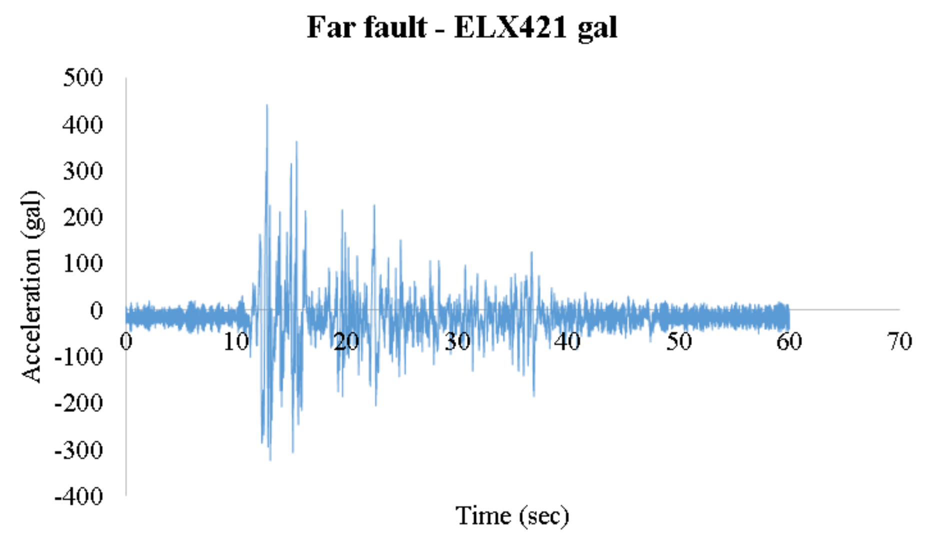

Figure 3. 30 Far fault of ELX421 with peak ground acceleration 421 gal

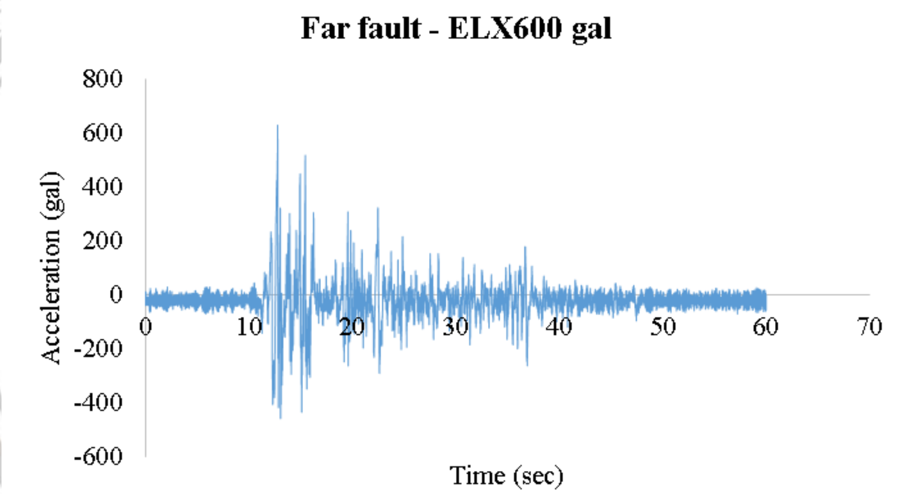

Figure 3. 31 Far fault of ELX600 with peak ground acceleration 600 gal

loading input, this chapter is further explanation of scaling method that used to determine the Peak Ground Acceleration of the near fault ground motion. Response spectrum determine as a plot of quantity response as a function of the natural frequency ω_n, natural period T_n, or cyclic frequency f_n for the fixed damping ratio ζ. Plot of response spectrum can be as deformation response spectrum u_0, relative velocity response spectrum $\dot{u}_0$, and $\ddot{u}_0{}^t$ as the acceleration response spectrum.

Based on equation of motion of single degree of freedom in eq. 3.3, gives the differential governing equation of free vibration system with damping:

$$m\ddot{u} + c\dot{u} + ku = 0 \qquad \textit{eq. 3. 20}$$

Dividing with m as a mass and damping coefficient $c = 2m\zeta\omega_n$ and acknowledge natural frequency $\omega_n = \sqrt{k/m}$ and subjected to ground acceleration $\ddot{u}_g(t)$:

$$\ddot{u} + 2\zeta\omega_n\dot{u} + \omega_n{}^2u = -\ddot{u}_g(t) \qquad \textit{eq. 3. 21}$$

Equation 3.29 shows that natural frequency $\omega_n$or natural period $T_n$of the system also damping ratio ζ contribute the deformation response u(t) for a given$\ddot{u}_g(t)$. Simply means that for two systems that have same values of ω_n and ζ shall have same deformation response u(t) although one of them is greater than the other one, also even though one system is stiffer than the other one. The system with light damping shall respond more than the system with larger damping, thus if there are several systems with the same of their natural period, their response will be similar for the time that required to complete a cycle of vibration and in peak time either maximum or minimum point, (Chopra, A., 2013).

In a structural analysis, equivalent static force preferred to choose since the building code specified the earthquake force relation, static force of f_s expressing k in terms of the mass m in the eq. 3.30:

$$f_s(t) = m\omega_n{}^2u(t) = mA(t) \qquad \textit{eq. 3. 22}$$

Simply means that:

$$A(t) = \omega_n{}^2u(t) \qquad \textit{eq. 3. 23}$$

This equivalent static force mentions A(t) as its pseudo-acceleration that multiply with m as mass. From the deformation response of the structure of u(t) is the basic response to calculate pseudo-acceleration A(t). Pseudo-acceleration is a plot of acceleration as a function of the natural period (Anil K. Chopra, 2014). Meanwhile the structure have the true acceleration $\ddot{u}_0{}^t$, pseudo-acceleration is undergoing acceleration of mass that associated with inertial force to calculate the base shear v_{b0}, related with eq. 3.30 then the value of base shear considered as:

$$v_{b0} = f_{s0} = mA \qquad \textit{eq. 3. 24}$$

With function of weight, then we get:

$$v_{b0} = {}^{A}/_{g} \cdot w \qquad \textit{eq. 3. 25}$$

Then $^{A}/_{g}$ represented base shear coefficient and used in building codes to interpret the obtain base shear that multiplied by the weight.

From the near fault ground motion of TCU052, TCU068, and TCU102. Take place the construction site is in Taichung city meanwhile Chi-Chi earthquake is a fault activity near Nantou county. Due to the site location and soil condition reason, design spectra of the original ground motion of TCU052, TCU068, and, TCU102 must be scaled to consider the existing condition of construction site. Figure 3.32 until figure 3.34 show the plot function of the response spectra of TCU052, TCU068, and TCU102 that normalized by the standard design spectra plot function of Taichung city, as mention before that the system that even though one system is larger than another one as long as the natural period and the damping ratio is the same, they will provide the same response, this concept applied to calculate the design spectra that in further these normalized ground motion shall be used as input of the ground motion data.

Response spectrum is the plot data of the original data as a function of accelerogram that had been filtering to be time history of the ground motion data as a function of the natural frequency or natural period, yet natural period is the preferred parameter that use as a response spectrum plot function. Related with equation 3.31, since the response of u(t) represent as D ($D \equiv u_0$), pseudo-acceleration function of the original ground motion A calculated from this equation:

$$A = \omega_n^{\,2} D = (2\pi/T_n)^2 D \qquad \textit{eq. 3. 26}$$

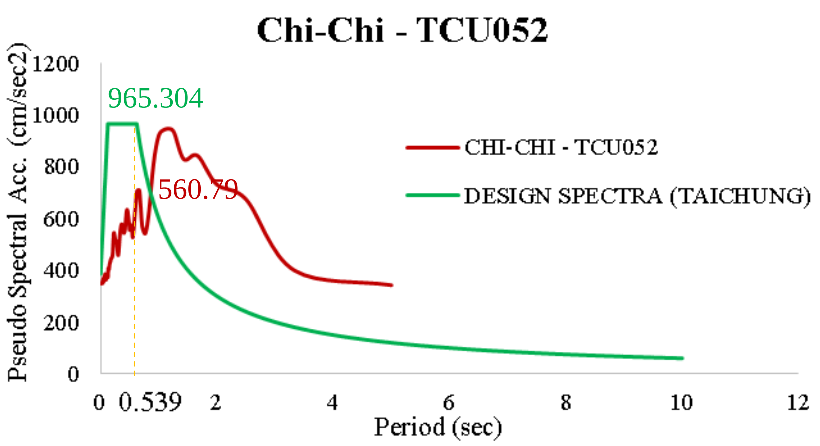

Figure 3. 32 Response spectrum design of TCU052

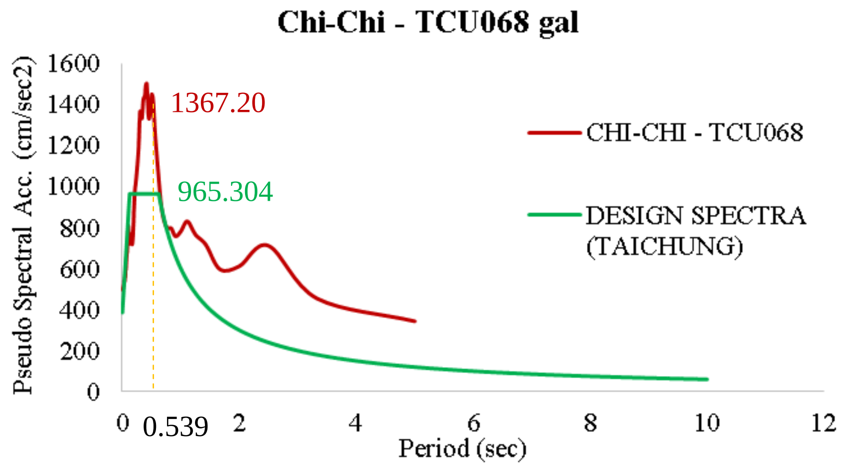

Figure 3. 33 Response spectrum design of TCU068

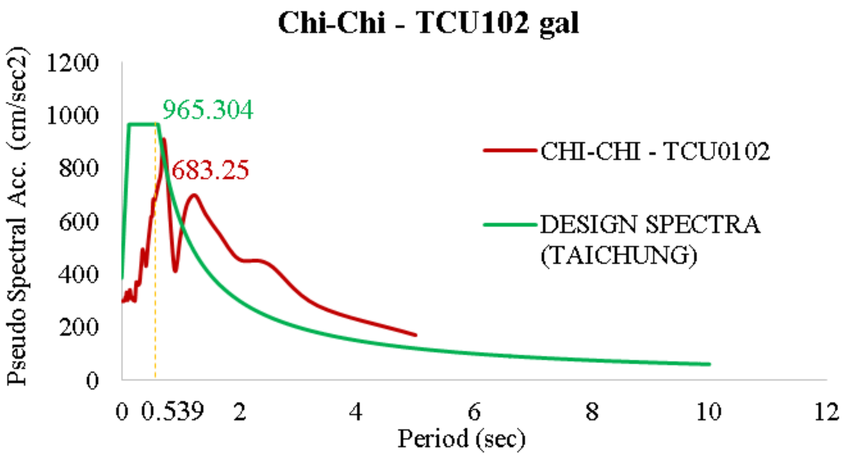

Figure 3. 34 Response spectrum design of TCU102

Since structure natural period is the important parameter that need to consider to normalized the ground motion using response spectrum concept, structural mass of the bridge model as shown in figure 3.20 associated with the stiffness equivalent of the structure as a relation of $\omega_n = \sqrt{k/m}$ and $T_n = 2\pi/\omega_n$ then the value of bridge structural natural period computed as large as 0.539 sec.

Standard design spectra that considering Taichung city as a site location, calculated using software of earthquake standard design that published by National Center Research of Earthquake and Engineering (NCREE) considering Taiwan building code. Response spectrum of the original ground motion TCU052, TCU068, and TCU102 plot merged with the standard design spectra based on Taiwan building code to find out how much scaling number that need to multiplied in original ground motion to calibrate based on the construction site condition. In a diagram of comparison between response spectrum design and standard design spectra, in a same value of structural period that computed as amount 0.539 sec, then the different value of pseudo-acceleration of both spectra can be found. Furthermore, the different value of pseudo-acceleration between response spectrum design and standard design spectra is the value of scaling that here in after used to scale the original ground motion to be normalized ground motion, then it can be calculated that the scaling factor of TCU052 is 1.721, TCU068 is 0.706, and TCU102 is 1.413.

3.7 Bearing System

Rubber bearing system carried out as seismic isolation system in a bridge shaking table test model related with functional bearing model (FBM) analysis. Rubber bearing is a conventional elastomeric bearing that consist of several layer of thin steel plates and rubber layer, steel material in rubber bearing system shall prohibit excessively deformation in rubber bearing itself. Following rubber bearing system of Liu et. al. in 2013, the physical looks of the rubber bearing system shown as figure 3.35.

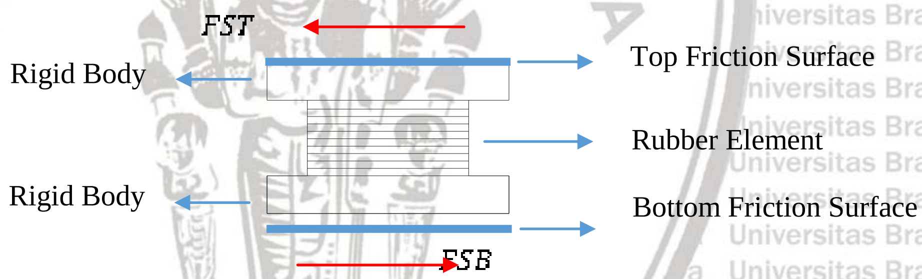

Figure 3. 35 Rubber bearing system

Generally, isolation system in a bridge designed to reduce the structural response with preventing the excessive displacement, same purpose proposed for this rubber bearing system. At the time when the earthquake happens, and the external force from the ground transmitted to the bridge structure, with applying rubber bearing instead, flexibility of the rubber bearing will reduce the strength capability of the structure to develop the loads and elongate the fundamental period of the structure beyond the predominant period of the earthquake, thus the base shear shall be reduced because of the energy dissipation capability of the rubber bearing system. As advance as the technology of the rubber bearing that applied, as effective as the rubber bearing capable to dissipate the energy.

Jangid RS. 2006, mention that isolation system shall be very important and vulnerable to consider in a structure near fault. With an unpredictability response of a structure under the near fault earthquake, applying rubber bearing system and analyzing using functional bearing model (FBM) analysis is a well consideration to improve the prediction of bridge response under the near fault earthquake. A proposed model of the rubber bearing system shown in figure 3.35, there is a rubber element consist of rubber and thin steel plates layer instead and covered by rigid body in the top and bottom side of it, and each outer surface is covered by friction layer and its variate based on the material of the surface roughness. Assume that the rubber has low horizontal stiffness K_R about 4.8 KN/cm and the rigid bodies are 1000xK_R its about 4800 KN/cm. And the rigid bodies made by concrete and with variation of surface roughness as the variation of coefficient of friction based on the design code and based on the experimental test that was done by Liu et.al.

3.7.1 Functional Bearing Model (FBM) and Link Definition

Functional bearing model is an element modeling assumption based on each element function of a rubber bearing system, associated with the purpose to calculate the contribution of the shear element of the rubber to prevent the sliding displacement and to calculate the rubber deformation independently, then a rubber bearing system divide into three links as top friction link of top rigid body, rubber link, and bottom friction link of bottom rigid body. Because there is very large stiffness close to the rigid of the rigid bodies, then the behavior of the first and third links are sliding due to the friction, and low stiffness of the rubber link shall provide pure deformation of the rubber bearing system. The functional bearing model (FBM) of the rubber bearing system shown in figure 3.36.

The analysis was done by SAP2000 software, single span bridge built with the section properties and material as mention in previous subchapter. Three springs of SAP2000 2 joint link created to assume each spring system, in further named Top Friction Link, Rubber Link, and Bottom Friction Link. Top Friction and Bottom Friction Link defined as multilinear plastic link with similar value of the stiffness K_{ST} and K_{SB} equal with 4800 KN/cm, horizontal x direction only. Meanwhile, Rubber Link defined as linear link with the value of K_{RB} is 4.8 KN/cm, also in horizontal x direction only.

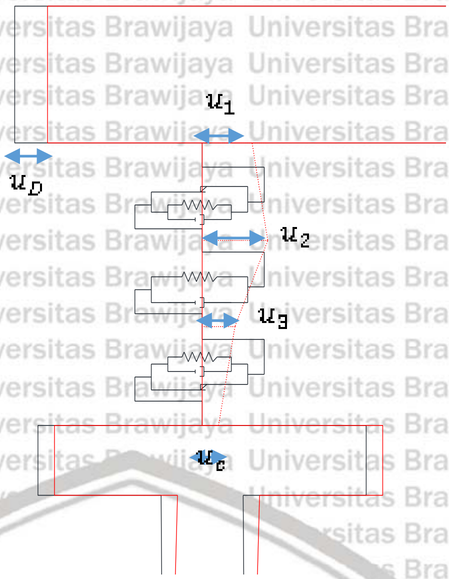

Figure 3. 36 Functional Bearing Model (FBM) assumption of the rubber bearing system

3.7.2 Non Linear Boundary Condition

Rubber link is the main element of the rubber bearing system, it working on linear. Linear link of rubber link that defined in SAP2000 modelling will keep the stiffness of the rubber bearing and behave linearly at any time. Consider K_R = 4.8 KN/cm and the Normal Force of the deck that transmitted into each column N_D is 32.42 KN.

Since the top friction link and bottom friction link defined as multilinear plastic link, boundary condition of non-linear parameter should be determined to limit the yield force and first plastic deformation, also to limit the ultimate value of shear force and maximum allowed deformation. Assume that the sliding will be happen right after rubber reach maximum shear force and plastic deformation, and it is make sure that the failure does not happen in the rubber because of the rubber maximum shear force and deformation are under the allowed maximum shear force and deformation based on building code. Define the value K_{SB} = K_{ST} = 4800 KN/cm and considering the normal force N_D = 32.42 KN. To define top friction link, μ_{ST} is the variation value of friction coefficient in the top friction interface that explain in subchapter 3.8, the $f_y = \mu_{ST}.N_D$, with the slope of K_{ST} then Δ_y can be defined, for the ultimate point, $f_y = f_u$ and maximum deformation is infinity since the deformation target is the maximum deformation response of the link under defined loading. Similar way to define bottom friction link, if μ_{SB} is the variation value of friction coefficient in the bottom friction interface, then the value of $f_y = \mu_{SB}.N_D$, with the slope of K_{SB} then Δ_y can be defined, for the ultimate point, $f_y = f_u$, maximum deformation is infinity.

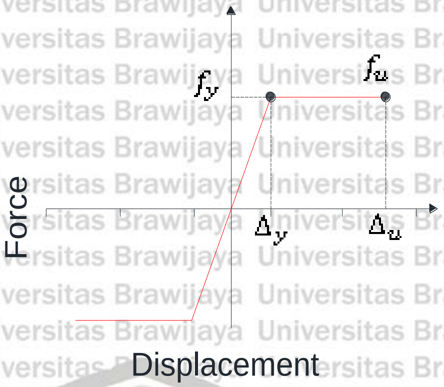

Figure 3. 37 Non-linear boundary condition of top and bottom friction links

3.8 Variation of the Coefficient of Friction

Chang, et. al., 2011 proposed the friction coefficient test of the friction system between rubber bearing pad and concrete. The friction coefficient is inversely proportional toward the sliding speed. The relation between the friction coefficient and the sliding speed will be close to the normal speed when the sliding speed is very high. As high as the sliding speed as wear as the sliding surface. Reaffirmed by Liu et. al., 2013, that the value of friction coefficient increased in line with increasing of the velocity and then saturated. There also mention that the bearing’s elastic deformation and sliding deformation cannot be separated. The relation shown in figure 3.38. The friction coefficient test that was done by Chang, et. al. present in table 3.4.

Take the concern on rubber bearing system and considering the sliding in the top and in the bottom interface of the rubber bearing, then the shear force that caused by the surface roughness become very important parameter that need to considered. Several value of coefficient of friction have been proposed. In his previous experimental model, Chang,et. al. expected the coefficient of friction value in range 0.35 - 0.5 as the result of friction coefficient test of the rubber pad and concrete layer. By inputting a reasonable coefficient of dynamic friction, the accuracy of dynamic analysis of the bridge should be improved. The coefficient is significantly higher than the standard recommended value of 0.15 and further

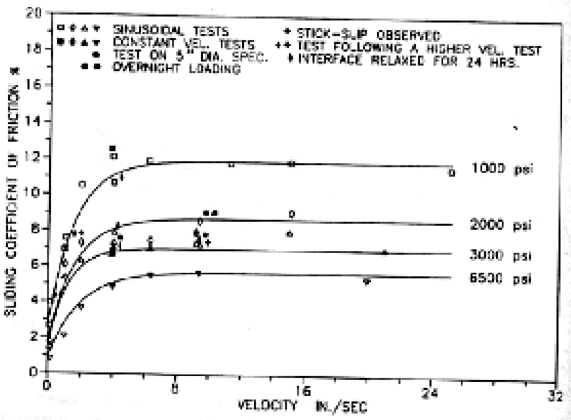

Figure 3. 38 Relationship between friction coefficient and the sliding velocity, (Chang, et. al., 2011).

Table 3. 3 Friction coefficient test result. (Chang, et. al., 2011)

Group	Force (MPa)	Velocity (mm/s)	Shape system	Friction coefficient
01	2.25	1.06	3.75	0.500
02	2.49	60	3.75	0.456
03	2.38	120	3.75	0.364
04	2.12	240	3.75	0.310
05	4.06	1.06	3.75	0.269
06	4.43	60	3.75	0.223
07	4.61	120	3.75	0.209
08	4.35	240	3.75	0.153
09	6.88	1.06	3.75	0.217
10	6.44	60	3.75	0.150
11	6.75	120	3.75	0.152
12	6.73	240	3.75	0.115

Table 3. 4 Case details based on variation of coefficient of friction

Case A : Design Code - Based			
Friction Link	Friction coefficient		
Case	A1	A2	A4
Top Link	0.2	0.2	0.4
Bottom Link	0.2	0.4	0.4
Case B : Experimental - Based			
Case	B1	B2	B4
Top Link	0.35	0.35	0.5
Bottom Link	0.35	0.5	0.5

research need to reviewed more, (Liu, 2013). This is the fundamental explanation of coefficient of friction 0.35 is different 0.15 from design code that require the coefficient value about 0,2 – 0.4.

Friction force as a function of normal force and static/kinematic coefficient of friction as in eq. 3.7 shall be the important parameter to consider the sliding time and sliding distance, since the normal force is a constant value, then variation of coefficient of friction need to study more to find out the value of coefficient of friction that relevant to apply in a structure based on material friction. Here is proposed several value of coefficient of friction based on experimental test that was done by Liu on 2013 and several friction coefficient value based on design code as shown in table 3.5. As reminder that friction coefficient owned by top link is μ_{ST} and for the bottom link is μ_{SB}.

3.9 System Analysis

Analysis was done in 2 Dimension analysis of SAP2000 of a shaking table test model all direction of motion defined on global x direction based on sap2000 axis definition, considering dead load of the bridge and earthquake excitation loading.

3.9.1 Loading Definition and Loading Case

Bridge analysis considering the dead load that already include the additional load of the vehicle, secondary load is several earthquake loading that mention before in earthquake input. Dead load and additional vehicle load assigned as a frame with uniform density and section properties. Meanwhile, earthquake loading defined as time history loading with scaling factor value as the result of normalization of the design spectra based on site and soil condition that explained before in sub chapter of design spectra.

Direct integration was chosen as non-linear method since direct integration provide more accurate calculation than modal analysis. Since the column of the bridge model is short column, then p-delta effect did not consider in this analysis. With the earthquake duration is 85 second for the near fault earthquake and 60 second for the far fault earthquake, time step convergence analysis was done before in order to get more accurate result of the integration, based on the maximum time integration that provide steady response, integration was done with the time step 0.005 second.

Time integration method shall be the important parameter of SAP2000 analysis, Newmark's method was chosen since this method is family of single step, which mean each step is treated independently and step size Δ_t can be changed at any time. And Newmark's method categorized as implicit method which mean the equation of motion establish at i+1 and capable in large step size considering small value of the time step, thus make Newmark's method capable in longer calculation time and more accurate. Newmark's method also was chosen since this method available for both linear and non-linear analysis.

Damping system calculated and defined using Rayleigh damping. Rayleigh damping is one type of the classical damping that consider mass proportional damping and stiffness proportional damping as:

$$c = a_0\boldsymbol{m} + a_1\boldsymbol{k} \qquad \textit{eq. 3. 27}$$

With the damping ratio:

$$\zeta_n = \frac{a_0}{2}\frac{1}{\omega_n} + \frac{a_1}{2}\omega_n \qquad \textit{eq. 3. 28}$$

Since Rayleigh damping depend on the damping ratio and the frequency in mode i and j:

$$\frac{1}{2}\begin{bmatrix} 1/\omega_i & \omega_i \\ 1/\omega_j & \omega_j \end{bmatrix}\begin{bmatrix} a_0 \\ a_1 \end{bmatrix} = \begin{bmatrix} \zeta_i \\ \zeta_j \end{bmatrix} \qquad \textit{eq. 3. 29}$$

Mode i and mode j is the first and second dominant mode of modal participating mass ratio, it is known $T_i = 0.5385$ second and $T_j = 0.0104$ second and with $\zeta_n = 0.05$ then Rayleigh damping was considered in the system analysis.

CHAPTER IV – NUMERICAL ANALYSIS: VARIATION OF FRICTION COEFFICIENT EFFECT ON FUNCTIONAL BEARING MODEL (FBM) ANALYSIS

4.1 Case Details

First objectives of this research is to study the variation of coefficient of friction that applied in the top and bottom surface friction of the rubber bearing system. Friction surface on the rubber bearing system that shown in figure 3.31 depend on the material friction that lied on both of it. Top friction surface is the friction element that connect the rubber bearing system with the deck, bottom friction surface is the friction element that connect the rubber bearing system with the column. The friction surface material may be different with the column or deck, also may be the same. Friction force happen due to the contact surface between two elements due to the different material between two surface, friction coefficient is the dimensionless value as representation of the surface roughness that will provide friction force, since friction force direction is the opposite with the motion, then the existing of friction force shall prohibit the motion. And the friction material surface in the top and the bottom side may be the same or may be different.

Since friction surface of the rubber bearing system is made from Poly Tetra Fluoro Ethylene (PTFE) layer. Applying variation of friction coefficient in rubber bearing system shall provide the information about the effective material of PTFE, take a range value of 0.2-0.4 based on the design coda and increase 0.15 higher than the design code at range 0.35-0.5 based on experimental test.

Case details in this study are based on table 3.3 that is based on the variation of friction coefficient in the top and bottom interface. If the μ_{ST} is the coefficient of friction value in the top surface and μ_{SB} is the coefficient of friction value in the bottom surface, thus there are six case proposed:

Based on the design code

Case A1: applying same value of friction coefficient both in the top and bottom interface,

$\mu_{ST} = 0.2$ and $\mu_{SB} = 0.2$.

Case A2: applying larger value of friction coefficient in the bottom interface,

$\mu_{ST} = 0.2$ and $\mu_{SB} = 0.4$.

Case A4: applying same value of friction coefficient in both interface but larger than case A1, $\mu_{ST} = 0.4$ and $\mu_{SB} = 0.4$

Based on the experimental test

Case B1: applying same value of friction coefficient both in the top and bottom interface, $\mu_{ST} = 0.35$ and $\mu_{SB} = 0.35$.

Case B2: applying larger value of friction coefficient in the bottom interface, $\mu_{ST} = 0.35$ and $\mu_{SB} = 0.5$.

Case B4: applying same value of friction coefficient in both interface but larger than case B1, $\mu_{ST} = 0.5$ and $\mu_{SB} = 0.5$

4.2 Near Fault Analysis

4.2.1 Duration of the Peak Response

Each combination of friction coefficient in the rubber bearing provide the different structure response. There is time sequence of the peak response in each case, which mean there are time delayed in one case to reach the maximum response compare with another. The time reference analyzed at the time when the maximum sliding of the top friction surface, maximum deformation of the rubber bearing itself, maximum sliding of the bottom friction surface, and at the time when peak ground acceleration happens. As shown on table 4.1 until 4.4, there mention that in a different case under the different earthquake input, the maximum response of an element also different. Variation of the time when the maximum response happen is due to the variation of the friction coefficient. Remember that increasing the value of friction coefficient will be increasing the roughness friction surface, variation of friction coefficient configuration between top and the bottom friction surface will more affected on a structure response in a different case under different earthquakes. This time difference is the beginning assumption of there are some effect related with the variation of friction coefficient in the link configuration.

Table 4. 1 Near fault - time table of the maximum sliding displacement of top friction surface

CASE	TIME REFERENCE (SEC)		
	TCU068	TCU102	TCU052
A1	35.775	47.27	33.755
A2	35.765	47.265	33.74
A4	35.71	48.335	33.585
B1	35.72	47.205	33.625
B2	35.725	48.345	33.61
B4	35.69	48.315	33.54

Table 4. 2 Near fault - time table of the maximum deformation of the rubber

Case	Time reference (sec)		
	TCU068	**TCU102**	**TCU052**
A1	35.58	36.18	33.405
A2	35.58	36.18	33.395
A4	35.58	48.235	33.39
B1	35.58	48.24	33.39
B2	35.58	48.235	33.385
B4	35.585	48.235	33.385

Table 4. 3 Near fault - time table of the maximum sliding displacement of the bottom friction surface

Case	Time reference (sec)		
	TCU068	**TCU102**	**TCU052**
A1	35.775	47.27	33.755
A2	35.69	48.31	33.585
A4	35.71	48.335	33.585
B1	35.72	47.205	33.625
B2	35.68	48.305	33.54
B4	35.69	48.315	33.54

Table 4. 4 Near fault - time table of the maximum peak ground acceleration of the earthquake input

Case	Time reference (sec)		
	TCU068	**TCU102**	**TCU052**
A1	35.18	36.115	33.33
A2	35.18	36.115	33.33
A4	35.18	36.115	33.33
B1	35.18	36.115	33.33
B2	35.18	36.115	33.33
B4	35.18	36.115	33.33

4.2.2 Displacement Contribution

Rubber bearing system as the main target of the study about functional bearing take an important part to be analyzed. Rubber bearing system that consist of rubber bearing element that will absorb the energy with the restoring capability of its low stiffness, also top and bottom friction surface that will absorb the energy excess from the rubber element with the sliding capability of the friction surface that capable to limit the motion. With modeling the rubber bearing system using functional bearing model (FBM) is clearly explain the contribution of each element of the rubber bearing system. Under the design spectra normalized ground motion of TCU068 (354 gal), TCU102 (421 gal), and TCU052 (600 gal), if the time when the rubber deformed in maximum consider as the reference time to take a data for another element as in table 4.2, then the percentage of the displacement contribution as the result of the total structure displacement shows in figure 4.1 until figure 4.3.

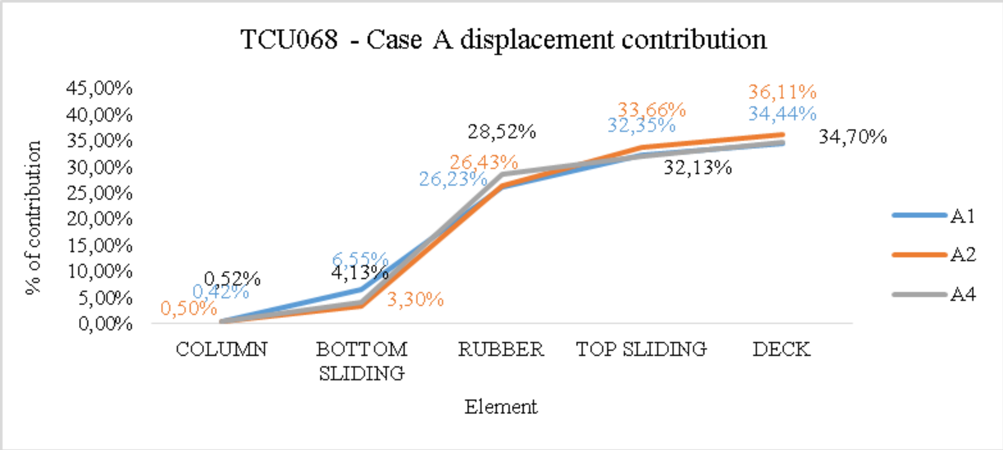

(a)

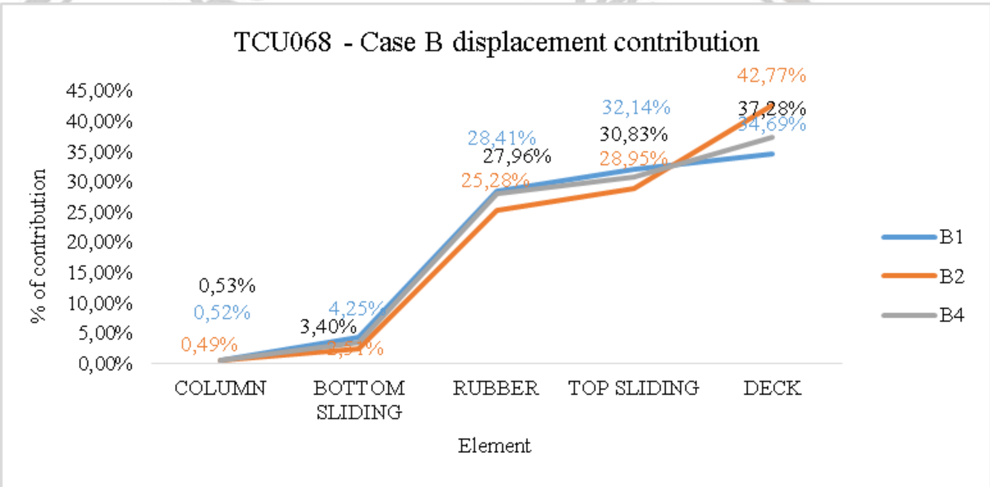

(b)

Figure 4. 1 TCU068 - 354 gal, (a) Displacement contribution of the case A, (b) Displacement contribution of the case B

Figure 4.1 until figure 4.3 explain that the structure both in case A and case B under near fault ground motion have similar pattern of element displacement contribution. Column always give small contribution of displacement compare with another element, and a deck displacement always larger than another. Simply means that under different near fault earthquake, column contribute the smallest displacement, then the slope of incremental percentage of the rubber deformation is sharper than other which mean that the rubber absorbs more energy, and the left over energy absorbed by the sliding surface in the top and the bottom friction surface. Top sliding surface displaced more than the bottom sliding surface, it is found that the sliding in the top is more dominant than the sliding in the bottom.

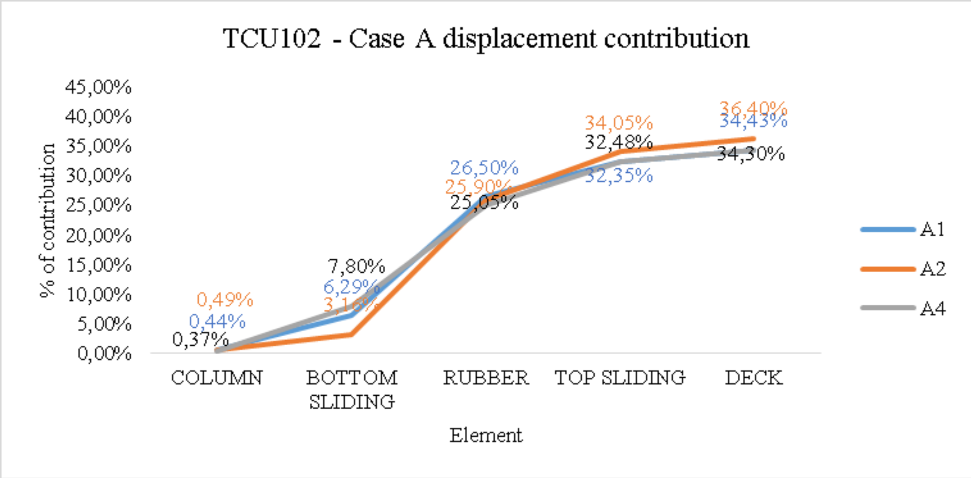

(a)

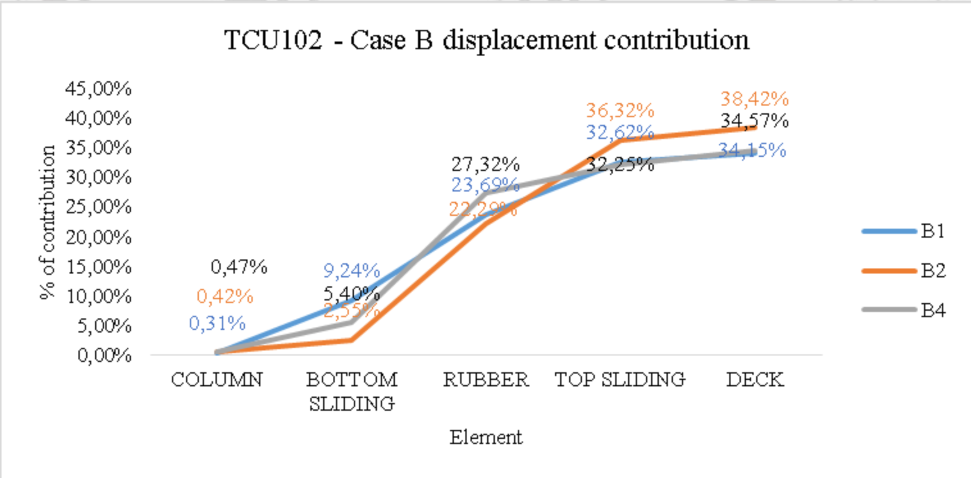

(b)

Figure 4. 2 TCU102 – 421 gal, (a) Displacement contribution of the case A, (b) Displacement contribution of the case B

Case A is applying value of friction coefficient based on the design code and case B is based on the experimental test. Under the smallest PGA of the near fault TCU068 (354 gal), applying different value or different combination of friction coefficient give small effect in element displacement in case A. But increasing friction coefficient become 0.35-0.5 in case B, effect on the deck displacement. In figure 4.1 (b) Orange line of B2 is the different combination of friction coefficient in the top and bottom surface, case B2 provide smaller displacement percentage than the other case in column, bottom sliding surface, rubber deformation, and top sliding surface, but B2 provide the largest displacement on the deck.

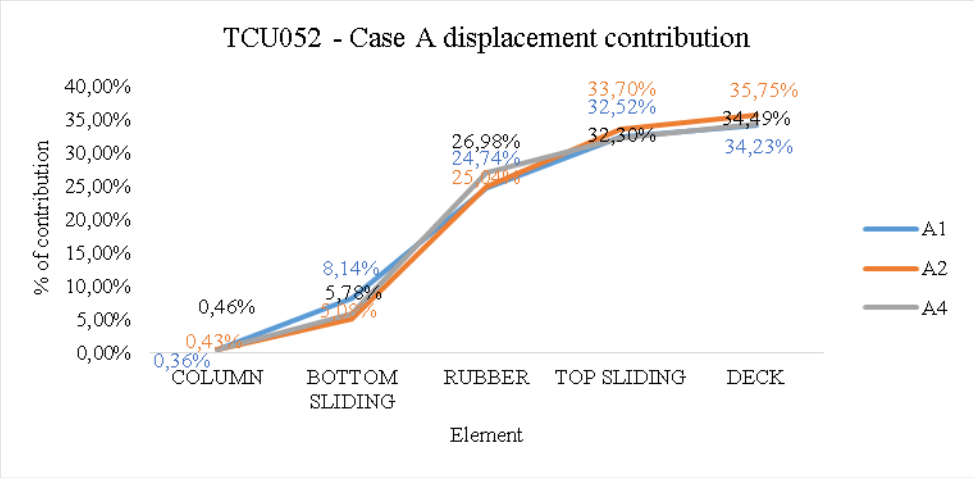

(a)

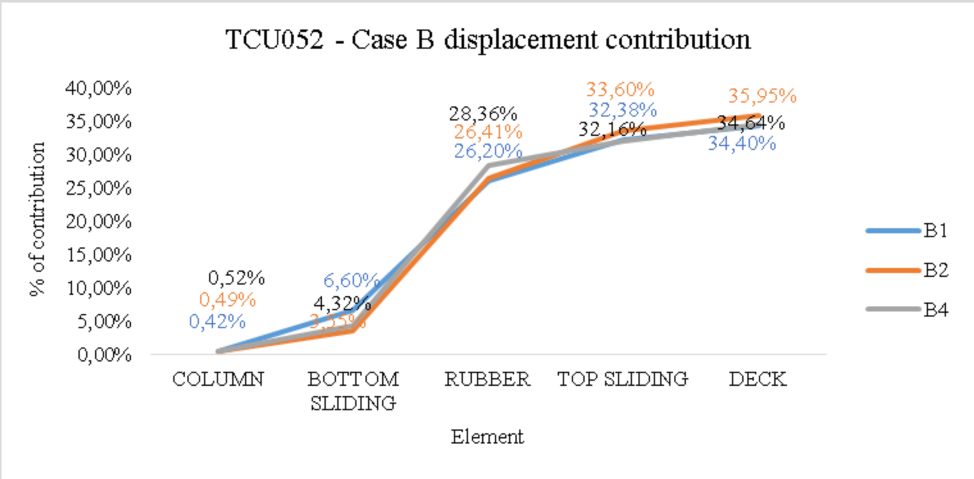

(b)

Figure 4. 3 TCU052 – 600 gal, (a) Displacement contribution of the case A, (b) Displacement contribution of the case B

Meanwhile, in case B1 and B4 there are a little different between them, and for the final displacement of the deck, B4 provide larger deck displacement than B1, it is due to increasing the value of friction coefficient make the friction surface more rigid and not easy to slip. B1 have the smallest value of friction coefficient than B4, its mean that the sliding surfaces of B1 are more flexible to move than B4, due to this reason the sliding surfaces of B1 shall work better than B4, thus the energy that transferred to the deck can be decrease and the displacement shall be decrease also.

Increase the loading under the middle PGA of the near fault TCU102 (421 gal). Displacement behavior of the case A under TCU102 (421 gal) is similar with case B under

TCU068 (354 gal), yet the difference show in case B. Case B1 under TCU102 produce more bottom sliding displacement than B2 and B4, but B4 produce more top sliding displacement than B1 and B2, its mean that in the same configuration value of friction coefficient, smaller value of friction coefficient contribute more in the bottom sliding surface, yet the larger value of friction coefficient contribute more in the top sliding surface. And the difference configuration value of friction coefficient value in top and the bottom sliding surface produce smallest sliding in the bottom surface but highest displacement on the top sliding surface and deck. A significant effect shows in the near fault TCU102.

In the largest PGA of the near fault TCU058 (600 gal), all behavior in case A and case B is similar, yet still A1 and B1 provide large deck displacement than another. It is look like increasing or varying friction coefficient give small effect in structural behavior, it may be friction coefficient will give small effect in 600 gal of the near fault earthquake.

4.2.3 Energy Absorptions

Energy dissipation calculated from the cyclic area of non-linear relation between displacement and force of the top and bottom friction link as representation of the top and bottom sliding surface. In order to design the rubber bearing system which effectively dissipate the energy that transmitted to the structure, variation of friction coefficient was proposed to find out which configuration that better to apply in a structure. In range value of 0.2-0.4 of case A and in range value of 0.35-0.5 of case B, both under three input of the near fault ground motion, the energy dissipation capability of each configuration shall be studied. Under TCU068, TCU102, and TCU052, figure 4.4 (a) and (b) shows the total energy dissipation capability of each configuration both in case A and case B.

In figure 4.4, the blue line is the energy dissipation under TCU068 (354 gal), the orange line is the energy dissipation under TCU102 (421 gal), and grey line is under TCU052 (600 gal). The result of blue line always smaller than another line it shows that the energy that need to provide is small since TCU068 is the smallest PGA. And the grey line is one level above the blue line, since TCU052 is larger than TCU068. But the orange line shows a special behavior, even though TCU102 is not under the largest PGA, but the energy that need to provide under TCU068 is the largest.

Related with the pattern of the ground motion of TCU052 (600 gal), TCU068 (354 gal), and TCU102 (421 gal) in figure 3.22 until figure 3.24, these three ground motion was taken under the same earthquake, that is Chi-Chi Earthquake in 1999 but in different location.

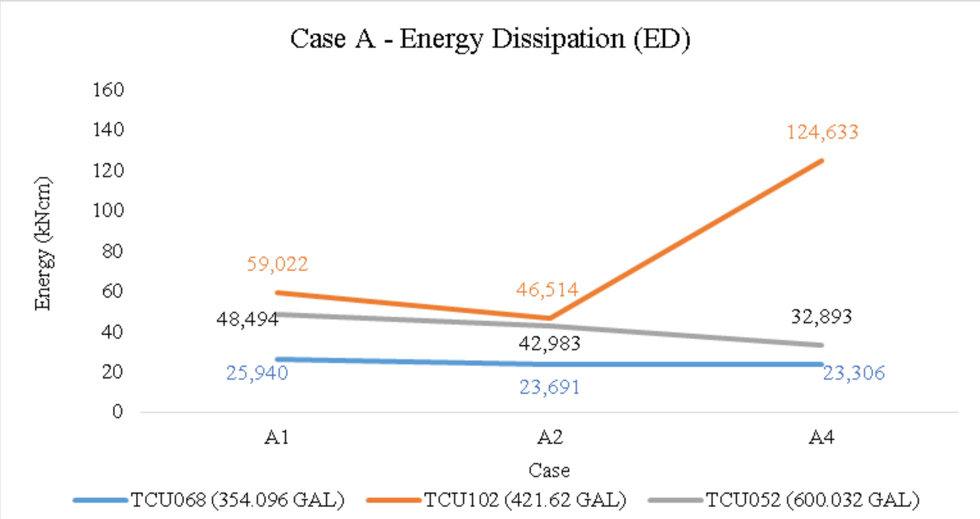

(a)

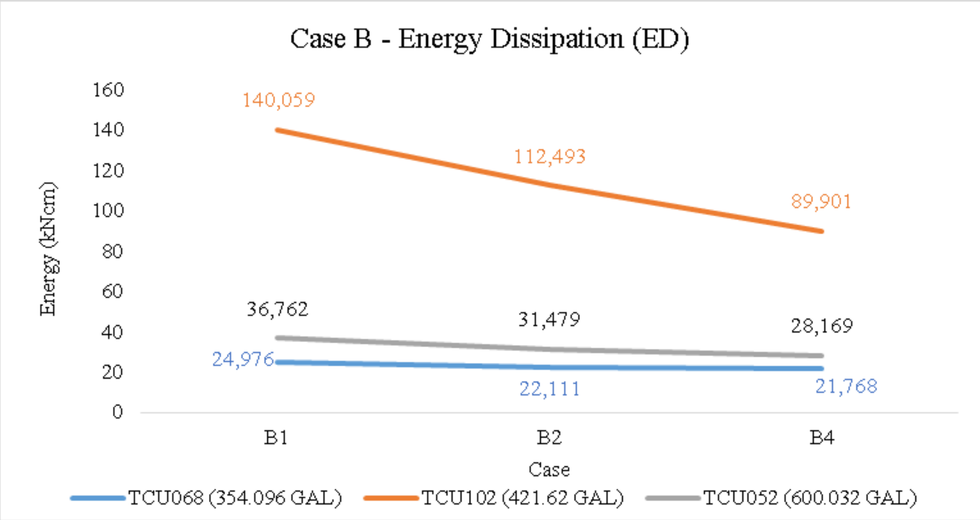

(b)

Figure 4. 4 Near fault - (a) Energy Dissipation of case A, (b) Energy Dissipation of case B

TCU 068 and TCU052 have one peak dominant, this is the presumption of a structure under TCU068 and TCU052 will have similar behavior, yet under the different PGA. But for TCU102 that shows in figure 3.24, there are two peak dominants that make the structure under TCU102 is more sensitive and the structural behavior is different with other. With this reason, the structure releases more energy under TCU102.

Previous study explain the energy dissipation capability based on input of the ground motion. Under the same ground motion, variation of friction coefficient give contributions to decrease the energy. Figure 4.4 (a), under the same characteristic of TCU068 and TCU052 increasing the value of friction force from A1 to A4 will be reduce the energy dissipation capability. Since A1 have smaller friction coefficient than A4, then increasing the coefficient of friction value will be decreasing the energy dissipating capability, similar behavior for case B in figure 4.4 (b).

In a special case under TCU102, different result of increasing friction coefficient happens in case A and case B. in case A, applied different value of friction coefficient on the top and the bottom friction surface give a big impact. As shown in figure 4.4 (a), the energy dissipated from A1 will be decrease if the friction coefficient configured in different value as in A2, and will be largely increase in the same configuration but in larger value of friction coefficient as in A4. Which means that under the ground motion TCU102, applying different value of friction coefficient will be decrease the energy dissipating capability of the structure. Opposite result happens in case B under TCU102, increasing value of friction force caused decreasing energy, and applying different value of friction force in the top and bottom friction surface is decrease less than applying the same larger value in both surface.

Overall, under TCU068 and TCU052, increasing friction coefficient value will be decreasing the energy dissipation capability. Under TCU102, in the small value of friction coefficient of case A, increasing friction coefficient value will be increasing the energy, but in the larger value of friction coefficient in case B, increasing friction coefficient value will be decreasing the energy dissipation capability.

Strain energy considered as the energy contribution of the rubber. Due to the excitation energy that transmitted to the rubber bearing system firstly shall be overcame by the rubber, after rubber reach its maximum capacity, then the excessive energy will be transmitted to the friction surface. If the total energy absorption by the rubber bearing system is E, then the strain energy that provide by the rubber is E_S, and the surface friction will be contribute the energy dissipation E_D.

$$E = E_S + E_D \qquad \text{Eq. 4. 1}$$

Rubber bearing assumed to behave linear, so that the maximum deformation of the rubber is on allowed deformation. Strain energy calculated from the area under the linear curve of the rubber link. Strain energy equal to the potential energy of the spring. The definition of the strain energy and energy dissipation describe on figure 4.5. The energy dissipation curve that mention in figure 4.4 is the energy that contributed by the friction surface in the top and in the bottom. Then figure 4.6 is the strain energy that was done by the rubber.

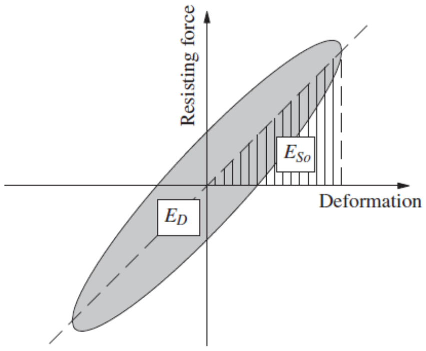

Figure 4. 5 Definition of energy loss E_D in a cycle of harmonic vibration and maximum Strain Energy E_{S0}, (Chopra, A.,K., 2014)

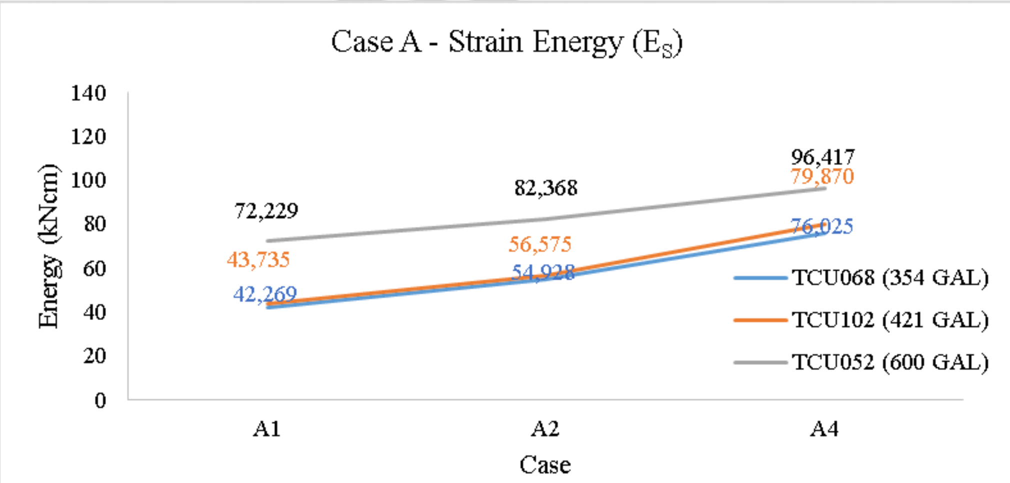

(a)

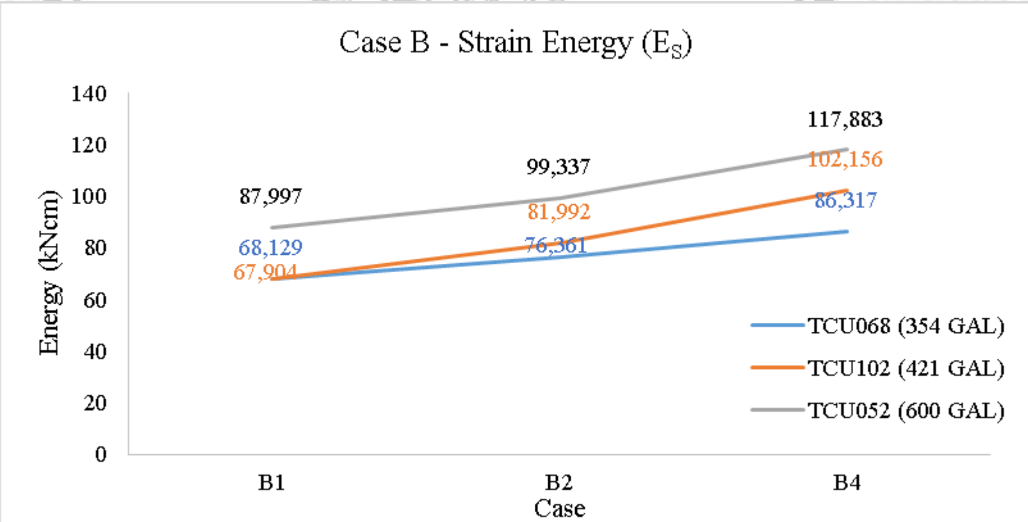

(b)

Figure 4. 6 Near fault - (a) Strain Energy of case A, (b) Strain Energy of case B

If the input energy that transmitted to the bridge is E_I, then the percentage of total energy absorption calculate using Eq. 4.2. and the result shown in figure 4.7.

$$\%\ Energy\ Absorption = \frac{E}{E_I} x100\% \qquad \textit{Eq. 4. 2}$$

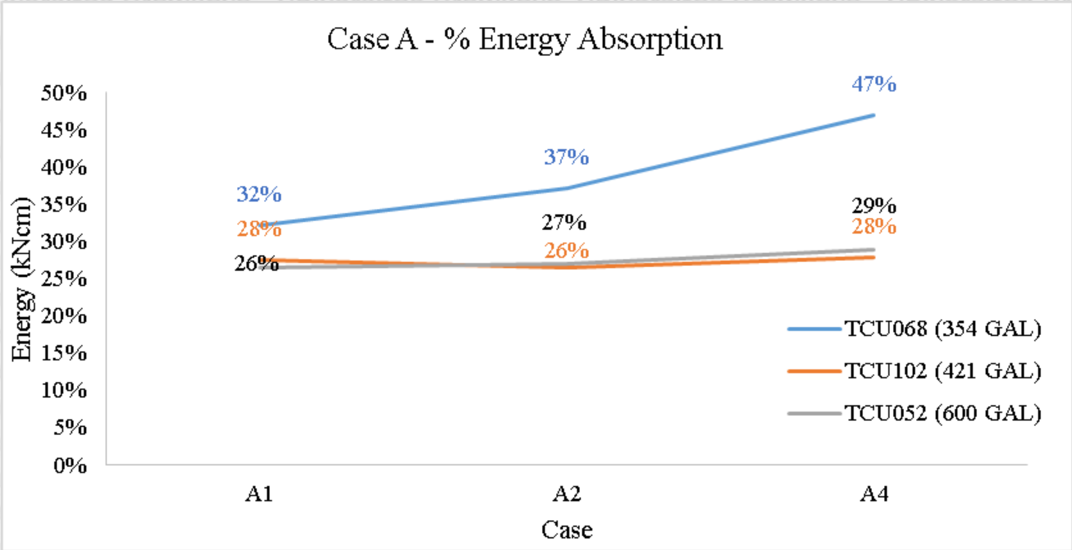

(a)

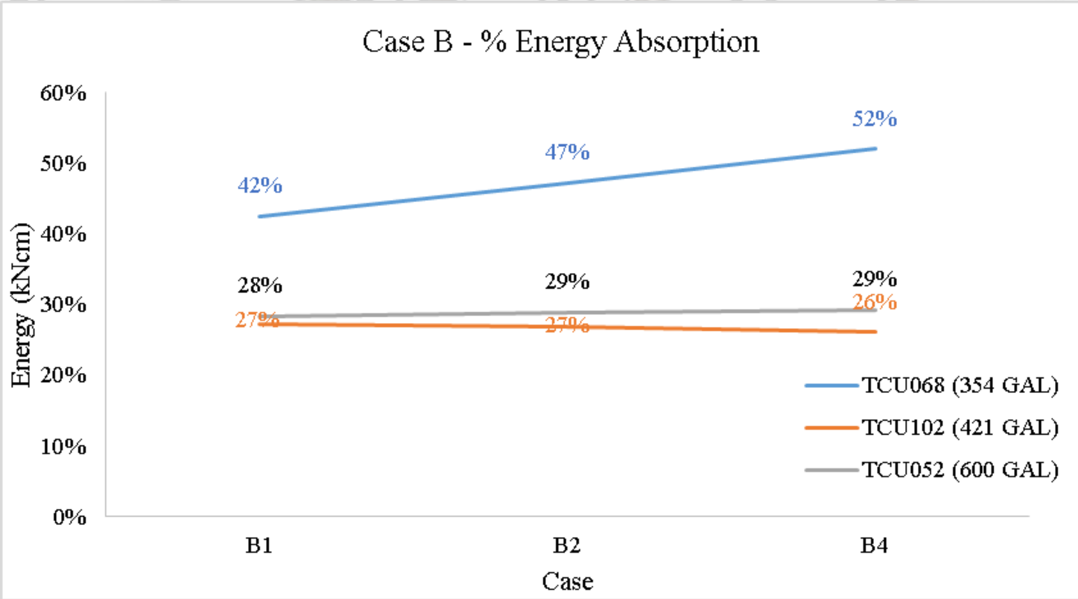

(b)

Figure 4. 7 Near fault, (a). Percentage of Energy Absorption of case A, (b). Percentage of Energy Absorption of case B

4.2.4 Friction Element Contribution

Since the deck, column, and the rubber bearing only allowed to behave in linear, then the energy dissipation calculated from the nonlinear cycle that provided by top and bottom friction surface. Since there are top and bottom friction surface that will absorb the excess energy, all the excess energy from the rubber shall be transmitted to the top surface and bottom surface friction right after rubber reach the limit. Figure 4.8 until 4.10 shows the contribution of the top friction surface and bottom friction surface in case of absorbing the excess energy.

The excessive energy of the rubber element transmitted toward the top and the bottom friction surface, and applying friction coefficient equally or differently in the top and bottom surface can be observe by the percentage energy relation of both friction surface. Figure 4.8 shows the relation of case A and case B under the smallest PGA of the ground motion TCU068 (354 gal), figure 4.9 is under the special ground motion of TCU102 (421 gal), and figure 4.10 is under the largest PGA of the ground motion TCU052 (600 gal). Overall result explained that in the same configuration such in case A1, A4, B1, and B4, the energy will be transmitted equally as amount of 50% each on the top friction surface and bottom friction surface.

In the different configuration of friction coefficient such in case A2 and B2, the energy shall be handled more by the top friction surface, it is due to the smaller value of friction coefficient applied on the top friction surface that make the surface easier to give a movement.

Related with the ground motion, comparing TCU068 (354 gal) and TCU052 (600 gal), even though TCU052 much larger than TCU068, but the energy that transmitted to the top and bottom friction surface in case A2 and B2 is almost the same. And for the special ground motion of TCU102 (421 gal), even though the PGA is not the largest, but the energy transmitted to the top and bottom friction surface is the largest than the other. Which means, that variation of friction coefficient in rubber bearing system under the near fault earthquake is not depend on the magnitude of the earthquake ground motion, but it is depend on the characteristic of the near fault ground motion.

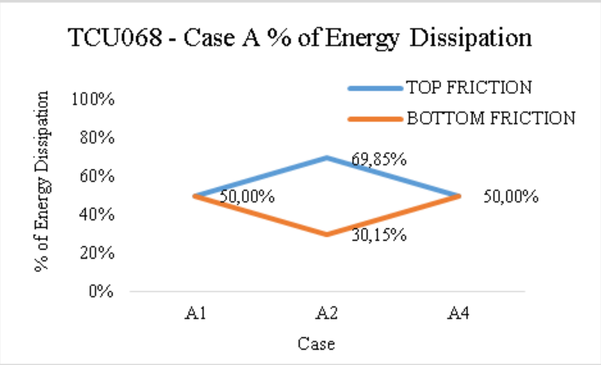

(a)

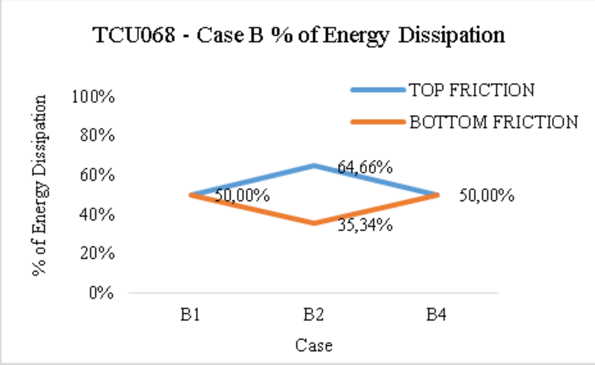

(b)

Figure 4. 8 TCU068 – 354 gal, (a) Energy Dissipation of the friction surface in case A, (b) Energy Dissipation of friction surface in case B

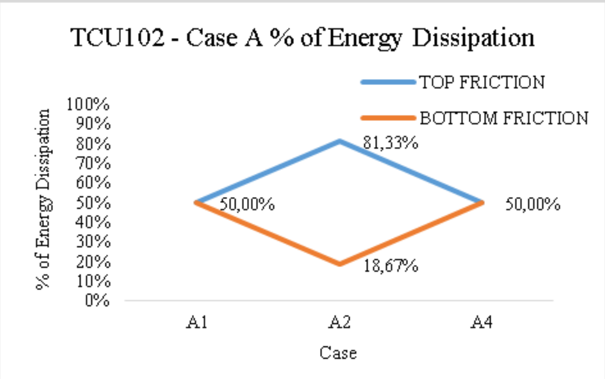

(a)

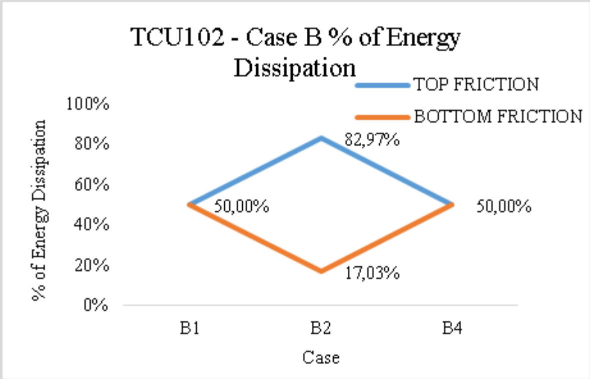

(b)

Figure 4. 9TCU102 – 421 gal, (a) Energy Dissipation of the friction surface in case A, (b) Energy Dissipation of friction surface in case B

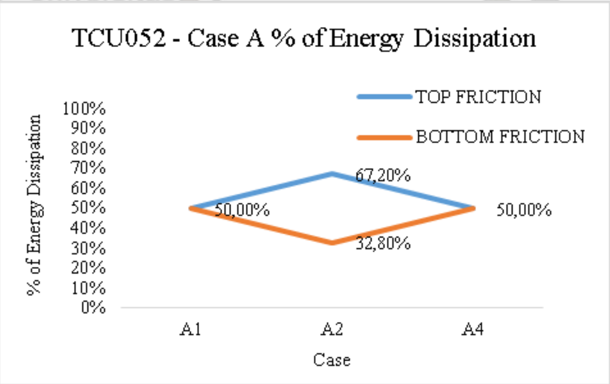

(a)

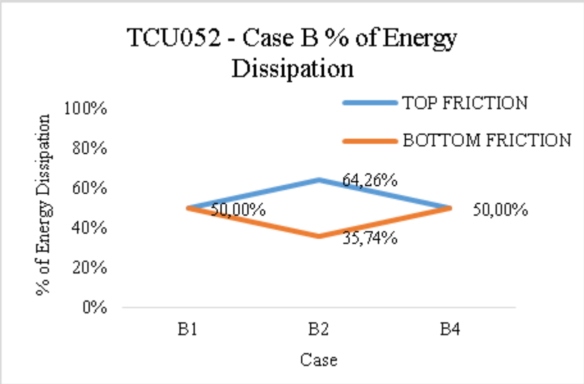

(b)

Figure 4. 10TCU102 – 421 gal, (a) Energy Dissipation of the friction surface in case A, (b) Energy Dissipation of friction surface in case B

4.3 Far Fault Analysis

4.3.1 Duration of the Peak Response

As the comparison result of the near fault that studied before, here is the analysis of the same model under far fault earthquake of El-Centro 1940. Time duration also studied in order to compare the time duration of the near fault earthquake. Table 4.5 is the time table when the top friction surface reached the maximum sliding, table 4.6 is the time table when the rubber deformed in maximum, table 4.7 is the time table when the bottom friction surface sliding in maximum, and table 4.8 is the time when the peak ground accelerations occur. All the time in each case under the different ground motion are different, yet the time in table 4.8 is the same in each case since under the same ground motion the PGA point will not change.

Under the far fault earthquake but in the same magnitude, ELX354 means El-Centro earthquake with the PGA 354 gal, ELX421 with the PGA 421 gal, and ELX600 with the PGA 600 gal. In the same value of PGA of far fault, the peak point time responses of each element are different with the time table in near fault analysis, which means that even though under the same PGA, the structure response of this analysis is different either in near fault or far fault earthquake.

Table 4. 5 Far fault - Time table of the maximum sliding displacement of the top friction surface

Case	Time reference (sec)		
	ELX354	**ELX421**	**ELX600**
A1	37.17	37.18	37.19
A2	37.175	37.19	37.185
A4	12.89	12.6	12.62
B1	12.595	12.605	37.165
B2	12.605	12.605	37.175
B4	15.585	15.595	12.605

Table 4. 6 Far fault - Time table of the maximum deformation of the rubber

Case	Time reference (sec)		
	ELX354	**ELX421**	**ELX600**
A1	12.82	12.82	12.825
A2	12.815	12.815	12.795
A4	12.81	12.81	12.785
B1	12.81	12.815	12.82
B2	12.81	12.81	12.815
B4	12.81	12.81	12.815

Table 4. 7 Far fault - Time table of the maximum sliding displacement of the bottom friction surface

Case	Time reference (sec)		
	ELX354	**ELX421**	**ELX600**
A1	37.17	37.18	37.19
A2	12.88	15.565	12.79
A4	12.89	12.6	12.62
B1	12.595	12.605	37.165
B2	15.55	15.575	12.6
B4	15.585	15.595	12.605

Table 4. 8 Far fault - Time table of the maximum PGA

Case	Time reference (sec)		
	ELX354	**ELX421**	**ELX600**
A1	12.79	12.79	12.79
A2	12.79	12.79	12.79
A4	12.79	12.79	12.79
B1	12.79	12.79	12.79
B2	12.79	12.79	12.79
B4	12.79	12.79	12.79

4.3.2 Displacement Contribution

To compare the displacement contribution of each element in near fault analysis at the time when the rubber deformed in maximum, figure 4.11 until figure 4.13 are the result analysis in the same model under the same PGA of far fault analysis. Based on the displacement contribution result that shown in figure 4.11 to 4.13 explain that the far fault analysis results are depend on the amount of PGA, the structure will be more sensitive in line with increasing the PGA.

Figure 4.13 is the structure response under the largest PGA, rubber deformation capability on figure 4.13 (a) continuously decrease in line with increasing friction coefficient, due to some energy could not absorbed well by the rubber, then more energy transmitted to the friction surface, finally the rubber bearing system behavior is dominated by the sliding motion.

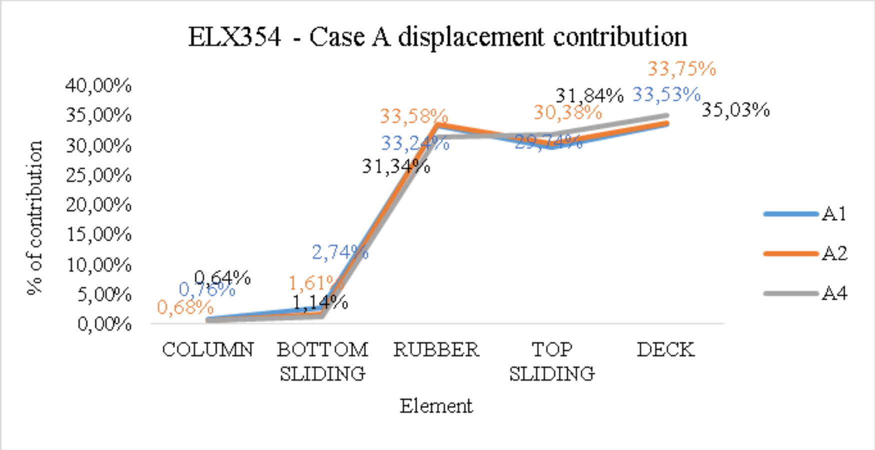

(a)

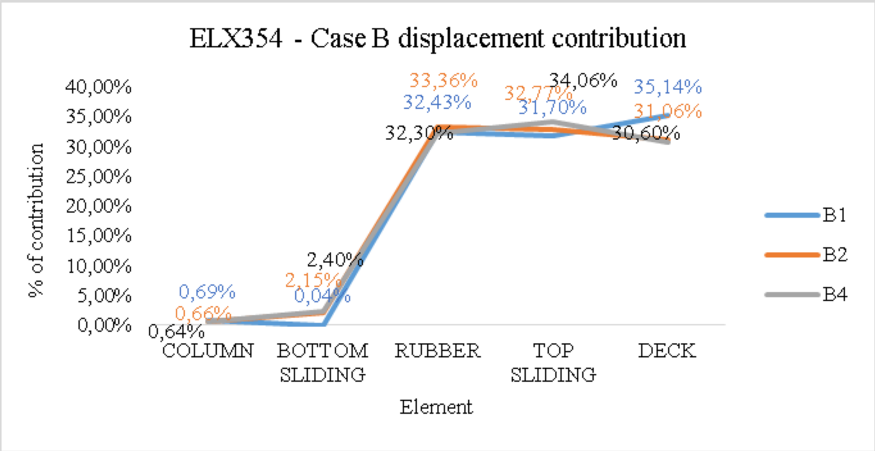

(b)

Figure 4. 11ELX354 - 354 gal, (a) Displacement contribution of the case A, (b) Displacement contribution of the case B

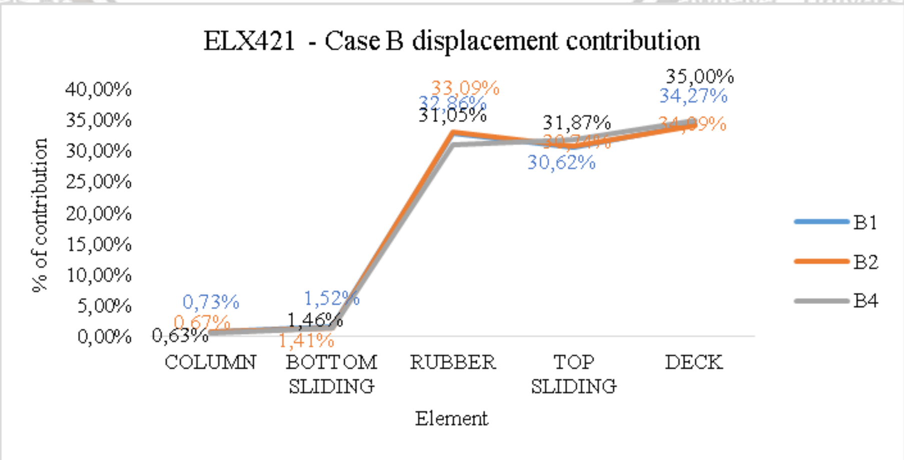

(a)

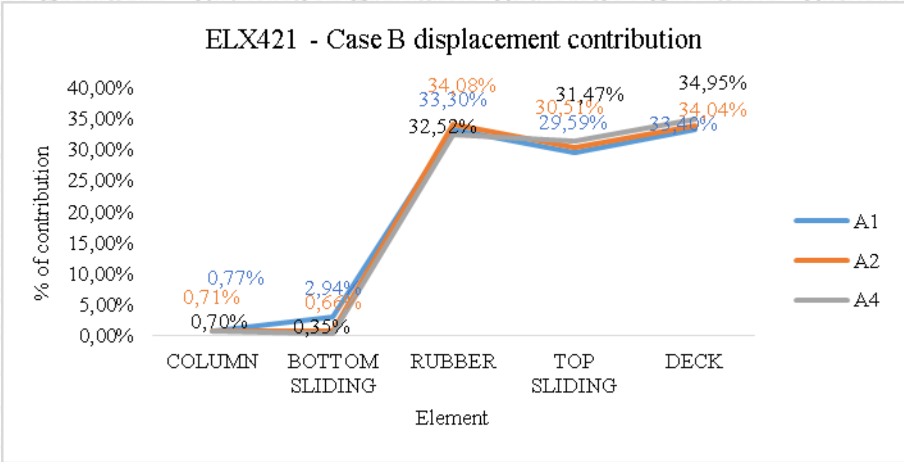

(b)

Figure 4. 12 ELX421 - 421 gal, (a) Displacement contribution of the case A, (b) Displacement contribution of the case B

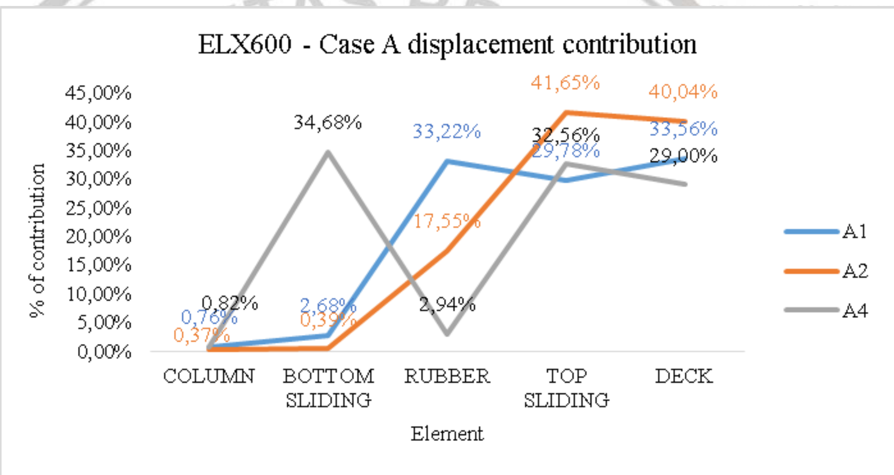

(a)

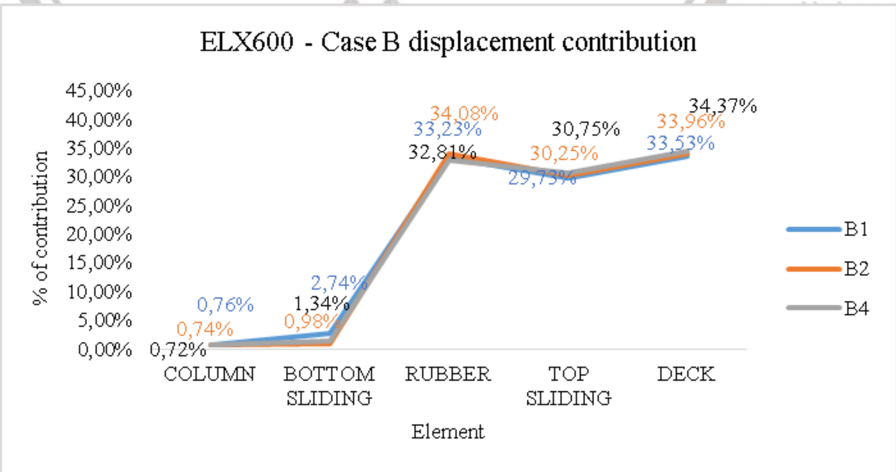

(b)

Figure 4. 13 ELX600 - 600 gal, (a) Displacement contribution of the case A, (b) Displacement contribution of the case B

4.3.3 Energy Absorptions

Total energy dissipation was calculated from the non-linear cycle area of the sliding surface, consider that only friction surfaces that behave non-linearly. Figure 4.17 and figure 4.18 explain the result of the summation energy dissipation capability of the top and bottom friction surface both in case A and case B. under ELX354 (354 gal) and ELX421 (421 gal) the equal combination of friction coefficient of the top and bottom friction surface as in case A1, A4, B1, and B4, they are capable to dissipate more energy than the different combination of friction coefficient as in case A2 and B2. But in case A, in the same combination as A1 and A4, as long as the friction coefficient increase then the energy dissipation will be increase. Different condition as in case B, for case B1 and B4, the energy will be decrease in line with increasing friction coefficient. From these reason, it is found that have a relation between A4 and B1, under ELX354 and ELX421, A4 and B1 is the combination which provide the maximum energy of each case, since friction coefficient of A4 is pair of 0.4-0.4 close with the friction coefficient of B1that is pair of 0.35-0.35, then we can assume that in this range value the friction surface will be an optimum combination.

Presumption result under ELX354 (354 gal) and ELX421 (421 gal) is not applicable for the system under ELX600 (600 gal), knowing that ELX600 is the largest input of the ground motion and the system under far fault earthquake is very sensitive with large PGA and small value of friction coefficient, then increasing friction coefficient in case A and case B in same combination of friction coefficient (A1, A4, B1, and B4) will be increasing the energy dissipation capability, but different combination of friction coefficient in top and bottom friction surface is provide some benefit for the sensitive result of case A under ELX600.

Total energy that absorbed by the rubber bearing system is the combination of strain energy E_S from the rubber and energy dissipation E_D from the surface friction. Figure 4.14 shows the energy dissipation of the surface friction in the top and the bottom side of the rubber bearing. Meanwhile, the strain energy of the rubber shown in figure 4.15 and the reduction energy that successfully absorbed by the rubber bearing system if its compares with the input energy shown in figure 4.16.

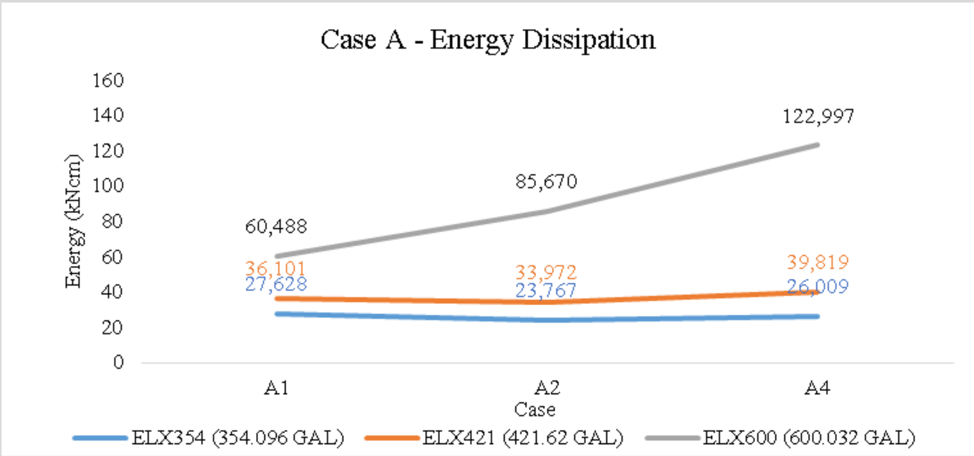

(a)

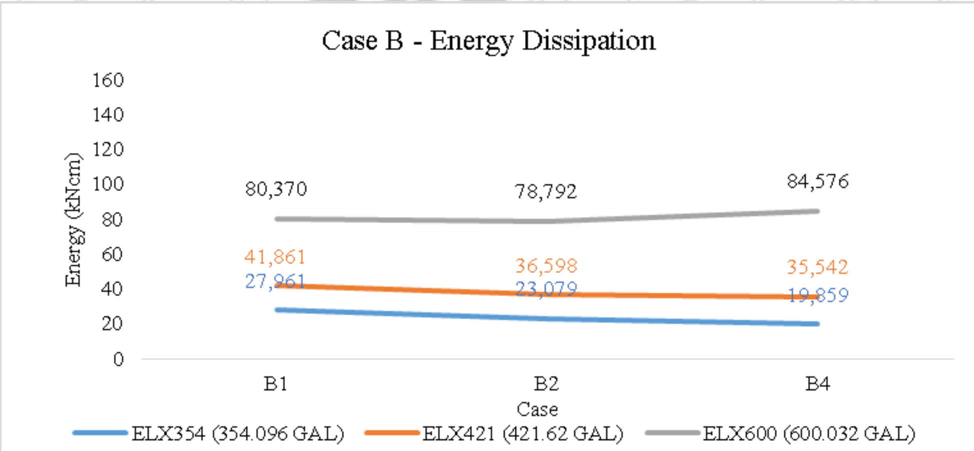

(b)

Figure 4. 14 Far Fault - (a) Energy Dissipation of case A, (b) Energy Dissipation of case B

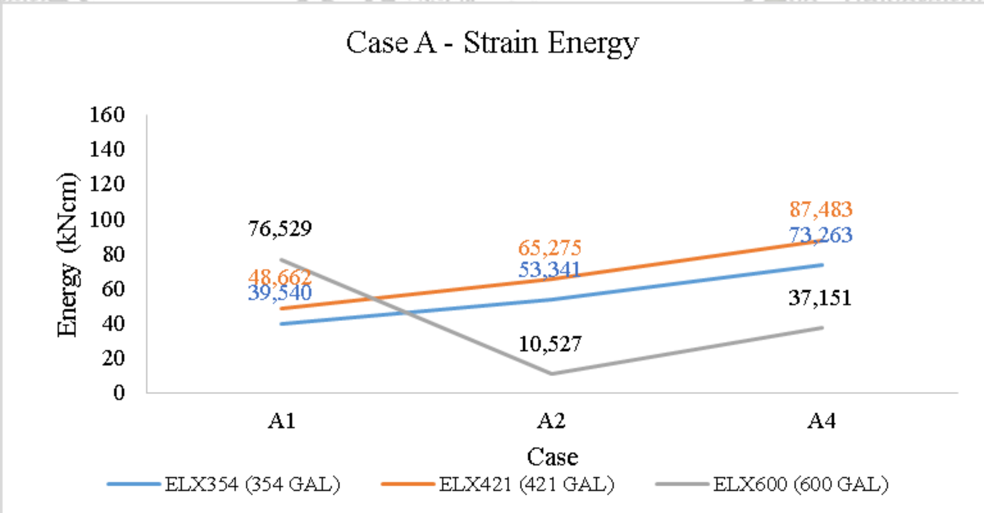

(a)

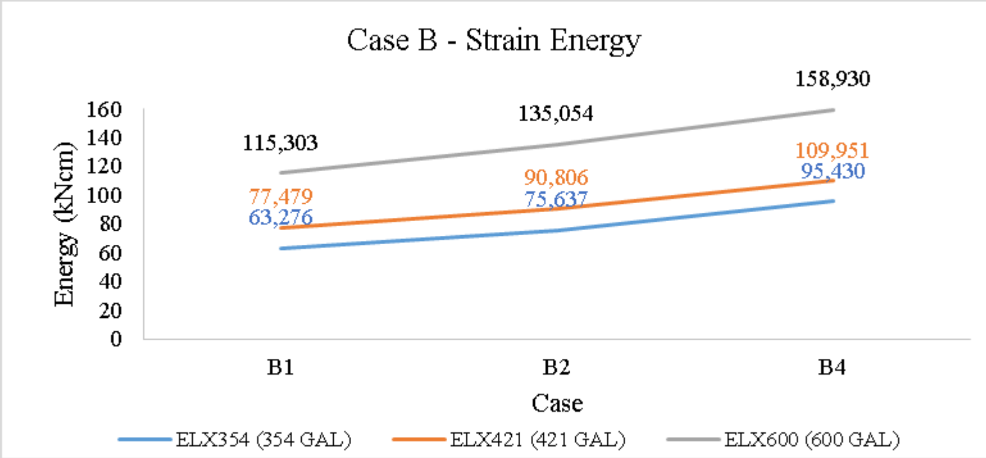

(b)

Figure 4. 15 Far Fault - (a) Strain Energy of case A, (b) Strain Energy of case B

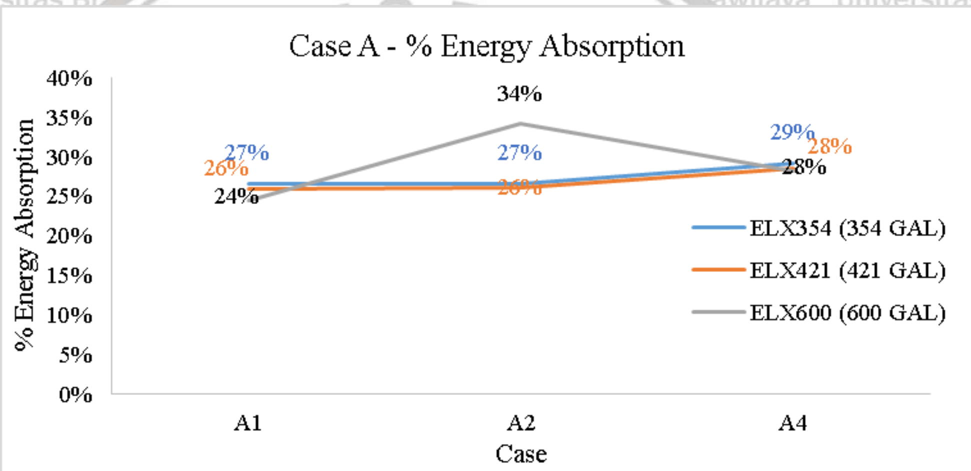

(a)

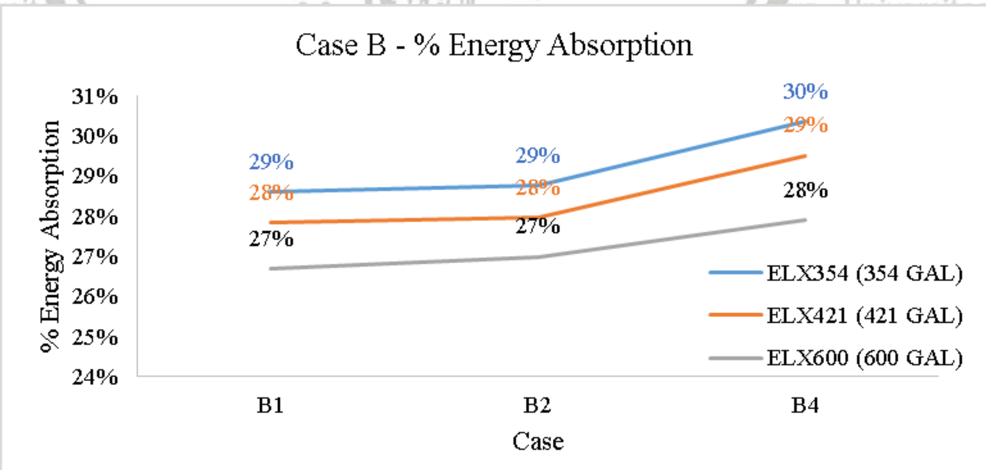

(b)

Figure 4. 16 Far fault - (a) % Energy Absorptions of case A, (b) % Energy Absorptions of case B

4.3.4 Friction Element Contribution

Since the energy dissipation capability of the rubber bearing system provided by the top and bottom friction surface, then the contribution of each surface will be studied as in figure 4.17 until figure 4.19. Under the far fault ground motion, energy contribution of the system in same combination of friction coefficient transferred equally toward top friction surface and bottom friction surface right 50% on each, it is similar with the system under the near fault ground motion. But for the system with different combination of friction coefficient in the top and bottom surface friction, without considering case A under ELX600 (600 gal), as long as the amount of PGA increase the contribution of the bottom friction will be increase, and finallyin case B under ELX600, even though the friction coefficient of the top friction surface is smaller than the friction coefficient in the bottom surface, but under the largest earthquake the contribution of top and bottom friction surface will be nearly equal. Case A (0.2-0.4) is the smaller range of friction coefficient value than the value of case B (0.35-0.5), under the largest PGA of the far fault and the smaller value of the friction coefficient, in this reason that the system in case A under ELX600 is the sensitive case. Since the value of friction coefficient is smaller, this combination provides more flexibility to move than in case B, due to the top friction surface is more dominant, in the different combination of friction coefficient as in case A2, almost all of the energy transmitted to the top friction surface, as shown in figure 4.19 (a).

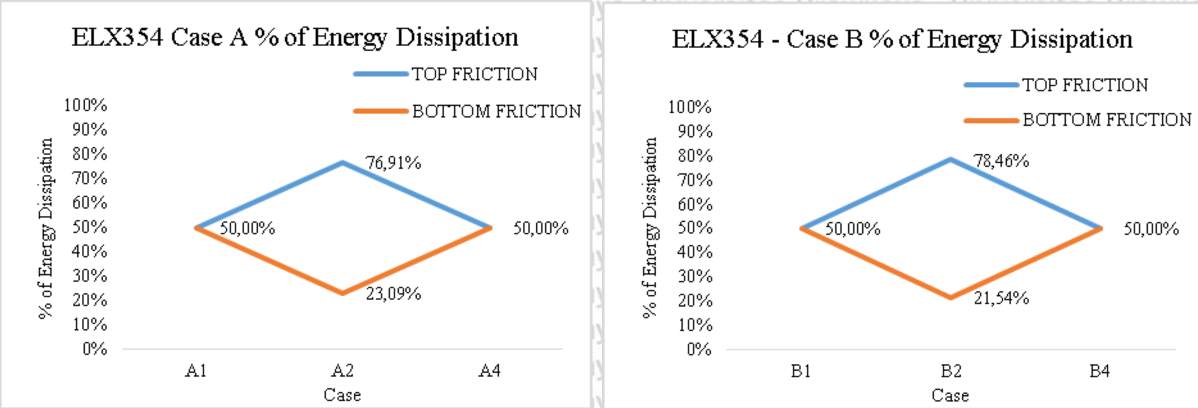

(a) (b)

Figure 4. 17ELX354 – 354 gal, (a) Energy Absorption of the friction surface in case A, (b) Energy Absorption of friction surface in case B

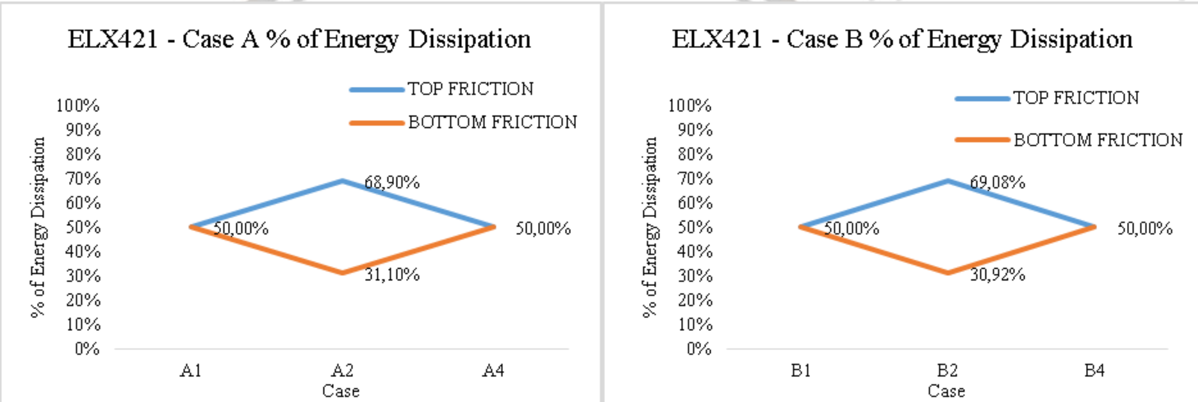

(a) (b)

Figure 4. 18ELX421 – 421 gal, (a) Energy Absorption of the friction surface in case A, (b) Energy Absorption of friction surface in case B

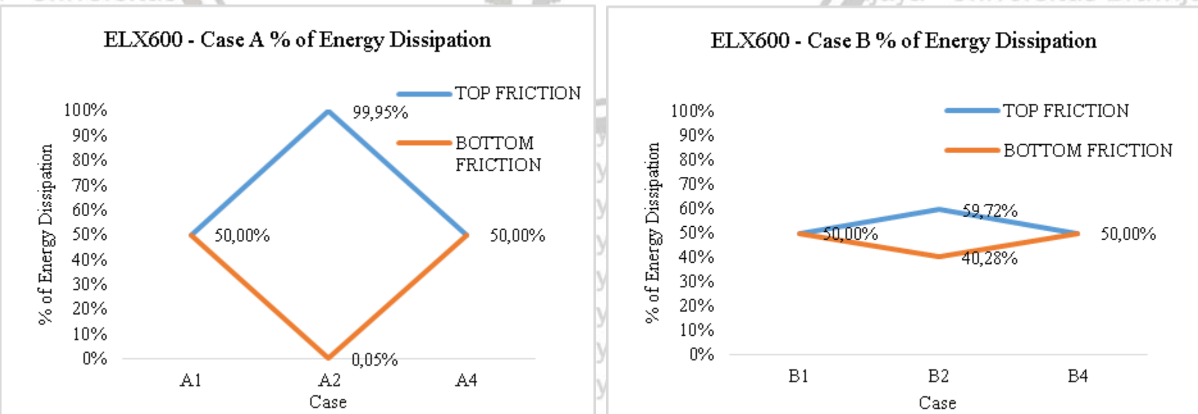

(a) (b)

Figure 4. 19ELX600 – 600 gal, (a) Energy Absorption of the friction surface in case A, (b) Energy Absorption of friction surface in case B

4.4 Conclusion

Here is the conclusion of the study about the effect of variation of the friction coefficient in functional bearing model (FBM) of the rubber bearing system under the near fault earthquake compare with the system under the far fault earthquake ground motion:

1. The bridge with Functional bearing model (FBM) analysis of the rubber bearing system is very sensitive with characteristic of the near fault earthquake ground motion. Meanwhile, the system will be very sensitive in lower value of friction coefficient under the high peak ground acceleration under the far fault earthquake ground motion.
2. Under the near fault ground motion, smaller value of friction coefficient as in case A1 dissipate more energy than the higher value of friction coefficient. Meanwhile, under the far fault earthquake A4 and B1 dissipate more energy than another case.
3. Special case under the near fault ground motion happen in the ground motion with two peaks dominant. Yet, special case under the far fault ground motion happen in the lower value of friction coefficient under the high peak ground acceleration.
4. Applying different value of friction coefficient give a middle impact under the near fault earthquake, but give a worst impact under the far fault earthquake.

CHAPTER V – NUMERICAL ANALYSIS: BRIDGE FALLING PREVENTION

5.1 Case Details

There are a lot of reason to explain the bridge falling phenomenon that mostly happen during the earthquake. First, it is because of the deck crashing due to the small gap between two decks. Second reason, un-proper design of the rubber bearing so that the rubber absorbs less energy, and the last is due to the small size of the cap beam that could not overcome more sliding of the rubber bearing system. Based on these reasons, the bridge shaking table test model analyzed using functional bearing model (FBM) to find out some parameters in each failure possibility.

If the μ_{ST} is the coefficient of friction value in the top surface and μ_{SB} is the coefficient of friction value in the bottom surface, here are the proposed cases to study about bridge falling prevention:

Based on the design code

Case A1: applying same value of friction coefficient both in the top and bottom interface, $\mu_{ST} = 0.2$ and $\mu_{SB} = 0.2$.

Case A2: applying larger value of friction coefficient in the bottom interface, $\mu_{ST} = 0.2$ and $\mu_{SB} = 0.4$.

Case A4: applying same value of friction coefficient in both interface but larger than case A1, $\mu_{ST} = 0.4$ and $\mu_{SB} = 0.4$

Based on the experimental test

Case B1: applying same value of friction coefficient both in the top and bottom interface, $\mu_{ST} = 0.35$ and $\mu_{SB} = 0.35$.

Case B2: applying larger value of friction coefficient in the bottom interface, $\mu_{ST} = 0.35$ and $\mu_{SB} = 0.5$.

Case B4: applying same value of friction coefficient in both interface but larger than case B1, $\mu_{ST} = 0.5$ and $\mu_{SB} = 0.5$

Based on the three main objectives that explained before, all of the case will be analyzed based on several time references. To design the proper rubber bearing, all of the system response will be analyzed at the time when the rubber deformed in maximum. And to design an enough gap distance of the deck to avoid inter deck crashing, all of the system response will be analyzed at the time when the sliding maximum happen at the top friction surface and consider about the deck displacement. And the last, to design an enough size of the cap beam as sitting place of the rubber bearing system, all of the system response will be analyzed at the time when the maximum sliding happen in the bottom friction surface and consider about the column displacement.

5.2 Design A Proper Rubber Bearing

5.2.1 Maximum Deformation of the Rubber

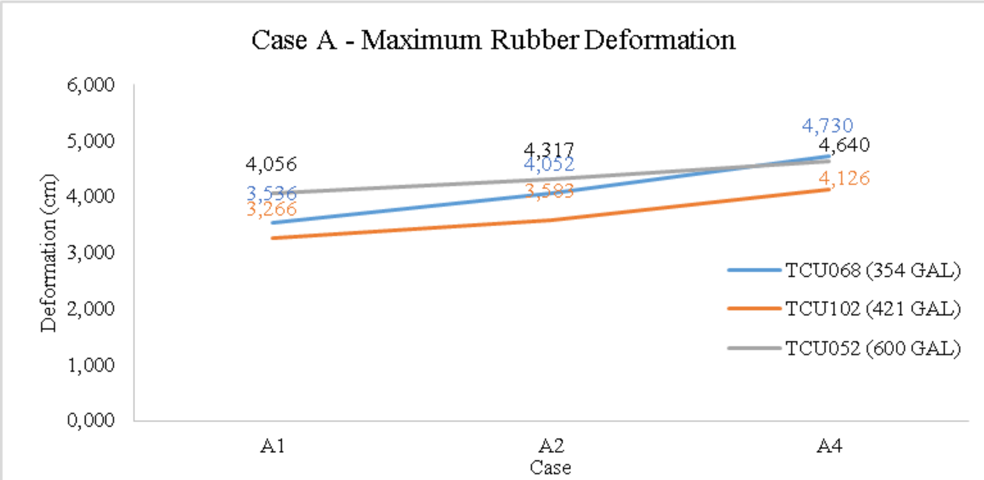

(a)

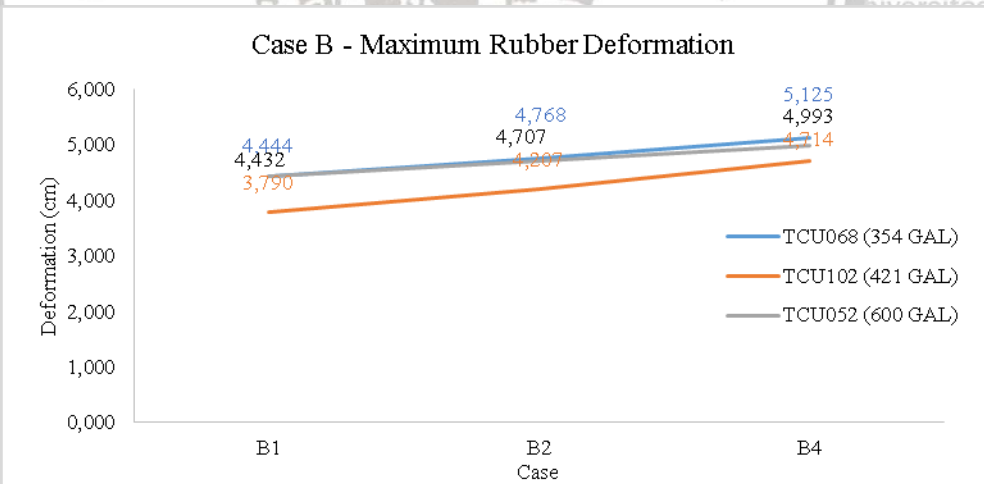

(b)

Figure 5. 1 Near fault, (a) Maximum rubber deformation of case A, (b) Maximum rubber deformation of case B

Figure 5.1 (a) and (b) are the overall result analysis of the rubber maximum deformation without considering any reference time. Variation of friction coefficient working on increasing the value of rubber deformation, it is naturally happened when the friction coefficient values have been increase, then the friction surface will limit its movement, finally most of the excitation energy absorbed by the rubber. Rubber maximum deformation become the first consideration to determine the parameter of designing a proper rubber element that will applied on the system since rubber element is the main object of the rubber bearing system.

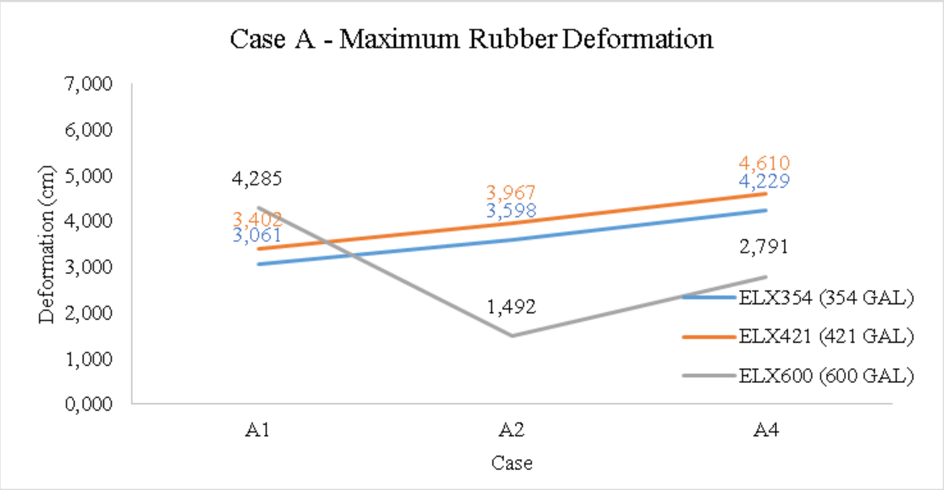

(a)

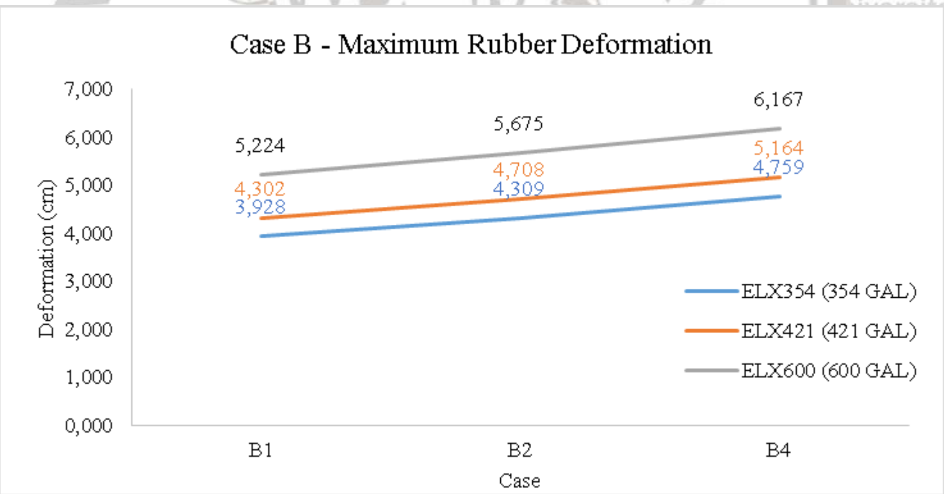

(b)

Figure 5. 2 Far fault, (a) Maximum rubber deformation of case A, (b) Maximum rubber deformation of case B

Under the near fault ground motion, TCU102 (421 gal) that known before as the special case of the near fault input provide smallest rubber maximum deformation, this is become one of the consideration of the near fault exception since TCU102 is not the input of the ground motion with smallest value of peak ground acceleration (PGA). In smaller configuration of friction coefficient in case A (0.2-0.4), responses of the TCU052 (600 gal) are larger than TCU068 in case A1 and A2, but decreasing when the system configured as case A4. Yet, in the higher configuration of friction coefficient in case B (0.35-0.5), there are small different responses of both in TCU068 and TCU052.

Under the far fault ground motion, since the special case of the far fault analysis is the one in same configuration of the smaller value of the friction coefficient under the largest peak ground acceleration of the far fault ground motion (case A under TCU052). Consider the rubber maximum deformation response in case A under ELX600 (600 gal) as an exception, similar with the near fault analysis, rubber maximum deformation increase in line with increasing friction coefficient value. And the rubber maximum deformation under the same case is increase in line with increasing the peak ground acceleration. Different configuration of the friction coefficient value of the top and bottom friction surface give the middle result of rubber deformation. For the special case, case A under TCU052, decreasing coefficient of friction value will be decreasing the rubber deformation, and put the larger friction value in the top surface provide an extreme decreasing of the rubber maximum deformation.

Overall, the one that need to pay more attention of the functional bearing model (FBM) analysis, under the near fault the characteristic of the ground motion will be very important, and under the far fault the peak ground acceleration for smaller value of friction coefficient will behave differently.

5.2.2 Time Reference

Since the study is to find out the parameter to design a proper rubber bearing system based on performance of the rubber element, the system was analyzed based on the time when the rubber maximum deformations occur. Based on the maximum deformation response of the rubber as shown on figure 5.1, then the time happening analyzed as the reference time to observe other element response. Recall the time table of the maximum rubber deformation on table 4.2 on chapter 4, table 5.1 is the time reference to determine the structure response in order to design a proper rubber bearing system. As the comparison, the time reference of the far fault analysis was observed. Recall the table 4.6 on chapter 4, Table 5.2 present the rubber maximum deformation time under far fault ground motion.

Table 5. 1 Near fault - Time table of the maximum deformation of the Rubber

Case	Time reference (sec)		
	TCU068	TCU102	TCU052
A1	35.58	36.18	33.405
A2	35.58	36.18	33.395
A4	35.58	48.235	33.39
B1	35.58	48.24	33.39
B2	35.58	48.235	33.385
B4	35.585	48.235	33.385

Table 5. 2 Far Fault - Time table of the maximum deformation of the Rubber

Case	Time reference (sec)		
	ELX354	ELX421	ELX600
A1	12.82	12.82	12.825
A2	12.815	12.815	12.795
A4	12.81	12.81	12.785
B1	12.81	12.815	12.82
B2	12.81	12.81	12.815
B4	12.81	12.81	12.815

5.2.3 Behavior of the Rubber Bearing System at the Certain Time

Rubber bearing system is a support system that consist of rubber element covered by friction surface in the top and the bottom side. Take the times that mention on table 5.1, under the near fault it had been analyzed the behavior of the other element in these certain time. Figure 5.3 until figure 5.5 shows the top sliding deformation, rubber deformation, and bottom sliding deformation of the rubber bearing system under the near fault ground motion.

At the time when the rubber deformed in maximum, under TCU068 (354 gal) and TCU052 (600 gal), increasing coefficient of friction means its limit the sliding motion of the friction surface, then increasing the value of the coefficient of friction will be increasing the rubber deformation and decreasing sliding displacement of the friction surface. It is perfectly shows on figure 5.3 (b) since the coefficient of friction value of case B are larger than in case A. In different combination of friction coefficient as in case A2 and B2, since the coefficient of friction in the top surface is less than in the bottom surface, thus the sliding displacement of the top surface is larger than the sliding displacement of the bottom surface.

In the special case of the near fault ground motion, the system under TCU102 (421 gal), rubber deformation will be increase in line with increasing coefficient of friction values. In the same configuration of friction coefficient as in case A1, A4, B1, and B4, since the friction increase then the friction sliding displacement will be decrease. Yet, in the different configuration of friction coefficient as in case A2 and B2, because of the friction coefficient of the top surface smaller than in the bottom surface, than the displacement of top surface will be larger than in the bottom, but in the bottom will be decrease become the smallest value compare with the other case. As the comparison, the system under far fault ground motion was analyzed. Figure 5.6 until figure 5.8 present the plot of top friction sliding, rubber deformation, and bottom friction sliding.

Under the far fault, rubber maximum deformation will be increase in line with increasing the friction coefficient values, and also will be increase in line with increasing the magnitude of the peak ground acceleration. Consider the special case of case A under ELX600 (600 gal) as an exception, in the special case of the far fault ground motion of case A under ELX600, case A1 is the same combination of the top and bottom friction surface with low value of friction coefficient, result of the case A1 still similar with the common result, but when the friction coefficient increase into A4, then the energy of ELX600 will be higher and the excess energy of the rubber element will be absorb well by the top and the bottom friction surface. Under the largest PGA of the far fault ELX600, the low part friction will be weaker than the rubber, it is due to the inertial mass of the deck that close with the top friction surface that applied small value of the friction coefficient. Thus in case A2, due to the inertial mass of the deck, the force will be directly concentrated on the top friction surface.

From the displacement result of each element, the displacement of each point can be calculated. Considering element point as in figure 3.2, u_c is the column displacement, u_{ST} is the top friction's sliding deformation, u_{RB} is the rubber deformation, and u_{SB} is the bottom friction sliding deformation. Then, the displacement of each point u_c, u_1, u_2, and u_3 can be calculated by:

$$u_c = u_c \quad \textit{Eq. 5. 1}$$

$$u_3 = u_{SB} + u_c \quad \textit{Eq. 5. 2}$$

$$u_2 = u_{RB} + u_3 \quad \textit{Eq. 5. 3}$$

$$u_1 = u_{ST} + u_2 \quad \textit{Eq. 5. 4}$$

Under the near fault earthquake, the displacement of each point of u shows on figure 5.9 until figure 5.11. In the similar characteristic of the ground motion TCU068 (354 gal) and TCU052 (600 gal), the accumulation result of TCU068 are smaller than the result of TCU052 due to

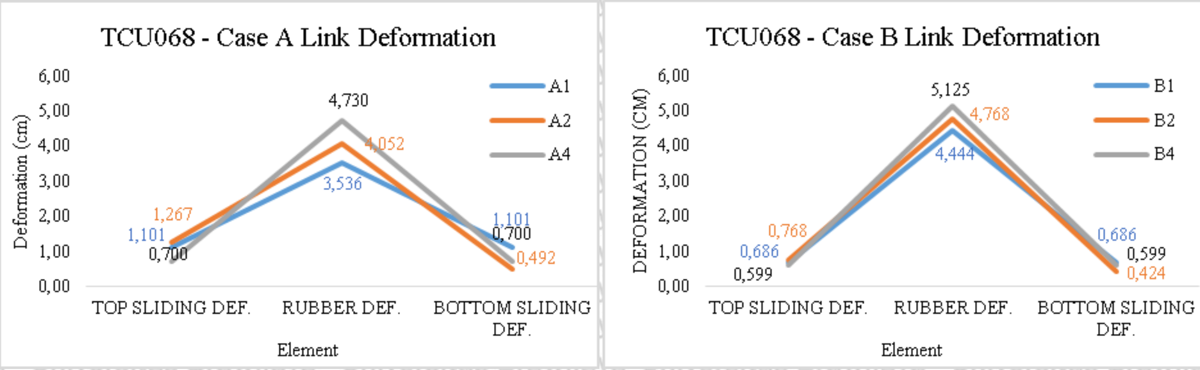

(a) (b)

Figure 5. 3 Near fault TCU068 (354 gal), (a) Link Deformation of case A, (b) Link Deformation of case B

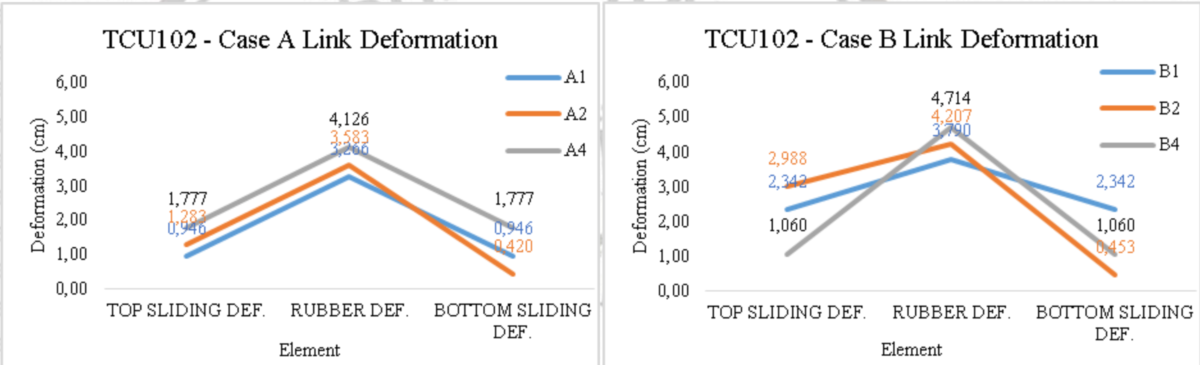

(a) (b)

Figure 5. 4 Near fault TCU102 (421 gal), (a) Link Deformation of case A, (b) Link Deformation of case B

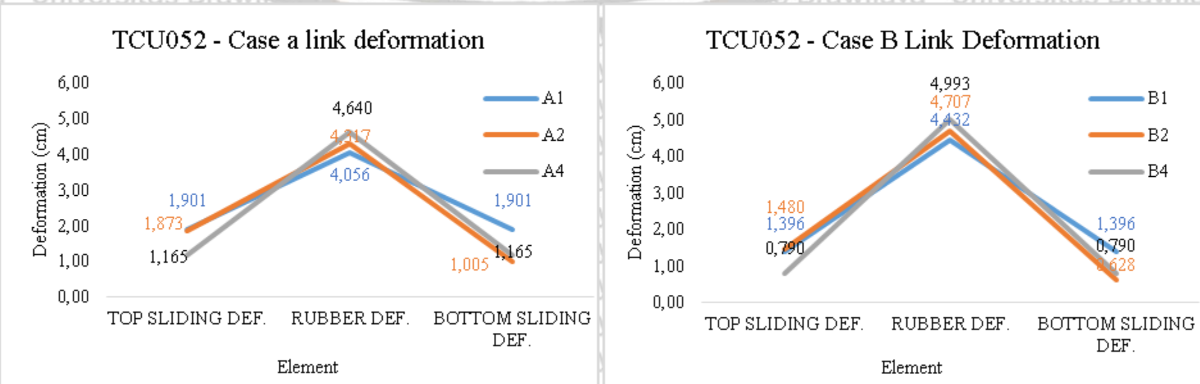

(a) (b)

Figure 5. 5 Near fault TCU052 (600 gal), (a) Link Deformation of case A, (b) Link Deformation of case B

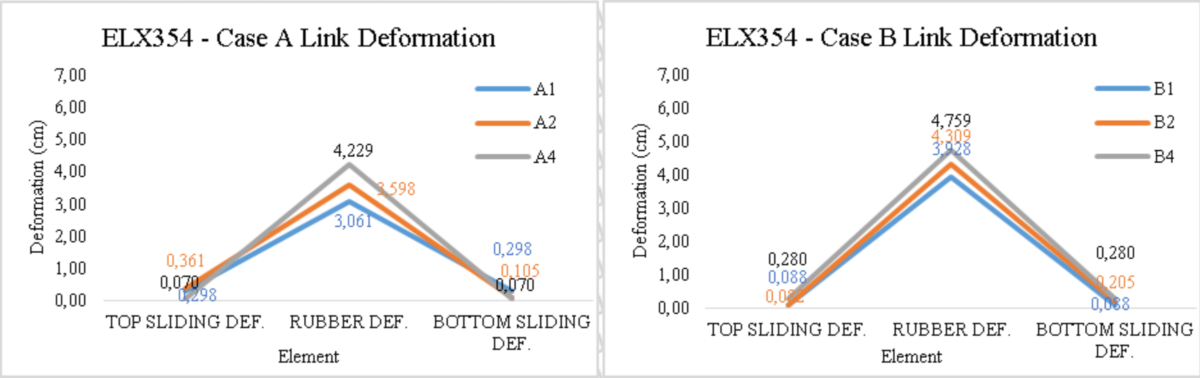

(a) (b)

Figure 5. 6 Far fault ELX354 (354 gal), (a) Link Deformation of case A, (b) Link Deformation of case B

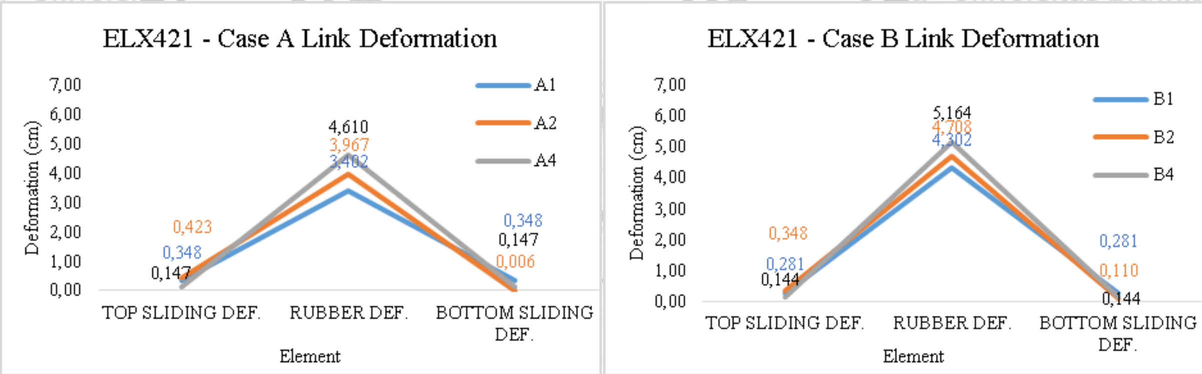

(a) (b)

Figure 5. 7 Far fault ELX421 (421 gal), (a) Link Deformation of case A, (b) Link Deformation of case B

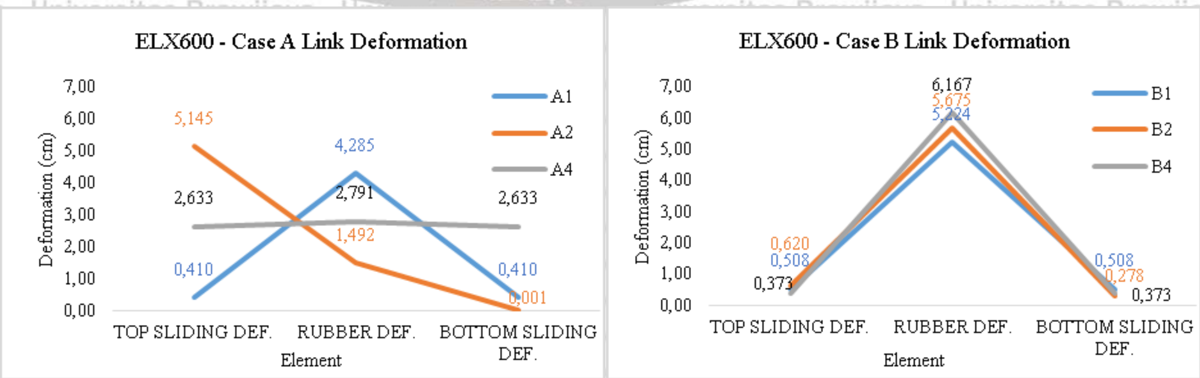

(a) (b)

Figure 5. 8 Far fault ELX600 (600 gal), (a) Link Deformation of case A, (b) Link Deformation of case B

the PGA. But, in the smaller PGA of TCU 102 (421 gal), overall results are larger than TCU052 (600 gal).

Under TCU068 (354 gal), in the same value of friction coefficient of the top and the bottom friction surface, if the friction value increase from A1 to A4, then the column displacement will be increase from 0.076 cm to 0.101 cm, so did rubber displacement of u_2. And the overlap energy will be transferred as displacement of u_1 and u_3, in the top friction surface A4 displaced more than A1, and in the bottom friction surface A4 displaced less than A1. Similar behavior happens in case B under TCU068, since in case B have larger value of friction coefficient, then the gap between case B1 and B4 is very close, which mean in the large value of friction coefficient, there are small effect on increasing friction coefficient value. Move to the different configuration of the friction coefficient of the top and bottom friction surface in case A2 and B2. A2 and B2 under TCU068 displaced less than the other case, but A2 closely behave like A1, so did B2 closely behave like B1, which means that applying low friction value of the top surface still behave like the applying the lowest friction value in same configuration.

Then the PGA increase to be TCU102 (421 gal). In the case A, case A4 displaced more than case A1 in all point, its happen since the energy of the system under TCU102 is very large, and if the friction surface limiting more, then the displacement will be large due to the rubber bearing receive more energy. Unstable condition happens when the system applied under TCU102, because of the condition in case A did not happen on case B, if case B1 is the same configuration with low value of the friction coefficient, then increasing friction value become B4 will be decrease overall displacement, its happen due to increasing the friction coefficient value means limiting the structural motion. Second condition if the system applied on different value of friction coefficient of the top and the bottom friction surface, the displacement behavior of case A2 closely similar with A1, since the value is bigger in the bottom surface then the sliding displacement of the bottom surface will be smaller than case A1. Yet, in case B, the displacement result of B2 is lower than B1. The pattern result of the system under TCU102 can be defined easily, so that the result under this ground motion is a little bit unstable.

Under the largest PGA of the near fault TCU052 (600 gal), all of the result in case A almost close each other, its mean the effect of varying of the friction coefficient are less impact in a higher earthquake, and the system with different combination of friction coefficient such like A2 and B2 provide less displacement than the same configuration (A1, A4, B1, B4).

If we pay more attention of the path of the grey line (A4 and B4), under the smallest PGA TCU068 (354 gal) and smaller value of the friction coefficient (case A), the grey line (A4) is outside the path of the A1 and A2, grey line come closer in the case with larger value of the friction coefficient (case B). Then increase the PGA into TCU102 (421 gal), when the system is on case A (low friction value), the grey line is far outside the area of the blue line (A1) and orange line (A2), the on case B (higher friction value), the grey line displacement B4 is inside the area of B1 and B2. Under the highest PGA of TCU052 (600 gal), the grey line of both case A4 and B4 are inside the area of the blue line and orange line, and the displacement lines are very close, which means that increasing friction value will give small effect in high PGA of the near fault ground motion.

In order to make sure the behavior of the near fault, several analyses proposed under TCU068, TCU102, and TCU052 in the same PGA about 421 Gal as shown in figure 5.12 until 5.14. Under the same PGA for all different ground motion, the system behave similarly as the system under the different PGA as in figure 5.9 until 5.11. It is mean that even though the PGA increase the behavior will be the same, thus the system analysis under near fault ground motions are depend on the characteristic of the ground motion and the value of the friction coefficient.

Another comparison was done under the far fault earthquake ground motion. Figure 5.15 until figure 5.17 shows the result of the bridge analysis under far fault ground motion. Generally, if the system working under far fault ground motion, as long as the coefficient of friction increase, then the force will be concentrated more toward the rubber, so that the rubber displacement will be larger, and the friction sliding of the top and the bottom surface friction influence by the rubber deformation, if the rubber deformation increase, then the friction sliding will be increase too. This is the reason to explain that under the far fault, case A4 and B4 always higher than case A1 and B1. And if the friction coefficient of the top sliding surface is smaller than in the top, the result always be in the middle of the result in same configuration of friction coefficient.

Overall, in order to design the proper rubber bearing element based on the functional bearing model (FBM) analysis, the most important parameter that need to paid more attentionis the earthquake input. If the system working under the near fault ground motion, then the characteristic of the ground motion is the most important consideration. And if the system working under far fault ground motion, then the smaller value of friction coefficient and the amount of the peak ground acceleration shall be more important.Under the near fault earthquake, as long as the value of friction force increased, the rubber deformation will be increase too, it is due to the movement of the friction surface limited by the higher value of the friction force,thus the force will be concentrated on the rubber. At the time when the rubber deformed in maximum, the result of case A1 and A2 or B1 and B2 mostly is closed each other, since the most sensitive case is the case A4 and B4, that continuously changing in line with increasing PGA of the near fault ground motion.

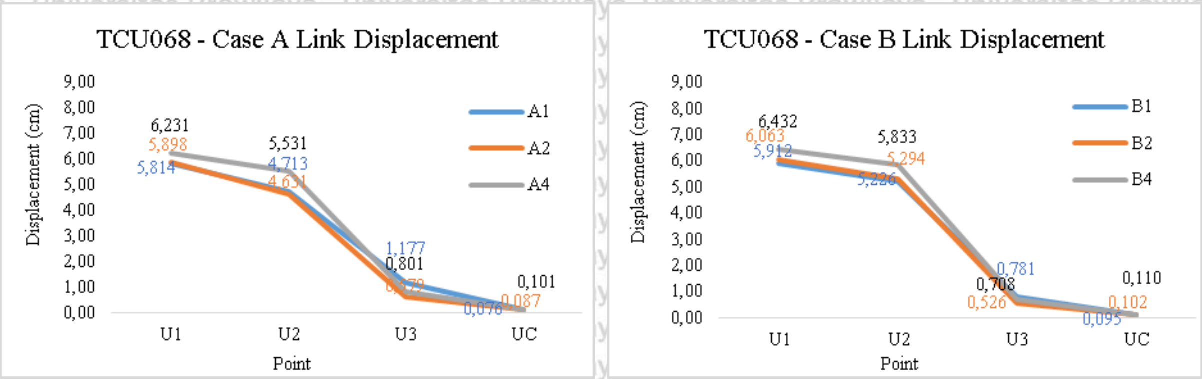

(a) (b)

Figure 5. 9 Near fault TCU068 (354 gal), (a) Displacement point of case A, (b) Displacement point of case B

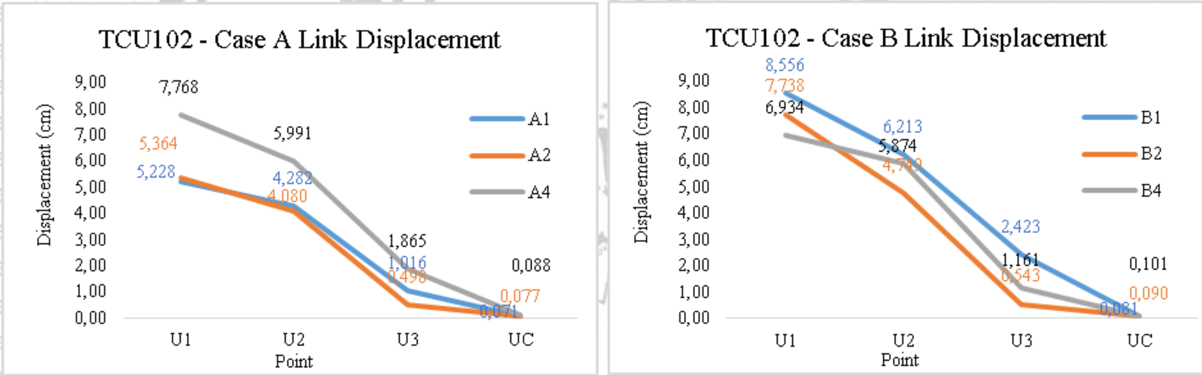

(a) (b)

Figure 5. 10 Near fault TCU102 (421 gal), (a) Displacement point of case A, (b) Displacement point of case B

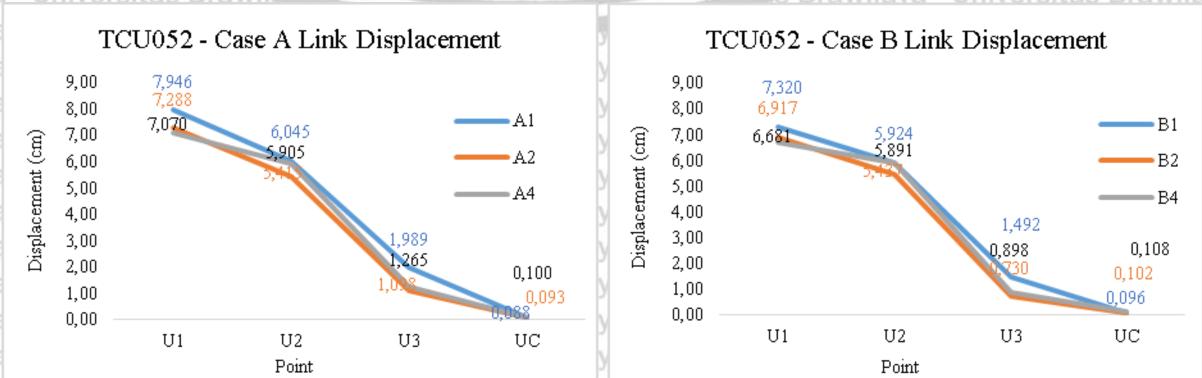

(a) (b)

Figure 5. 11 Near fault TCU052 (600 gal), (a) Displacement point of case A, (b) Displacement point of case B

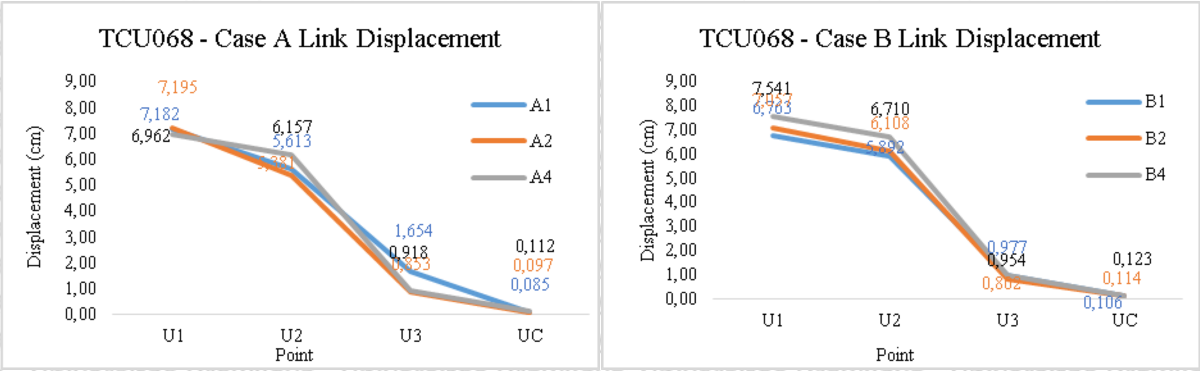

(a) (b)

Figure 5. 12 Near fault, TCU068 421 gal, (a) Displacement point of case A, (b) Displacement point of case B

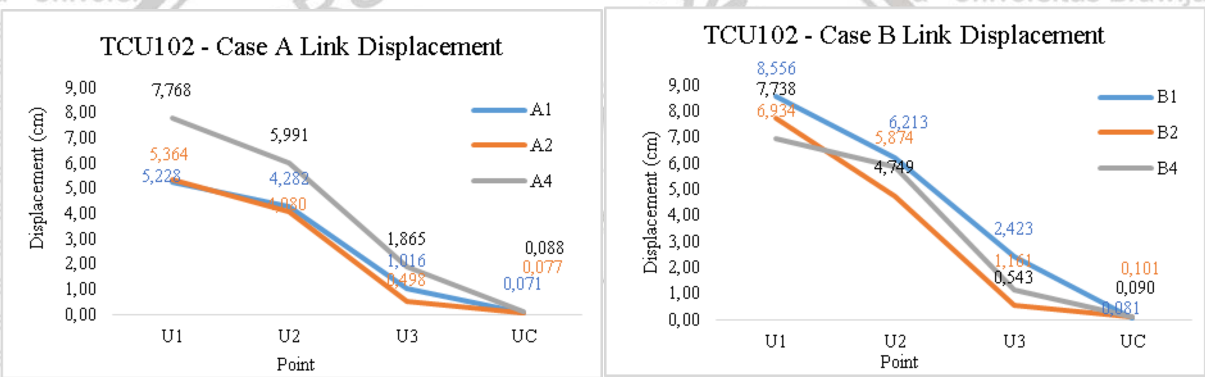

(a) (b)

Figure 5. 13 Near fault, TCU102 421 gal, (a) Displacement point of case A, (b) Displacement point of case B

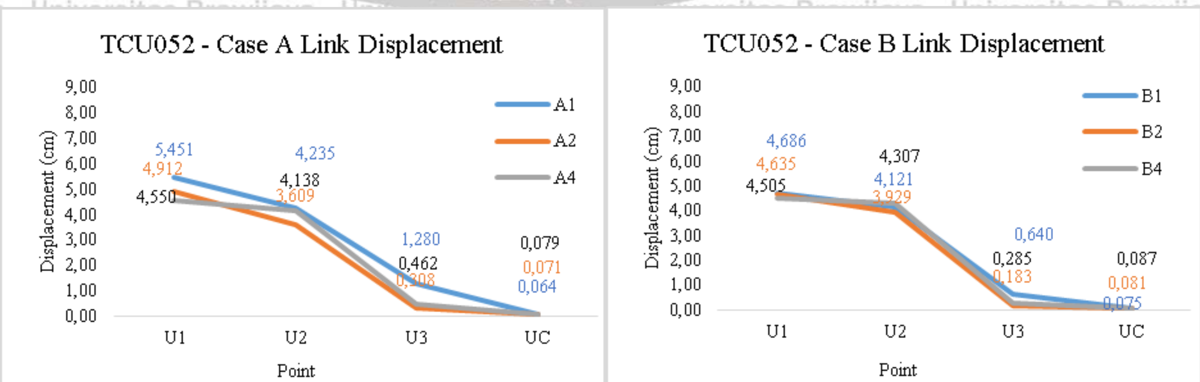

(a) (b)

Figure 5. 14 Near fault, TCU052 421 gal, (a) Displacement point of case A, (b) Displacement point of case B

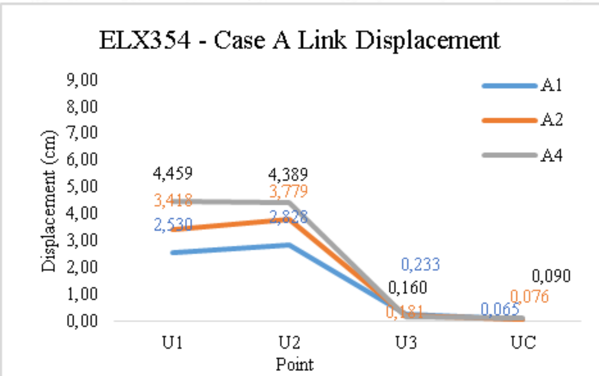

(a)

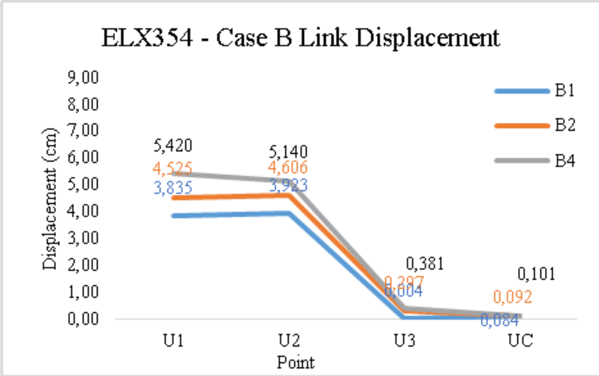

(b)

Figure 5. 15 Far fault, ELX354 (354 gal), (a) Displacement point of case A, (b) Displacement point of case B

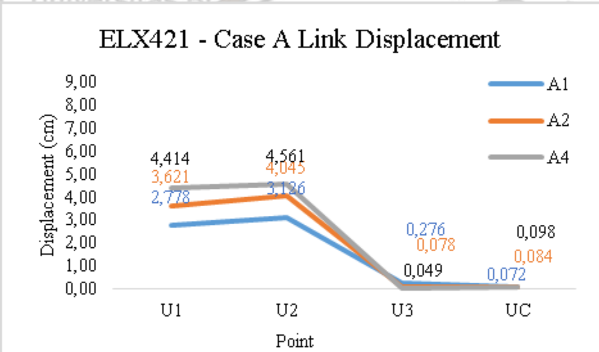

(a)

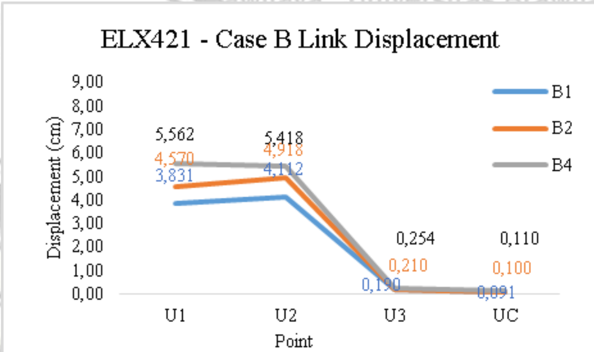

(b)

Figure 5. 16 Far fault, ELX421 (421 gal), (a) Displacement point of case A, (b) Displacement point of case B

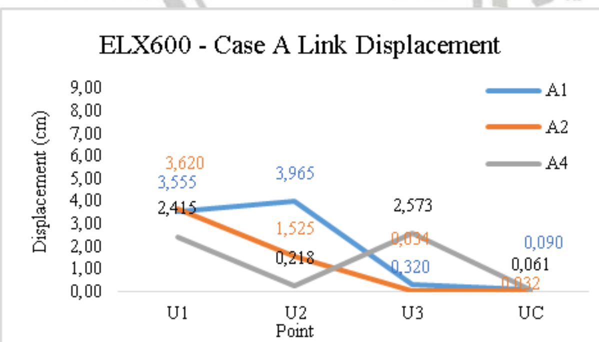

(a)

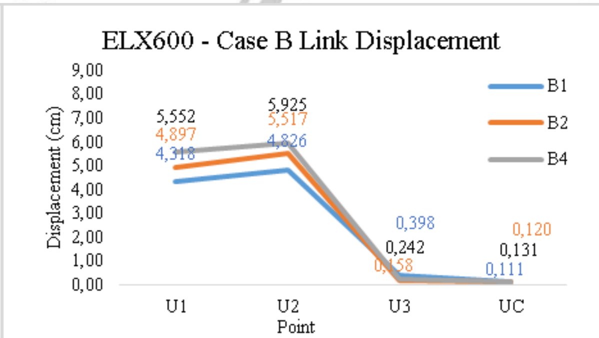

(b)

Figure 5. 17 Far fault, ELX052 (600 gal), (a) Displacement point of case A, (b) Displacement point of case B

5.3 Design the Gap Distance of the Deck

5.3.1 Maximum Deck Displacement

Before observing the parameters that need to consider of a bridge to prevent the deck crashing with designing an enough space between two decks, it will be important to analyze the deck maximum response under the existing ground motion. Figure 5.18 shows the deck response under the near fault ground motion.

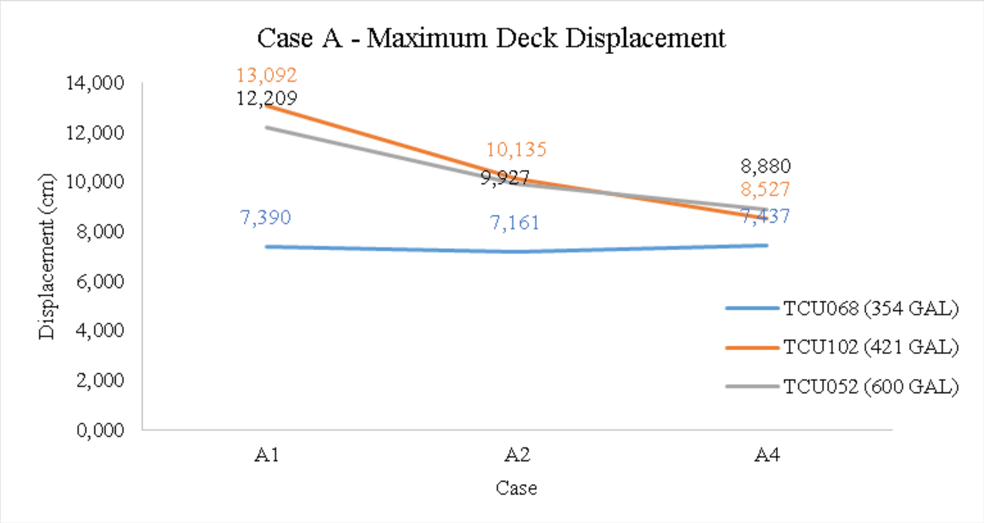

(a)

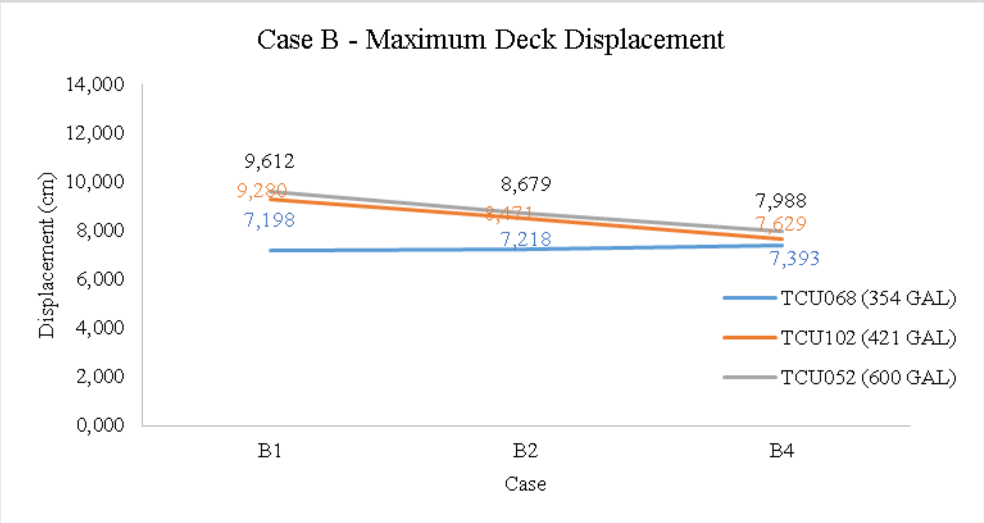

(b)

Figure 5. 18 Near fault, (a) Maximum Deck Displacement of case A, (b) Maximum Deck Displacement of case B

It can be analyze based on figure 5.18, deck displacement of the system under TCU102 is close with the deck displacement under the largest peak of TCU052 even though their magnitudes are different. And overall deck displacement will be decrease in line with

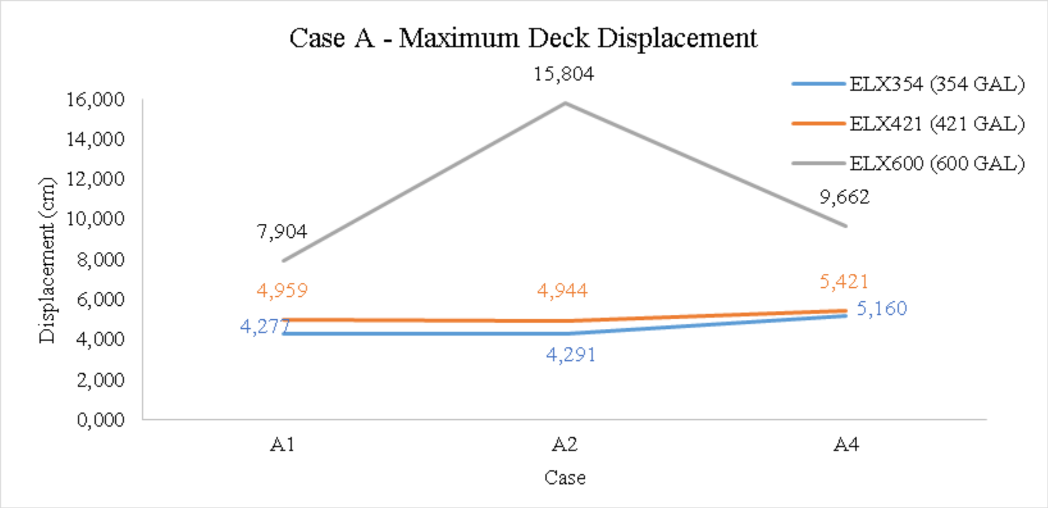

(a)

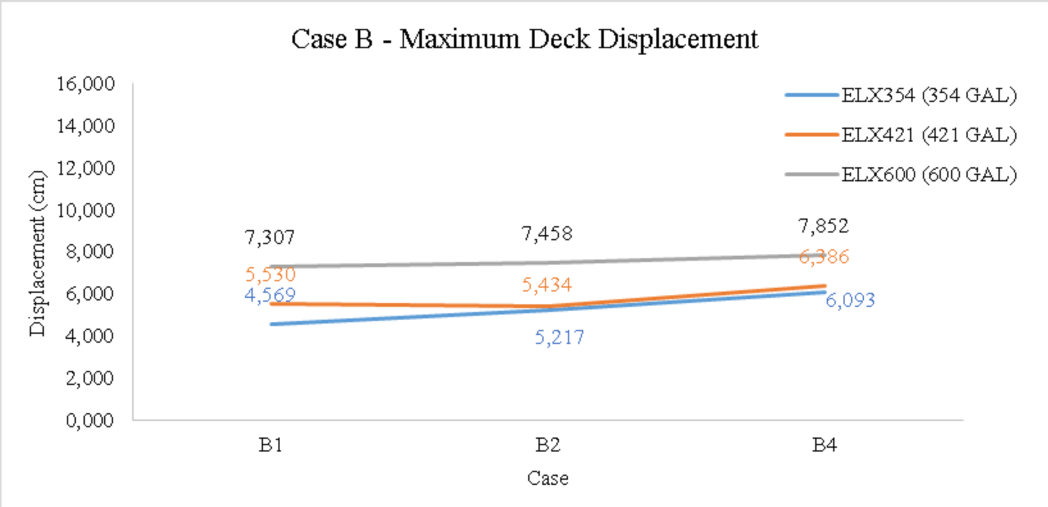

(b)

Figure 5. 19 Far fault, (a) Maximum Deck Displacement of case A, (b) Maximum Deck Displacement of case B

increasing the value of friction coefficient. Comparing figure 5.1 and figure 5.18, deck maximum displacements are in opposite with the rubber maximum deformations, thus a proper rubber bearing system is the one that capable to dissipate more energy so that the energy that received by the deck can be reduced.

Under the far fault earthquake, take some correlation in a special case of the case A under TCU052 between rubber maximum deformation and deck displacement from figure 5.2 (a) and 5.19 (a), case A2 has the smallest rubber deformation and the largest deck displacement, simply means that if the system configured on case A2, the rubber will absorb less energy, the effect is more energy transferred to the deck and the deck displacement will be larger.

5.3.2 Maximum Sliding Deformation of the Top Friction Surface

Top friction surface will be the second consideration to design the gap distance between two deck, since the dominant part of the friction surface is in the top, thus the sliding displacement in the top friction need to identify. Figure 5.20 shows the maximum sliding response of the top friction surface under the near fault earthquakes.

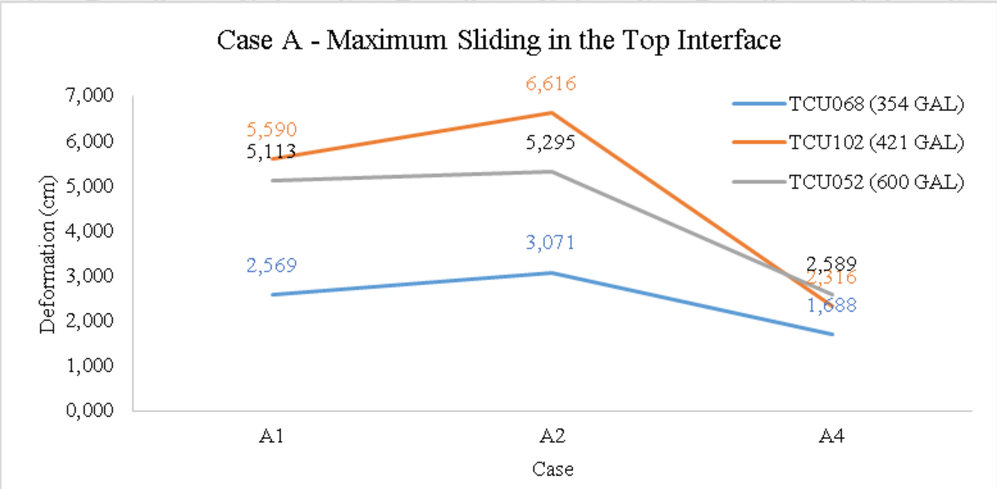

(a)

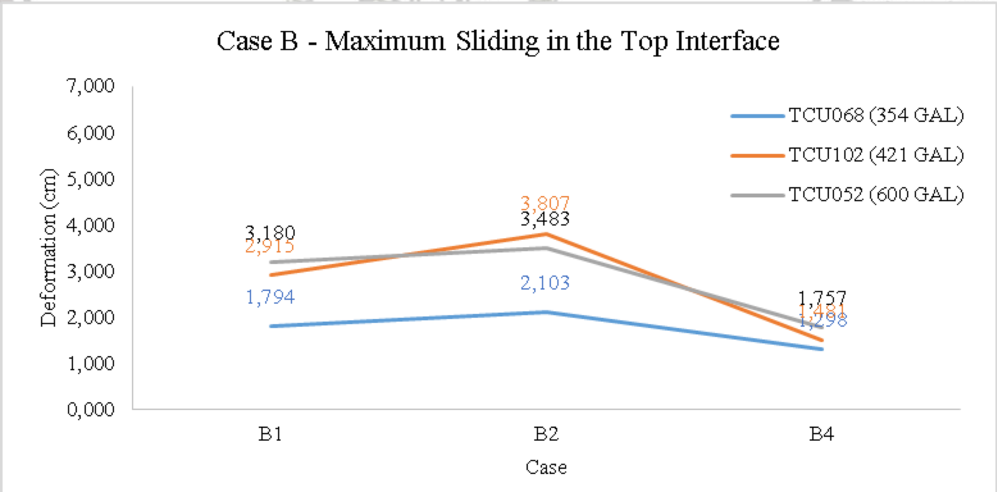

(b)

Figure 5. 20 Near fault, (a) Maximum sliding of the Top Interface on case A, (b) Maximum sliding of the Top Interface on case B

Theoretically, sliding displacement of the top friction surface increase as long as the peak ground acceleration increase, and also will be decrease in line with increasing the value of friction coefficient. This happen on the system under the near fault as in figure 5.20 but not in case A under TCU102, since it is the special case of near fault analysis. For the special case in case A1, the sliding displacement under TCU102 is the largest one, since the system need more energy, so that the sliding displacement of this case is the highest. For the overall result, case A2 and B2 since both of them have the small value of friction coefficient in the top friction sliding, thus the force in these case concentrated on the top friction surface, as the effect, the top surface received more energy and displaced more than another case.

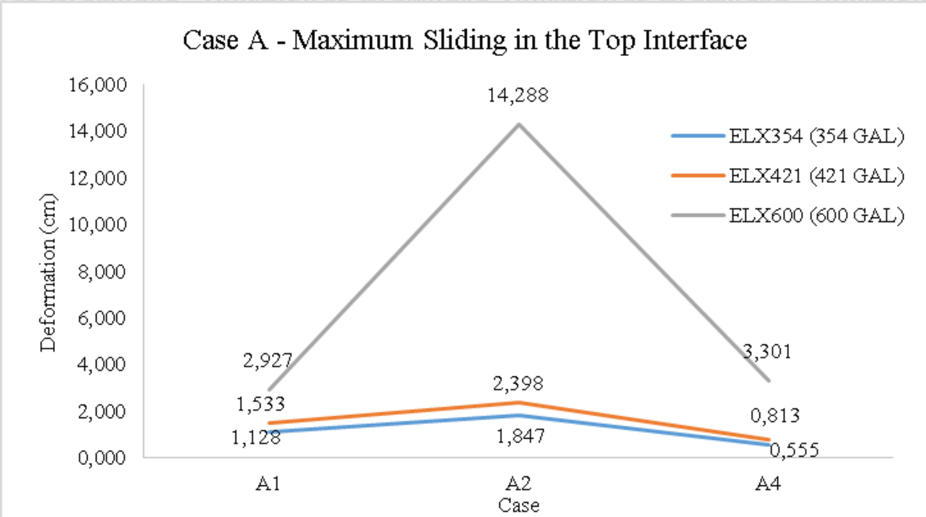

(a)

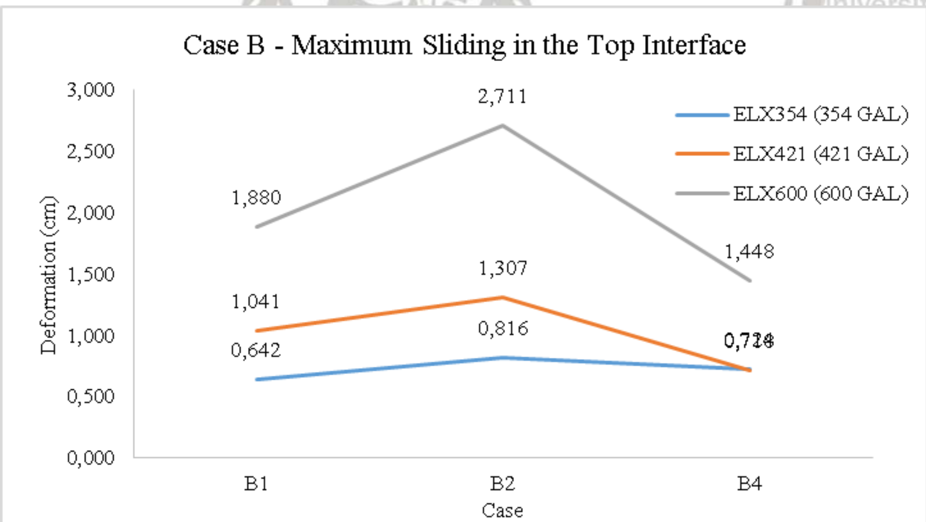

(b)

Figure 5. 21 Near fault, (a) Maximum sliding of the Top Interface on case A, (b) Maximum sliding of the Top Interface on case B

Under the far fault earthquakes as in figure 5.21, very large deformation happens in case A2 under TCU052 (600 gal), it is due to the energy that limited by the bottom friction transferred extremely to the top friction surface, as the result, deformation of the top friction sliding increase from 2.927 cm to 14.288 cm, and it brings the deck displaced very large as it can be seen on figure 5.19 (b).

5.3.3 Time Reference

The system analysis based on the time when the top surface reaches the maximum sliding need to be considered in order to design the gap distance between two decks. It is due to the deck motions influenced by the friction sliding in this interface. Table 5.3 is the time happening of the top surface when it reaches the maximum sliding displacement under the near fault, and table 5.4 is for those under the far fault earthquakes. At the time that written in table 5.3, the other element was analyzed and compare to find out the rubber bearing system at the reference time.

Table 5. 3 Near Fault, Time Table of the Top Friction Maximum Response

Case	Time reference (sec)		
	TCU068	TCU102	TCU052
A1	35.775	47.27	33.755
A2	35.765	47.265	33.74
A4	35.71	48.335	33.585
B1	35.72	47.205	33.625
B2	35.725	48.345	33.61
B4	35.69	48.315	33.54

Table 5. 4 Far Fault, Time Table of the Top Friction Maximum Response

Case	Time reference (sec)		
	ELX354	ELX421	ELX600
A1	37.17	37.18	37.19
A2	37.175	37.19	37.185
A4	12.89	12.6	12.62
B1	12.595	12.605	37.165
B2	12.605	12.605	37.175
B4	15.585	15.595	12.605

5.3.4 Behavior of the Rubber Bearing System at the Certain Time

At the reference time that mention in table 5.3 and 5.4 the system will observe under the near fault comparing with the far fault earthquake ground motions. Figure 5.22 shows the deformation value at the top surface, rubber, and the bottom surface at the time when the sliding maximum happen in the top surface under TCU068 (354 gal). Under TCU068, in case

A2 and B2 the rubber will be less deformed due to it have one weak part, that is the top friction surface, when the earthquake happens, the force will be concentrated on the weakest part of the rubber bearing system and the force that received by the rubber will be less than another case, this is the reason that the top friction deformation is large in case A2 and B2. Similar with the two cases before, case A1 and B1 also have similar behavior. In A1 and B1, due to the friction coefficient both in the top and the bottom surface is the same and small, the motions are limitless in the friction surface, so that the rubber and friction surface will work in balance, the result is the rubber will deform less because the leftover force will be dissipated by the friction surface in the top and the bottom side of the rubber bearing system. If the friction value increase to be as in case A4 and B4, the friction surface will be rougher and hard to provide a movement. Due to the friction surface in both side is more rigid, then the force will be received more by the rubber, the rubber deformation will be large and less in friction sliding.

Same behavior happens in the system under TCU102 (421 gal) and TCU052 (600 gal). In figure 5.23 as the result of TCU102, even though TCU102 is not the largest PGA of the ground motion, the deformation value under TCU102 is the largest, it is due to the near fault analysis is the special case as explain before. And overall, both under TCU102 and TCU052 provide the same behavior as the system under TCU068, the difference is about the deformation magnitude.

Under the near fault earthquakes at the time when the top surface reaches the maximum sliding displacement, different values that apply in the top friction surface (case A2 and B2) provide more deformation than applying same value in both surface (Case A1, A4, B1, and B4). For those case that with the higher rubber deformation have small in friction sliding deformation. In the same configuration value of the friction coefficient such in case A1, A4, B1 and B4, cases with the higher value of the friction coefficient provide smaller deformation. Its means that, even though at the time when the top surface deformed in maximum, applying larger friction coefficient will reduce the capability of the friction surface to move.

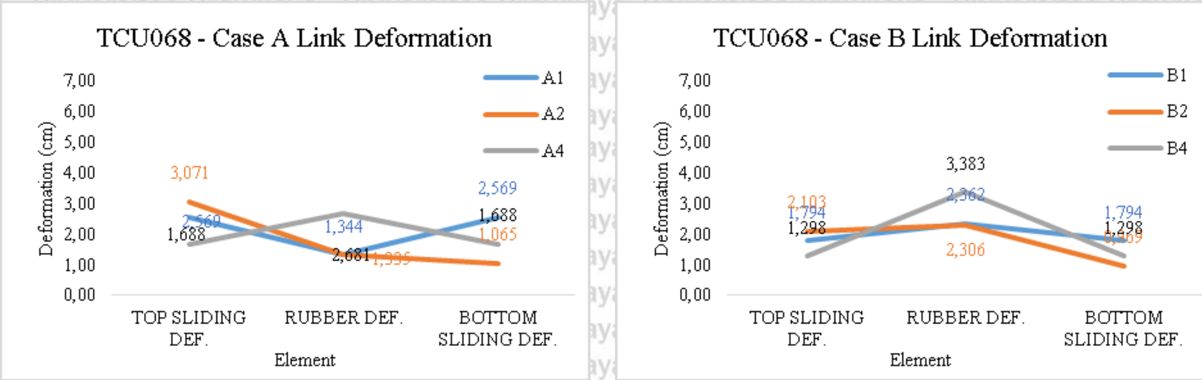

(a) (b)

Figure 5. 22 Near fault TCU068 (354 gal), (a) Link Deformation of case A, (b) Link Deformation of case B, (Top Sliding Maximum)

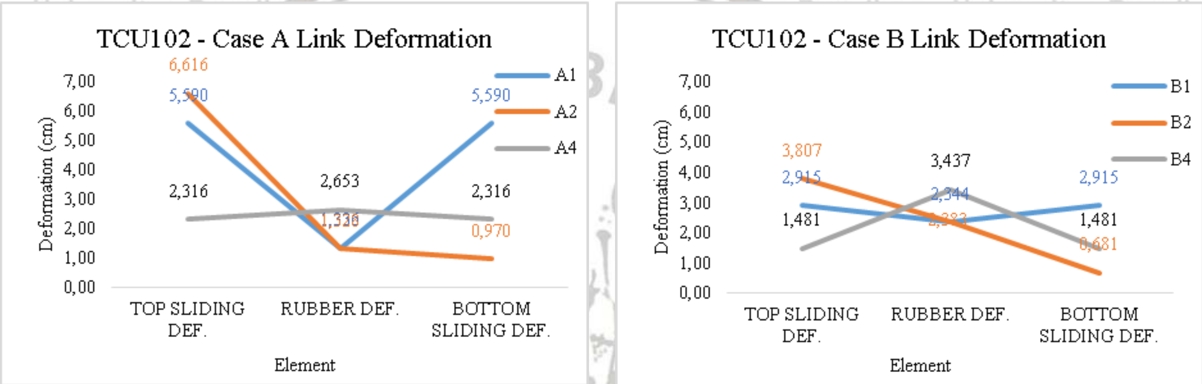

(a) (b)

Figure 5. 23 Near fault TCU102 (421 gal), (a) Link Deformation of case A, (b) Link Deformation of case B, (Top Sliding Maximum)

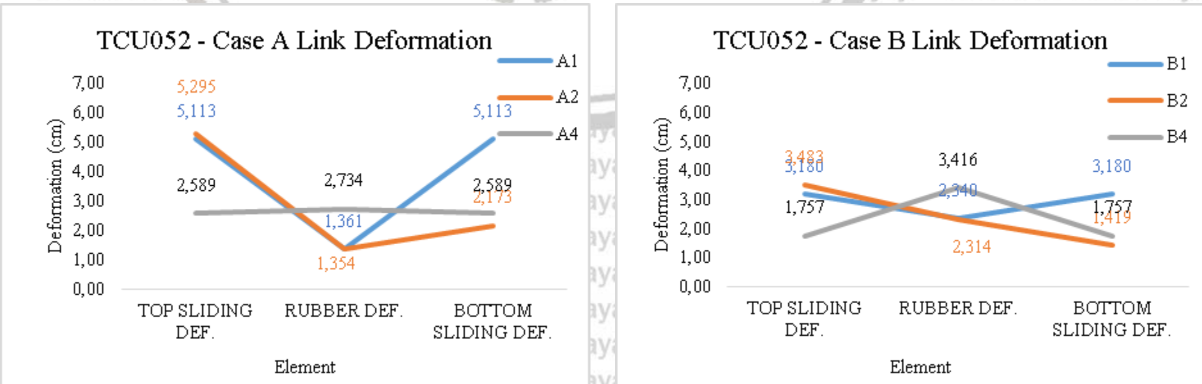

(a) (b)

Figure 5. 24 Near fault TCU052 (600 gal), (a) Link Deformation of case A, (b) Link Deformation of case B, (Top Sliding Maximum)

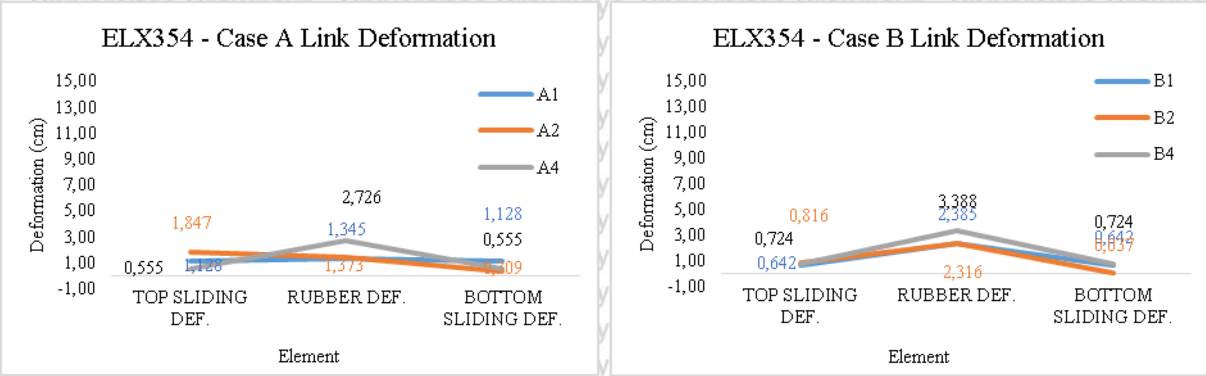

(a) (b)

Figure 5. 25 Far fault ELX354 (354 gal), (a) Link Deformation of case A, (b) Link Deformation of case B, (Top Sliding Maximum)

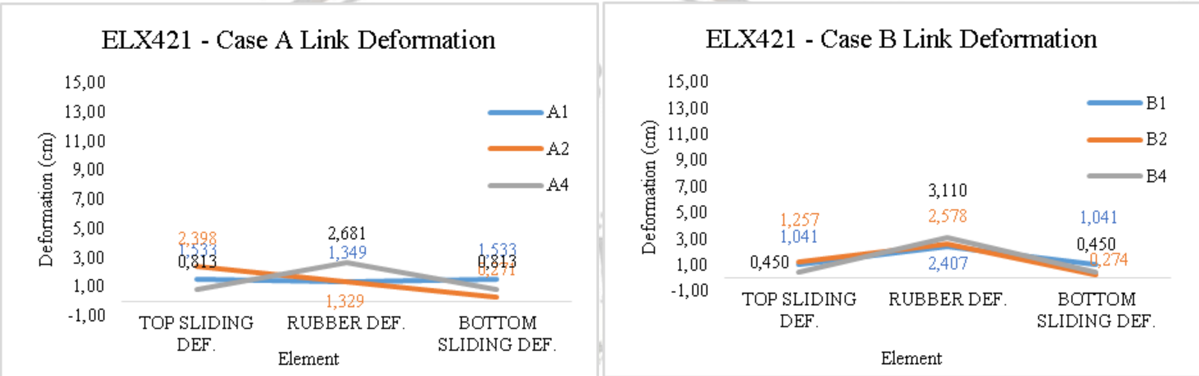

(a) (b)

Figure 5. 26 Far fault ELX421 (421 gal), (a) Link Deformation of case A, (b) Link Deformation of case B, (Top Sliding Maximum)

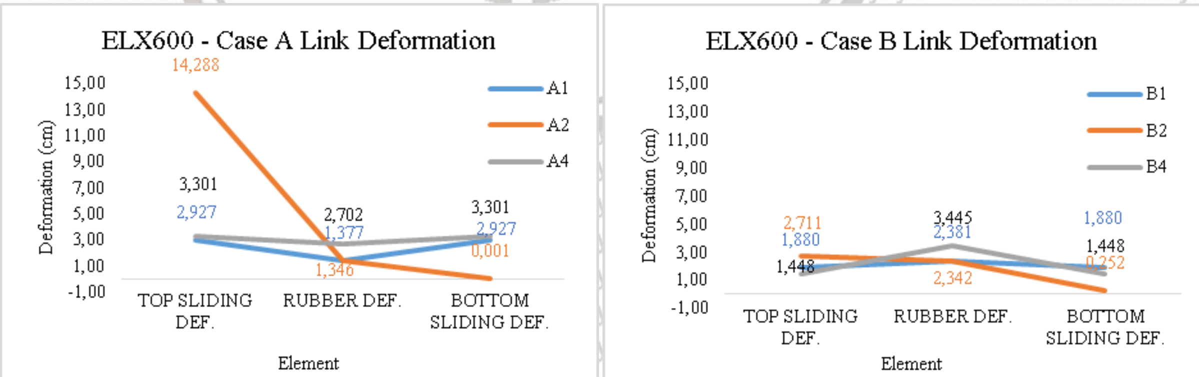

(a) (b)

Figure 5. 27 Far fault ELX600 (600 gal), (a) Link Deformation of case A, (b) Link Deformation of case B, (Top Sliding Maximum)

Comparing near fault analysis with far fault analysis. Figure 5.25 until figure 5.27 show the analysis result under the far fault earthquakes. Deformation of the rubber dominate more to the bearing behavior than the sliding, it can be seen in the figure, that mostly result shown the rubber always deformed higher than the friction sliding. It is means that under the far fault earthquakes rubber have an important role to handle the force than the friction surface. The same result as the near fault analysis that shown on the system that applied the small value of friction coefficient in the top surface, as in case A2 and B2. Since they easier to move due to the smaller friction coefficient, then the force will transmit more to the top surface, and the top surface will slide more than the bottom surface.

From the deformation of each element, then the displacement in each sliding point can be calculated. Consider the sliding points that mention in figure 3.2, figure 5.28 until 5.30 shows the displacement point under the near fault analysis. Each displacement point was calculated in equation 5.1 until equation 5.4, and each position as in figure 3.2 in the chapter 3. Under the smallest peak ground acceleration of TCU068 (354 gal), it shows in figure 5.28 that increasing the friction value in the same configuration (A1, A4, B1, B4) give the small impact, due to the curve of both smaller or higher value always close each other. The difference only shows by the case that have different friction configuration (A2, B2), because of there are unbalance in force transmission, in A2 and B2 case, rubber bearing system could not perform well, it is proven by the small displacement that can absorb compare with another case.

It has been observed before that the sensitivity response under the near fault is not caused by increasing magnitude of the peak ground acceleration, but it depended on the characteristic of the near fault ground motion itself. Compare the result of TCU102 (421 gal) and TCU052 (600 gal) in figure 5.29 and 5.30. Under both ground motion, the significant difference showed by case in the same configuration (A1, A4, B1, and B4). Case A1 and B1 still have larger displacement than A4 and B4. But they are not close each other, it is means that the difference effect of increasing the friction value will be shown in the larger ground motion, since TCU102 and TCU052's PGA is larger than TCU068.

When the system analyzed under the far fault ground motion. Due to the rubber will be more dominant to overcome the force, then the rubber bearing system behavior depend on how far the rubber deformed when the earthquakes happen. As shown in figure 5.31 until 5.33,

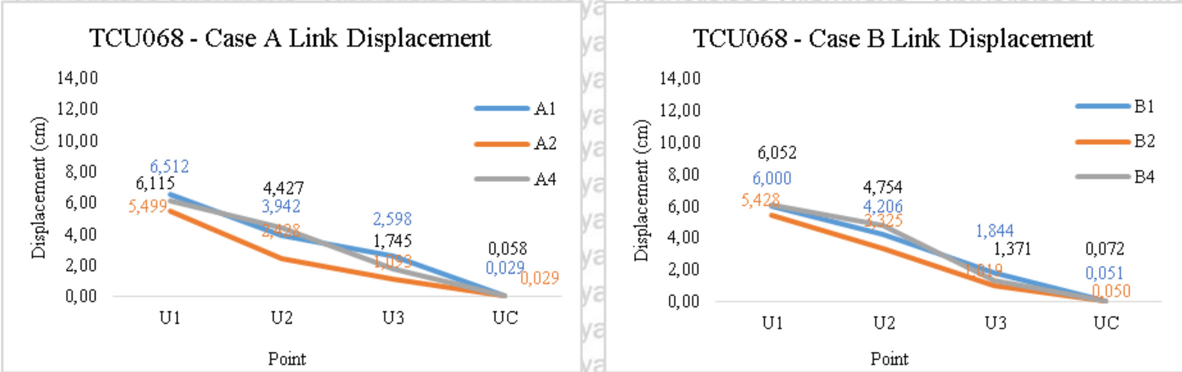

Figure 5. 28 Near fault TCU068 (354 gal), (a) Displacement point of case A, (b) Displacement point of case B, (Top Sliding Maximum)

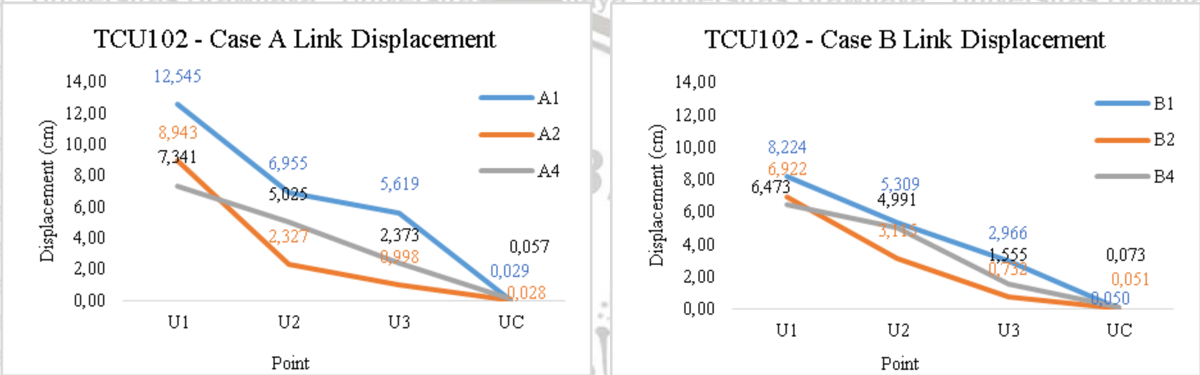

(a) (b)

Figure 5. 29 Near Fault TCU102 (421 gal), (a) Displacement point of case A, (b) Displacement point of case B, (Top Sliding Maximum)

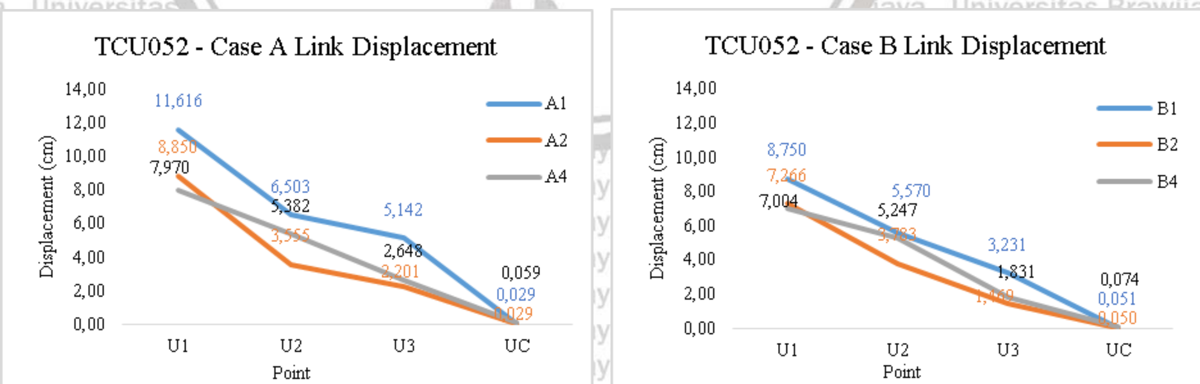

(a) (b)

Figure 5. 30 Near Fault TCU052 (600 gal), (a) Displacement point of case A, (b) Displacement point of case B, (Top Sliding Maximum)

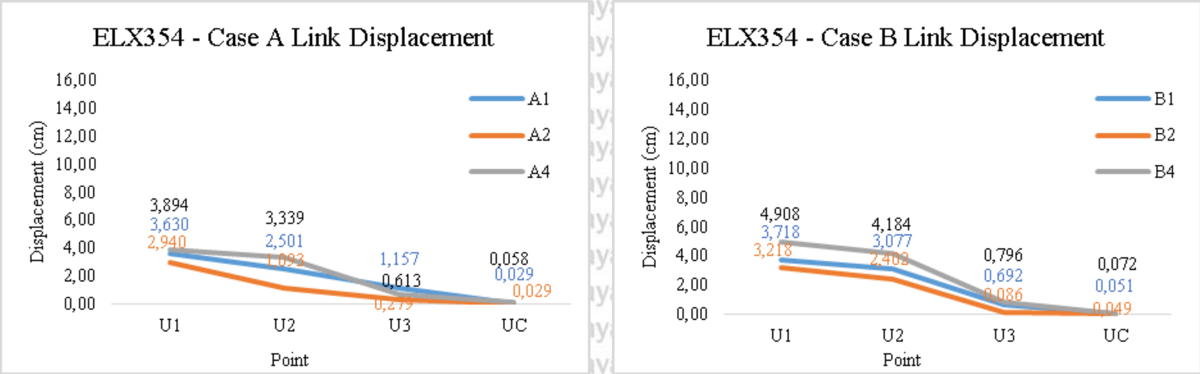

(a) (b)

Figure 5. 31 Far Fault ELX354 (354 gal), (a) Displacement point of case A, (b) Displacement point of case B, (Top Sliding Maximum)

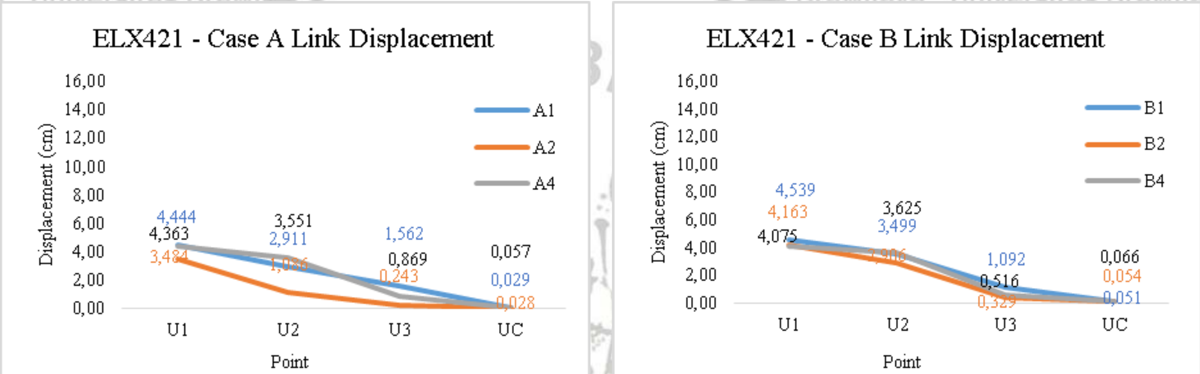

(a) (b)

Figure 5. 32 Far Fault ELX421 (421 gal), (a) Displacement point of case A, (b) Displacement point of case B, (Top Sliding Maximum)

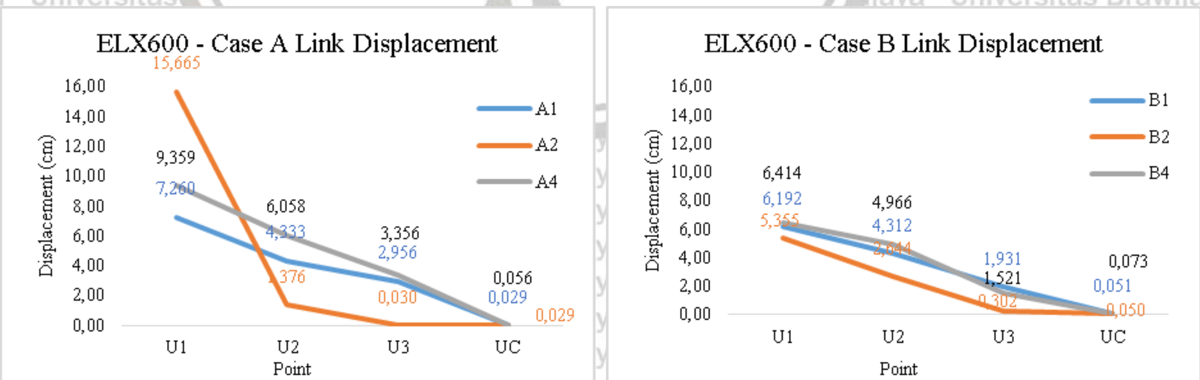

(a) (b)

Figure 5. 33 Far Fault ELX600 (600 gal), (a) Displacement point of case A, (b) Displacement point of case B, (Top Sliding Maximum)

except the result in case A under TCU052, the displacement in case A4 and B4 always larger than A1 and B1, but A4 and A1 also B4 and B1 are nearly close each other. It means that increasing friction value in the same configuration will be increasing the displacement but only give small differences. In the difference configuration of friction value as in case A2 and B2, due to there have concentrating force effects, then the force will be transmitted more to the rubber and the top friction surface, due to there have small contribution of the bottom surface friction, then the displacement that can be provided by case A2 and B2 is less than the other case. As long as the earthquake magnitude increase, the concentration energy will be more in the weaker part, as it shown in the figure 5.33 (a) and (b), the bottom surface almost does not give a contribution since the displacement value is close to zero.

5.4 Design the Column's Cap Beam Size

5.4.1 Maximum Column Displacement

For the last objective of this research, due to it is allowed the movement of the bottom side of the rubber bearing system, an enough size of the cap beam need to provide to prevent the bridge falling due to the rubber bearing movement. Since the column displacement considered in this analysis due to they have large inertial mass, the column displacement response observed as the first consideration. Overall response that shown in figure 5.34 both in case A and case B, increasing friction coefficient value will be increasing the column displacement response. Under the near fault ground motion, response of TCU102 (421 gal) is less than the results under TCU068 (354 gal) and TCU052 (600 gal). Maximum displacement of the column under TCU068 and TCU052 shows the difference in case A1, yet become closer as increase as the value of friction coefficient, and finally very close in case A4. Consider that the friction value of A4 is close to B1, start from B1 to B4, the column maximum displacement of the system under TCU068 and TCU052 are almost similar.

Under the far fault earthquakes as in figure 5.35, increasing the friction coefficient values will be increasing maximum displacement of the column, except on the case A under TCU052 (600 gal). Due to the behavior of the system will be change as long as the peak acceleration increase, then the column displacement under ELX421 (421 gal) always higher than under ELX354 (354 gal). Both in case A and case B, different configuration of the friction coefficient (A2 and B2) provide the middle column response, if it compares with case A1, A4, B1, and B4.

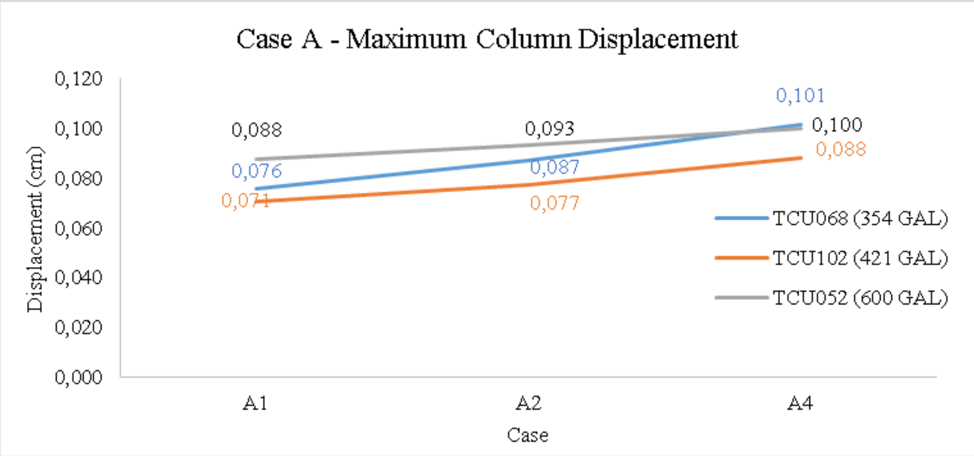

(a)

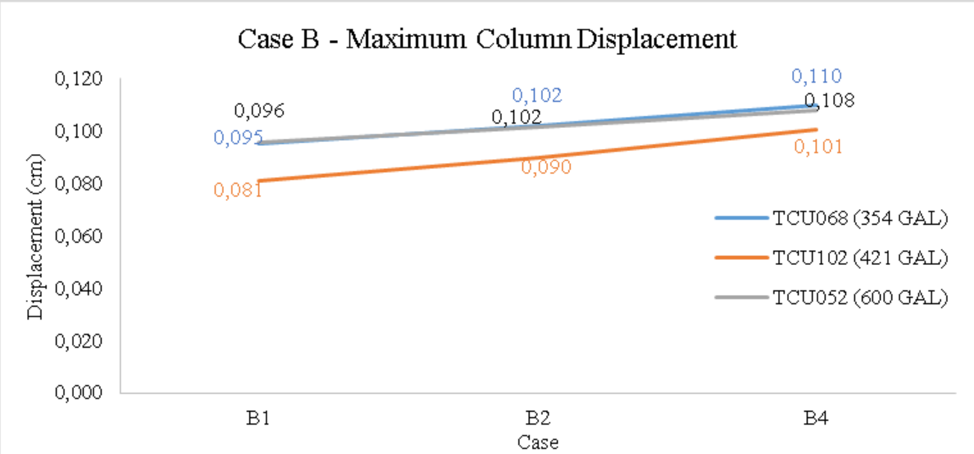

(b)

Figure 5. 34 Near fault, (a) Maximum Column Displacement of case A, (b) Maximum Column Displacement of case B

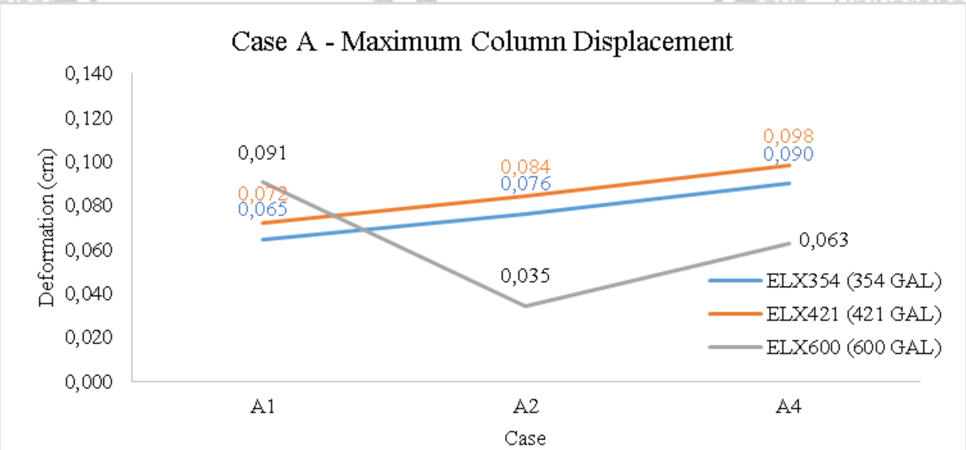

(a)

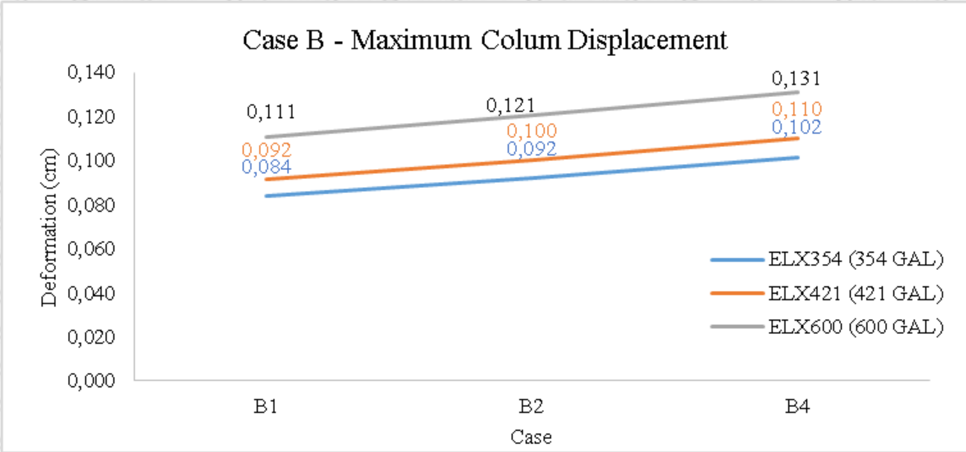

(b)

Figure 5. 35 Far fault, (a) Maximum Column Displacement of case A, (b) Maximum Column Displacement of case B

5.4.2 Maximum Sliding Deformation of the Bottom Friction Surface

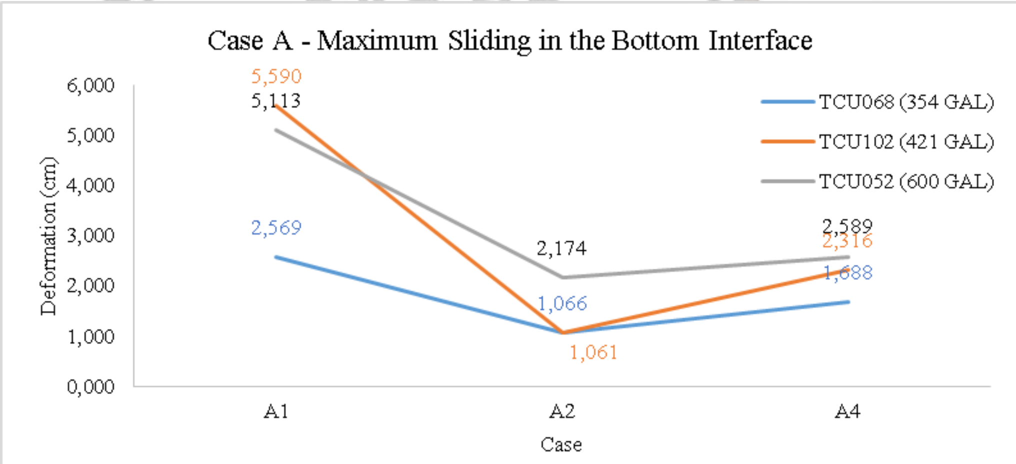

(a)

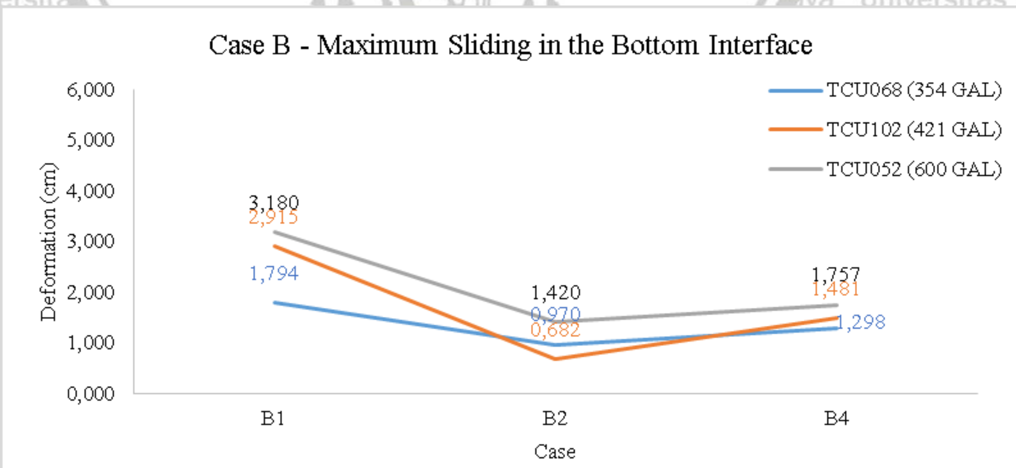

(b)

Figure 5. 36 Near fault, (a) Maximum Sliding of the Bottom Interface on case A, (b) Maximum Sliding of the Bottom Interface on case B

Second consideration yet the most important is the sliding displacement of the bottom surface friction. Put the case under TCU102 (421 gal) as an exception. Under TCU068 (354 gal) and TCU052 (600 gal) as shown in figure 5.36, sliding deformation of the bottom surface under TCU052 is larger than the sliding under TCU068, its related with increasing the magnitude of peak ground acceleration of the earthquake. And also increasing friction value of the same configuration from A1 to A4 and B1 to B4 will be decrease the deformation, since the movement will be limited on the large value of friction coefficient.

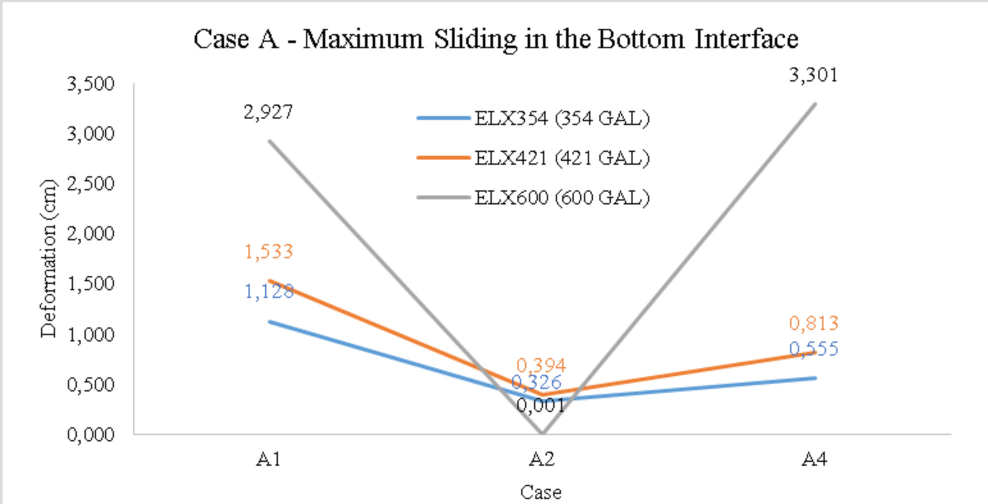

(a)

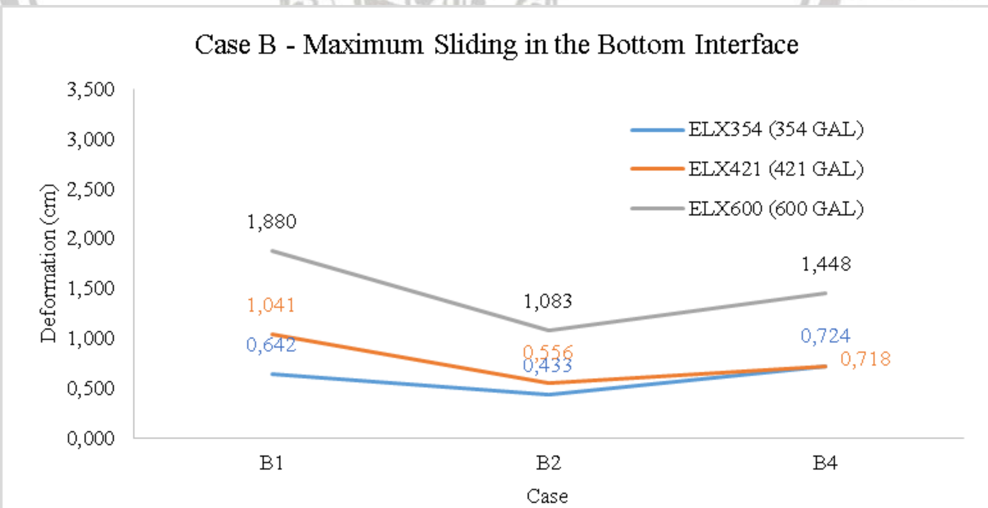

(b)

Figure 5. 37 Far fault, (a) Maximum Sliding of the Bottom Interface on case A, (b) Maximum Sliding of the Bottom Interface on case B

The different behavior that happen in case A2 under ELX600 answered in this study. When the large force transmitted to the structure, the force will be concentrated on the weakest element. The system with A2 configuration is applied the smaller coefficient value on the top surface friction, this surface friction became the weakest point. Because of ELX600 is the highest earthquakes input, then the force directly focused on the top surface and it caused the sliding in the top surface became very large and effected on the deck displacement. it is proven by the sliding displacement of the column and bottom surface that are very small, simply means that the force passed this element as a rigid element, due to the small force that need to overcome, they react the small force with small displacement.

5.4.3 Time Reference

The response of the bottom surface is the most important parameter to design the cap beam size, due to the bottom surface of the rubber bearing system is the element that connect directly to the cap beam. After the data response of the maximum deformation of the bottom friction surface have been analyzed at each time step. Then the time when the maximum responses were identified to analyzed other element at the same time with the maximum response of the bottom interface. Table 5.5 and 5.6 is the details of the time when the bottom surface deformations happen.

Table 5. 5 Near Fault, Time Table of the Bottom Friction Maximum Response

Case	Time reference (sec)		
	TCU068	**TCU102**	**TCU052**
A1	35.775	47.27	33.755
A2	35.69	48.31	33.585
A4	35.71	48.335	33.585
B1	35.72	47.205	33.625
B2	35.68	48.305	33.54
B4	35.69	48.315	33.54

Table 5. 6 Far Fault, Time Table of the Bottom Friction Maximum Response

Case	Time reference (sec)		
	ELX354	**ELX421**	**ELX600**
A1	37.17	37.18	37.19
A2	12.88	15.565	12.79
A4	12.89	12.6	12.62
B1	12.595	12.605	37.165
B2	15.55	15.575	12.6
B4	15.585	15.595	12.605

5.4.4 Behavior of the Rubber Bearing System at the Certain Time

Under the near fault analysis, if the consideration is on the maximum deformation of the bottom surface, comparing the same configuration of A1-A4 and B1-B4, due to the smaller value of friction coefficient, case A1 always provide largest deformation than A4, so do B1 always be larger than B4. The larger friction value of A4 and B4 have smaller deformation right after A1 and B1. Meanwhile, the different value of friction coefficient in case A2 and B2 provide the smallest deformation of the bottom friction. Even though, case A2 and B2 provide the smallest deformation, but as small as the deformation of the bottom surface, then the deformation in the top surface will be higher.

If these result compare with the analysis under far fault earthquakes as in figure 5.41 until figure 5.43. A1 and B1 always provide large deformation on the bottom surface than others, A2-A4 and B2-B4 will be closely similar, this condition happen except on the case A under ELX600 due to the special case that explained before.

Deformation result is a relative value of the element's displacement at the local point. If u_c is the column displacement, u_{ST} is the top friction's sliding deformation, u_{RB} is the rubber deformation, and u_{SB} is the bottom friction sliding deformation. Then, the displacement of each point u_c,u_1, u_2, and u_3 can be calculated by equation 5.1 until equation 5.4.

Under the near fault earthquake of TCU068 (354 gal), due to TCU068 is the smallest ground motion in the near fault earthquakes, so that the variation effect of the friction force still not be observed since the result is very close. And under TCU102 (421 gal), the effect of different friction coefficient began to show. Both in case A and case B, three case of A1, A2, and A4 shows their differences, so do them in case B. Smaller coefficient values in the same configuration (A1 and B1), at the time when the bottom surface deformed in maximum they always provide more displacement compare with another case. And the larger friction values (A4 and B4)'s result placed in the middle, and provide the smallest displacement in the top friction surface. And the smallest result provided by the different combination (A2 and B2) due to the bottom surface do not give more movement. Under TCU052 (600 gal), the displacement behaviors are similar with TCU102 (421 gal), due to TCU052 is not as stronger as TCU102, then differences are not as significance as in TCU102. But if it compares with the far fault earthquakes, at the smallest earthquakes on ELX354 (354 gal), A4 and B4 provide more displacement than A1 and B1. And case A2 and B2 (different configuration)

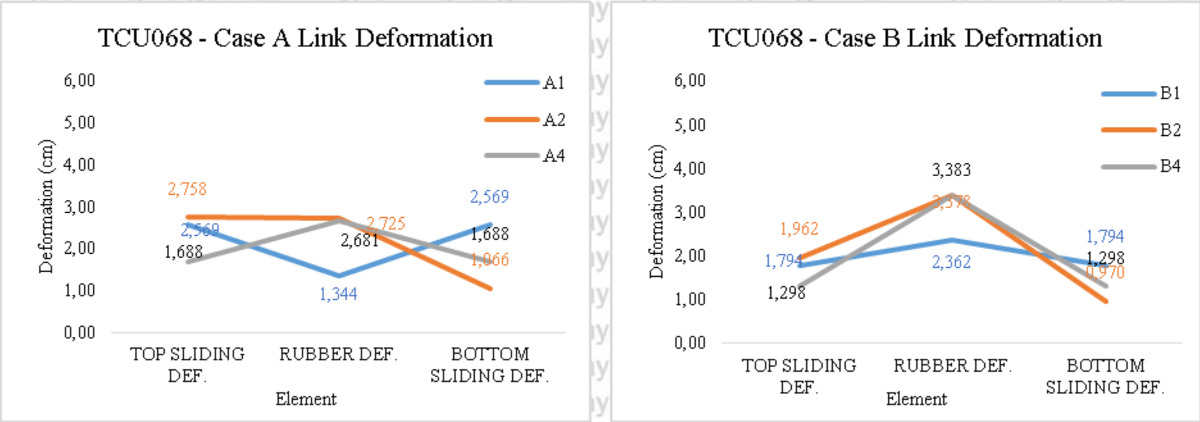

(a) (b)

Figure 5. 38 Near fault TCU068 (354 gal), (a) Link Deformation of case A, (b) Link Deformation of case B, (Bottom Sliding Maximum)

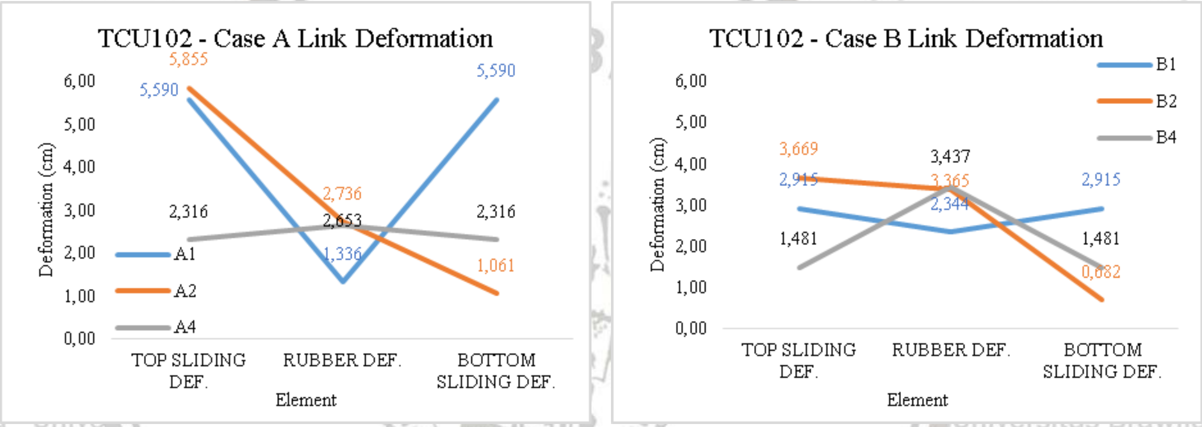

(a) (b)

Figure 5. 39 Near fault TCU102 (421 gal), (a) Link Deformation of case A, (b) Link Deformation of case B, (Bottom Sliding Maximum)

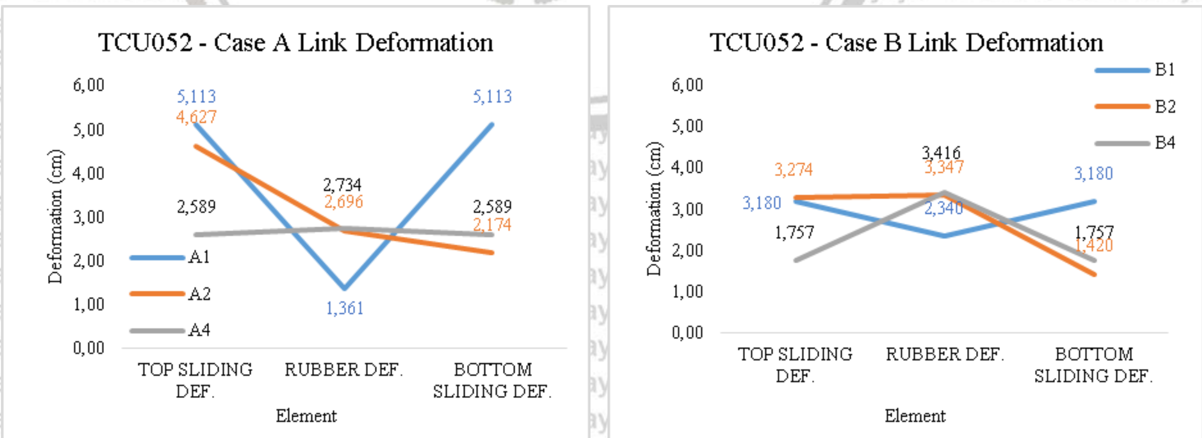

(a) (b)

Figure 5. 40 Near fault TCU052 (600 gal), (a) Link Deformation of case A, (b) Link Deformation of case B, (Bottom Sliding Maximum)

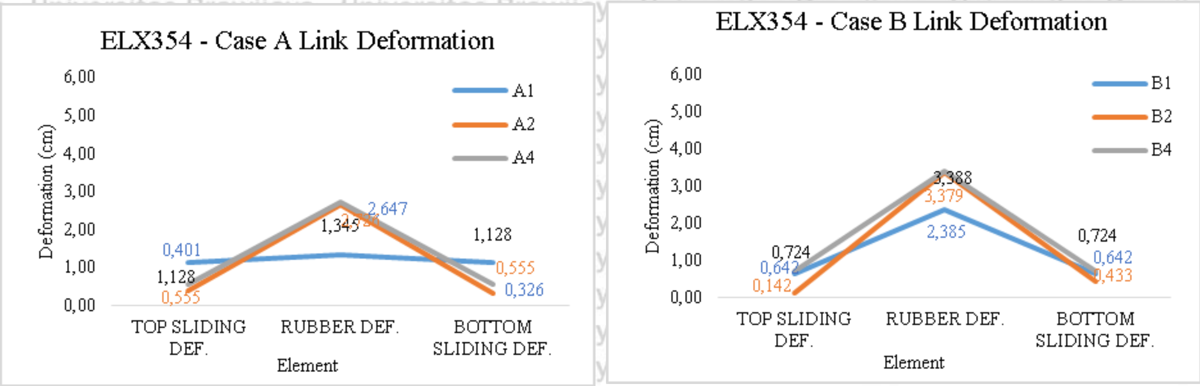

(a) (b)

Figure 5. 41 Far fault ELX354 (354 gal), (a) Link Deformation of case A, (b) Link Deformation of case B, (Bottom Sliding Maximum)

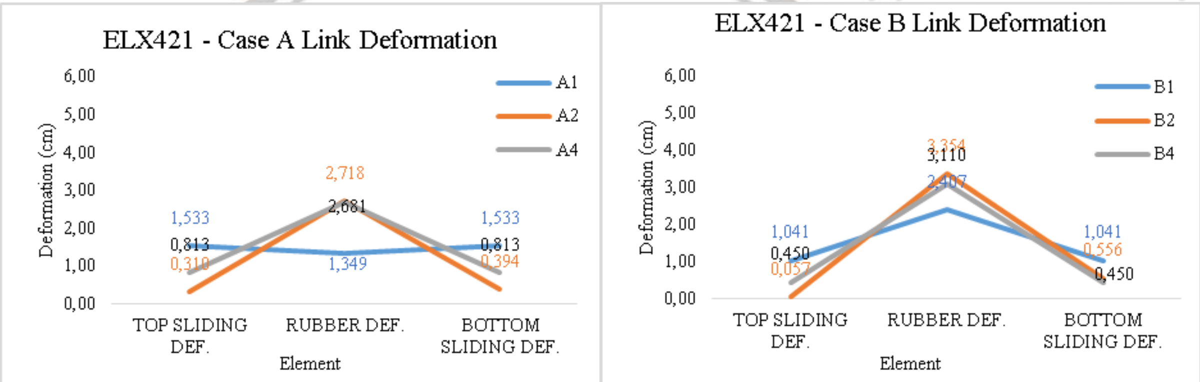

(a) (b)

Figure 5. 42 Far fault ELX421 (421 gal), (a) Link Deformation of case A, (b) Link Deformation of case B, (Bottom Sliding Maximum)

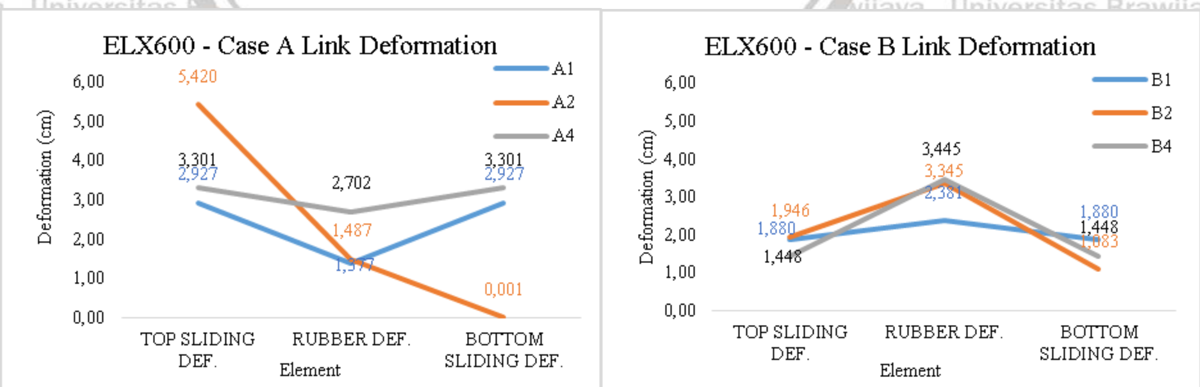

(a) (b)

Figure 5. 43 Far fault ELX354 (354 gal), (a) Link Deformation of case A, (b) Link Deformation of case B, (Bottom Sliding Maximum)

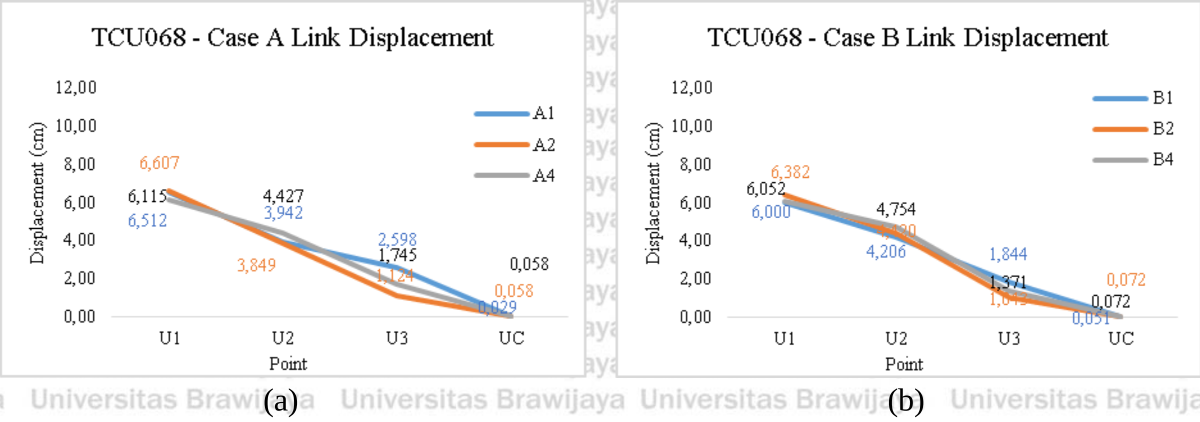

Figure 5. 44 Near fault TCU068 (354 gal), (a) Link Deformation of case A, (b) Link Deformation of case B, (Bottom Sliding Maximum)

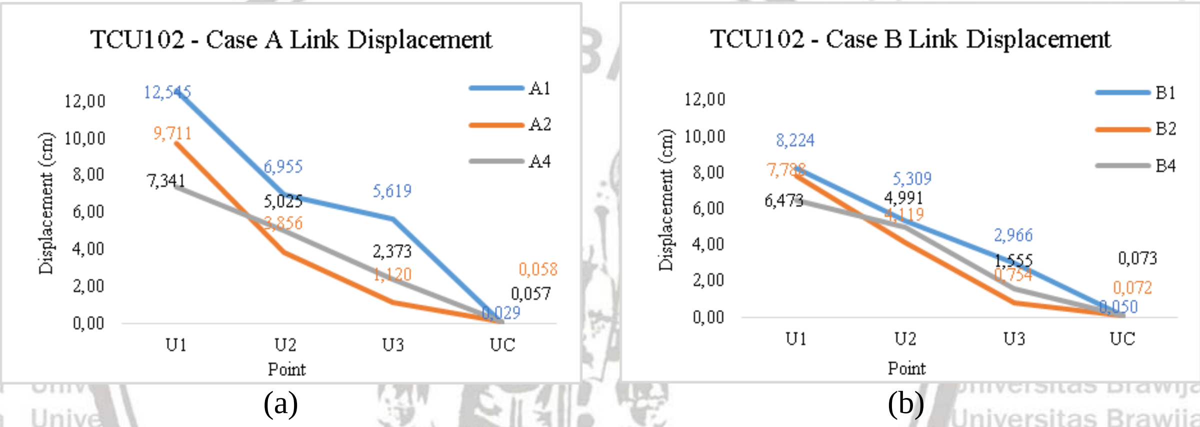

Figure 5. 45 Near fault TCU102 (421 gal), (a) Link Deformation of case A, (b) Link Deformation of case B, (Bottom Sliding Maximum)

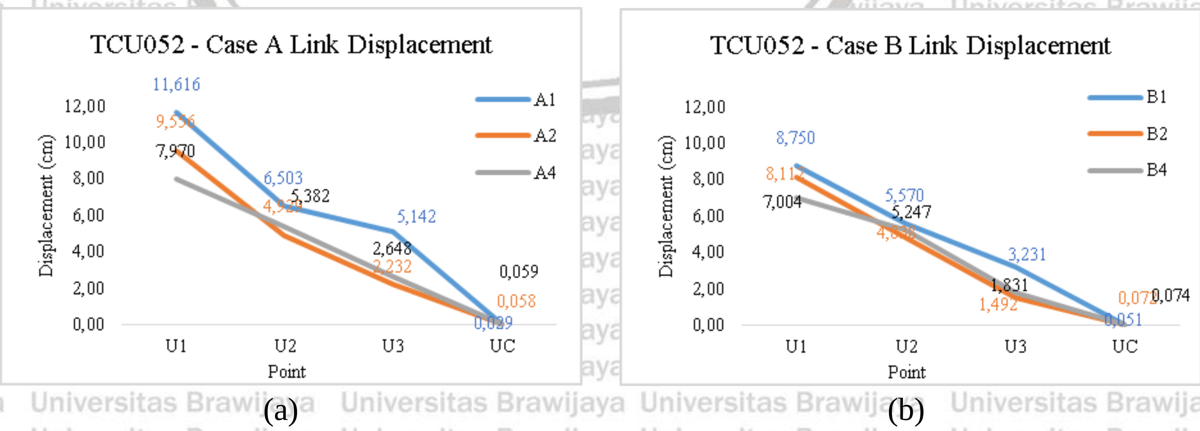

Figure 5. 46 Near fault TCU052 (600 gal), (a) Link Deformation of case A, (b) Link Deformation of case B, (Bottom Sliding Maximum)

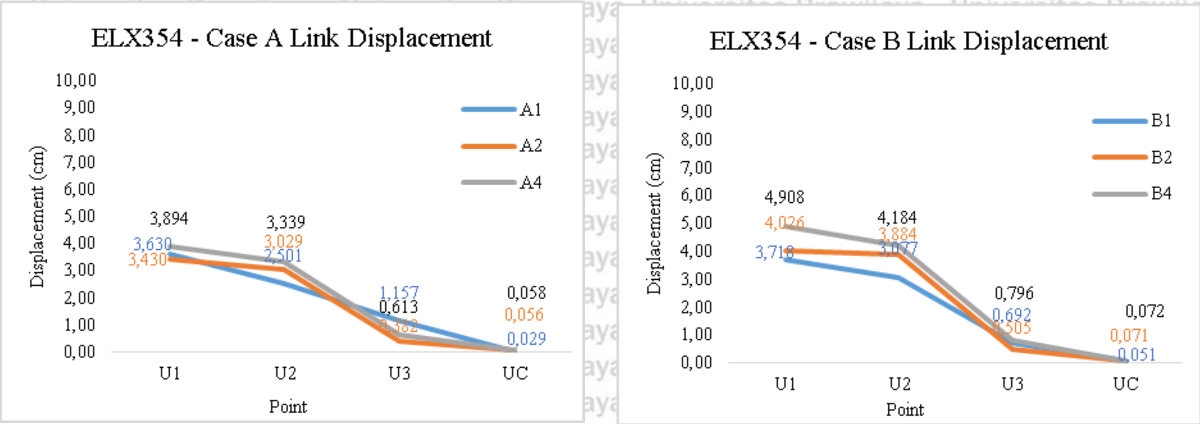

(a) (b)

Figure 5. 47 Far fault ELX354 (354 gal), (a) Link Deformation of case A, (b) Link Deformation of case B, (Bottom Sliding Maximum)

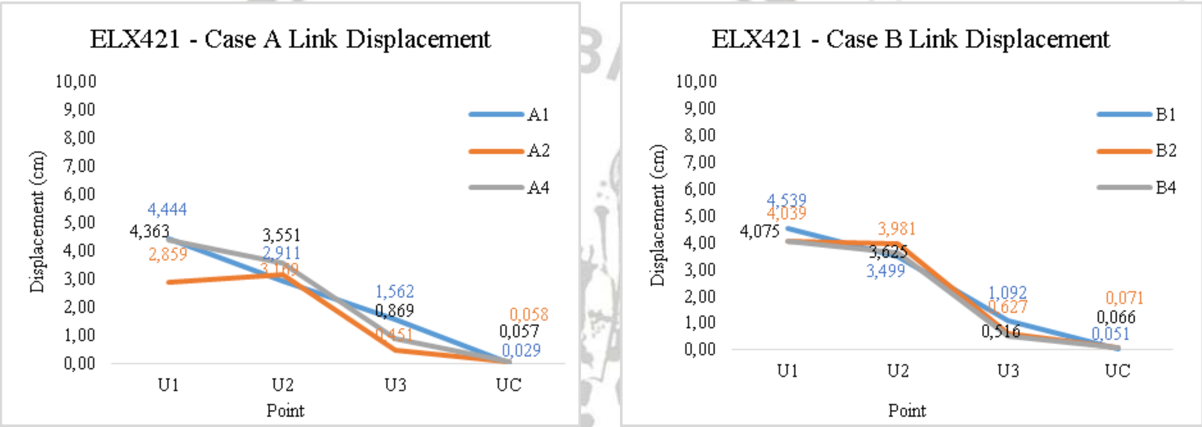

(a) (b)

Figure 5. 48 Far fault ELX421 (421 gal), (a) Link Deformation of case A, (b) Link Deformation of case B, (Bottom Sliding Maximum)

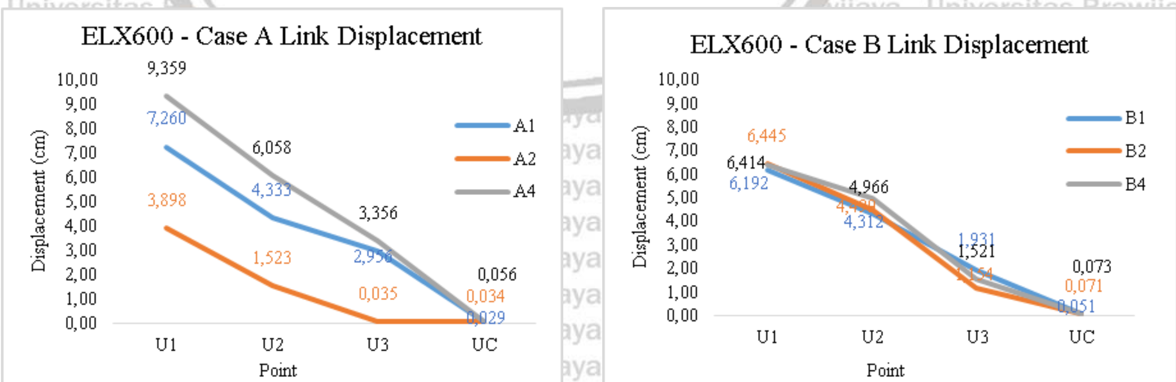

(a) (b)

Figure 5. 49 Far fault ELX600 (600 gal), (a) Link Deformation of case A, (b) Link Deformation of case B, (Bottom Sliding Maximum)

always be in the middle. Increase the PGA to be ELX421 (421 gal), the behavior is the same in case B, remember that case B's friction values are bigger than case A's. In case A, A1 will be higher in the top and bottom surface point but not in the rubber point, its means that rubber working less in case A1 due to the friction surface is lower. Case A2 provide less displacement than case A1. Case A2 become weaker with providing less displacement compare with case A1 and A4. Under the highest acceleration of the far fault ELX600 (600 gal), in case B, the difference of each case is very small, means in the strongest motion of the far fault earthquakes, the variation effect of friction coefficient is very small. But the big different happen in case A, A4 displaced more than A1, and A2 provide the smallest displacement due to the bottom surface did not give displacement contribution since the bottom surface in case A2 is rougher.

5.5 Standard Design Code

American Association of State Highway and Transportation Officials (AASHTO) is a guideline standard of bridge and highway construction design that used in America. Load Resistant Factor Design (LRFD) as the part of the standard design of AASHTO mention the standard design of the expansion joint, rubber capacity, and seating displacement that allowed.

In order to make sure that the deck pounding do not happen in a deck bridge and the abutment. The AASHTO LRFD that retrieved by Minnesota Department of Transportation mention about modular expansion joints on chapter 14.2.3 that list the opening between the deck and abutment should be less than 4 inches (10.16 cm). In table 14.7.6, the design code explained about the maximum allowed deformation of the elastomeric bearing pad based on the laminates thickness and number of laminates. Table 5.7 shows the standard design of the elastomeric bearing pad requirement.

Table 5. 7 Elastomeric bearing pad for prestressed concrete beam.
(AASHTO LRFR Table 14.7.3)

Interior Laminate Thickness (in)	D (in) ③	Number of Laminates	Total Elastomer Thickness, h_{rt} (in) ③	Maximum Movement Δ_s (in) ④
$^1/_2$"	$2^1/_2$	3 ⑤	2	1
	$4^3/_8$	6 ⑤	$3^1/_2$	$1^3/_4$
	5	7	4	2
	$5^5/_8$	8	$4^1/_2$	$2^1/_4$

Take the number of laminates is 3 due to there are 3 thin steel layer inside the rubber bearing system, then it can be found that the maximum movement of the bearing pad from the undeformed state to the point of maximum deformation is 1 inch (2.54 cm), considering the temperature change with a 1.3 load factor for the rubber design, then the allowable deformation based on the LRFD design code is 1.3 inch (3.302 cm). Sliding translation of the elastomeric bearing pad mention on the same design. They limit the translation until 4 inches (10.16 cm).

5.6 Conclusion

In order to design the bridge and avoid the bridge falling when the earthquakes happen. Several analyses related with the bridge falling reasons had been study to find out the parameter that need to pay more attention. Three main objectives consider in this study, first, to design a proper rubber bearing to avoid the bearing's failure. Second, to provide an enough gap between two decks, in order to prevent inter-deck crashing. And the third, to design the cap beam size, due to the provide an enough space of bearing to slide, related with column displacement. Several case had been proposed under the near fault of Chi-Chi Earthquakes that comparing with far fault earthquakes of El-Centro ground motions. Here are the conclusions:

Parameters to Design a proper rubber bearing system:

1. TCU102 (421 gal) is the strongest motion of the near fault earthquakes, but provide the lowest value of the overall result of the rubber maximum deformations.
2. The effect of variation of the friction coefficient under TCU068 (354 gal) and TCU052 (600 gal) give a big difference on case A1 and become closer in A2, suddenly almost the same in case A4. Yet no big differences in case B.
3. Rubber deformations are depending on the variation of the friction coefficient, as increase as the values of the friction coefficient, as large as the rubber deformation. It is due to increasing the friction values in the top and the bottom surface friction will limit the sliding movement of its, so that the force will be focused on the rubber, finally the rubber need to deformed more since the energy become larger.
4. As large as the rubber deformed, as small as the leftover energy that received by the top surface and the bottom surface, then the sliding deformation will be decrease.
5. Under TCU068 (354 gal) friction coefficient combinations as A4 and B4 will be provide more displacement than A1 and B1. Under TCU052 (600 gal) the combinations as in case A1 and B1 provide more displacement than A4 and B4. Under TCU102 (421 gal), in case A, friction coefficient combinations as A4 and B4 will be provide more displacement than

A1 and B1, but in case B, the combinations as in case A1 and B1 provide more displacement than A4 and B4.

6. Overall result shows that the different combination of the friction coefficient as in case A2 and B2 provide the smallest displacement.

Parameters to Design the gap distance of the deck:

7. Under the smallest ground motion of TCU068 (354 gal), increasing friction coefficient values will be less increasing on the deck displacement. But under TCU102 (421 gal) and TCU052 (600 gal), the deck displacement will be decrease in line with increasing the friction coefficient values.
8. Under the near fault ground motions, in the same configuration of the friction coefficient as in case A1, A4, B1, and B4, the sliding deformation of the top surface are increase in line with increasing friction coefficient. Different configuration as case A2 and B2 always provide the largest top surface sliding since the lower friction values applied than in the bottom surface.
9. Under the near fault analysis, case A2 and B2 always provide the highest top sliding deformation, case A1 and B2 will be the second highest, and A4 and B4 will be the lowest. As high as the top friction sliding deformation provided, as small as the deformation of the rubber.
10. At the time when the top surface in the maximum response, under the smallest near fault ground motion of TCU068 (354 gal), the effect of variation of the friction force is very small on the bearing displacement of the system that have same configuration as in case A1-A4 and B1-B4. Yet, case A2 and B2 always provide the smallest displacement. Under TCU052 (600 gal), displacement of case A1 and B1 increase and become larger than A4 and B4, it is due to A1 and B1 have smaller friction coefficient that allowed the surface to sliding more. Still case A2 and B2 provide the smallest displacement. Under TCU102 (421 gal), the bearing displacements are similar with the system under TCU052, but the displacement values are getting higher.

Parameters to Design the Column's Cap Beam size:

11. Overall result under the near fault ground motions, column displacement will be increase in line with increasing the coefficient of friction values. Under TCU068 (354 gal) and TCU052 (600 gal), the big difference shows on the column displacement in case A1 then become closer in case A2 and almost similar in case A4, and totally close in case B. The column displacement under TCU102 (421 gal) always be the smallest compare with TCU068 and TCU052, both in case A and case B.
12. Under the near fault ground motions, in the same configuration of the friction force (A1, A4, B1, B4), the bottom sliding deformation will be decrease in line with increasing the friction coefficient values. And the bottom sliding deformation will be much more decrease in case A2 and B2.
13. At the time when the bottom surface reaches the maximum response, the bottom sliding of case A1 and B1 always be larger than A4 and B4, so that the rubber deformation of A4 and B4 always be larger than A1 and B1, and the big changing happen on case A2 and B2, as small as the deformation of the bottom sliding in this case, as large as the deformation of the top sliding surface.
14. When the bottom surface is on maximum response, under the smallest ground motion of TCU068 (354 gal), the effect of increasing friction values is very small, and under TCU052 (600 gal) the elements displacement of the case A1 and B1 will be higher than A4 and B4, and case A2 and B2 are between them. Under TCU102 (421 gal), the displacement of A1 and B1 will be higher, and the gap with the displacement of A4 and B4 become wider. Meanwhile, A2 and B2 are become the smallest in all of the displacement point except on the top surface.

Table 5.7 until 5.12 resume the overall result of the expansion joint that need to provide in order to avoid the deck pounding, Rubber deformation capacity, and the seating displacement that need to provide in order to avoid the bridge falling under the near fault and far fault earthquakes. Take the standard design of AASHTO LRFD manual design code.

Table 5. 8 Near fault - Deck displacement.

Near Fault	Maximum Deck Displacement (cm)						Standard Expansion Joint
	A1	A2	A4	B1	B2	B4	
TCU068 (354 GAL)	7.390	7.161	7.437	7.198	7.218	7.393	10.16
TCU102 (421 GAL)	13.092	10.135	8.527	9.280	8.471	7.629	
TCU052 (600 GAL)	12.209	9.927	8.880	9.612	8.679	7.988	

Table 5. 9 Far fault - Deck displacement

Far Fault	Maximum Deck Displacement (cm)						Standard Expansion Joint
	A1	A2	A4	B1	B2	B4	
ELX354 (354 GAL)	4.277	4.291	5.160	4.569	5.217	6.093	10.16
ELX421 (421 GAL)	4.959	4.944	5.421	5.530	5.434	6.386	
ELX600 (600 GAL)	7.904	15.804	9.660	7.307	7.458	7.852	

Table 5. 10 Near fault - Rubber Capacity

Near Fault	Maximum Rubber Deformation (cm)						Standard Rubber Capacity
	A1	A2	A4	B1	B2	B4	
TCU068 (354 GAL)	3.536	4.052	4.730	4.444	4.768	5.125	3.302
TCU102 (421 GAL)	3.260	3.583	4.126	3.790	4.207	4.714	
TCU052 (600 GAL)	4.056	4.317	4.640	4.432	4.707	4.993	

Table 5. 11 Far fault – Rubber Capacity

Far Fault	Maximum Rubber Deformation (cm)						Standard Rubber Capacity
	A1	A2	A4	B1	B2	B4	
ELX354 (354 GAL)	3.061	3.598	4.229	3.928	4.309	4.759	3.302
ELX421 (421 GAL)	3.402	3.967	4.610	4.302	4.708	5.164	
ELX600 (600 GAL)	4.285	1.492	2.791	5.224	5.675	6.167	

Table 5. 12 Near fault – Bottom Sliding

Near Fault	Maximum Bottom Sliding (cm)						Standard Rubber Translation
	A1	A2	A4	B1	B2	B4	
TCU068 (354 GAL)	2.569	1.066	1.688	1.794	0.970	1.298	10.16
TCU102 (421 GAL)	5.590	1.061	2.316	2.915	0.682	1.481	
TCU052 (600 GAL)	5.113	2.174	2.589	3.180	1.420	1.757	

Table 5. 13 Far fault – Bottom Sliding

Far Fault	Maximum Bottom Sliding (cm)						Standard Rubber Translation
	A1	A2	A4	B1	B2	B4	
ELX354 (354 GAL)	1.128	0.326	0.555	0.642	0.433	0.724	10.16
ELX421 (421 GAL)	1.533	0.394	0.813	1.041	0.556	0.718	
ELX600 (600 GAL)	2.927	0.001	3.301	1.880	1.083	1.448	

CHAPTER VI – OVERALL CONCLUSIONS

6.1 Conclusions

Here is the conclusion of this research of Functional Bearing Model (FBM) Analysis under the Design Spectra Near Fault Ground Motions:

1. A good rubber bearing system is the one that dissipate more energy to decrease the deck force and deck displacement.
2. Friction combination in range of design code on case A (0.2-0.4) need to consider more than in range of the experimental test on case B (0.35-0.5), due to the smaller value of the friction coefficients are more increasing on the energy dissipation capability.
3. Top surface and the bottom surface friction will contribute each 50% on dissipating the leftover energy from the rubber element if they applied on the same friction coefficient value. And on the different friction value, the leftover energy will be distributed more to the top surface friction since there apply the smaller one.
4. In the same configuration of the friction value on the top and bottom surface friction, increasing friction value will be increasing the rubber deformations, decreasing the sliding deformations of the friction surfaces, and decrease the deck displacements.
5. In the different of configuration of the friction coefficient such in case A2 and B2, the result always be in the middle of the result in same configuration (A1-A4) and (B1-B4).
6. To overcome TCU068 (354 gal), TCU102 (421 gal), and TCU052 (600 gal), a deck will be displaced maximum as far 13.092 cm on case A1, 10.135 cm on case A2, 8.880 cm on case A4, 9.612 cm on case B1, 8.679 cm on case B2, and 7.988 cm on case B4.
7. Maximum deformation of the rubber under TCU068, TCU102, and TCU052 are: 4.056 cm on case A1, 4.317 cm on case A2, 4.730 cm on case A4, 4.444 cm on case B1, 4.768 cm on case B2, and 5.125 cm on case B4.
8. To avoid the bridge falling under TCU068 (354 gal), TCU102 (421 gal), and TCU052 (600 gal), as amount 5.590 cm on case A1, 2.174 cm on case A2, 2.589 cm on case A4, 3.180 cm on case B1, 1.420 cm on case B2, and 1.757 cm on case B4, the cap

9. beam need to enlarge to provide the sliding space on the bottom surface of the rubber bearing system.
10. The expansion joint that allowed by the design code is 10.16 cm, that is mean configuration A1 provide deck displacement that over the standard design. This is because A1 have small friction coefficient that drive the system to move more flexible than in other configuration. This is the reason that configuration A1 did not suitable in several type of near fault earthquakes.
11. The standard design code limits the elastomeric bearing translation up to 10.16 cm, that is means that the sliding translations in the bottom side of the rubber bearing system still under the limit.
12. The failure happens in the rubber capacity due to the maximum rubber deformation are beyond the limit. This condition unsophisticatedly happens in the real condition, that the superstructure and substructure is alright but the rubber bearing failure. This is due to the rubber bearing absorbed more energy to overcome the near fault earthquakes. So that in the future, the rubber bearing capacity expected to improve.
13. The result analysis under the near fault of TCU068 (354 gal), TCU102 (421 gal), and TCU052 (600 gal) is not only depend on the magnitude of the peak ground acceleration of the earthquakes, but also depend on the characteristic of the near fault ground motions.

6.2 Recommendations

Functional Bearing Model (FBM) analysis is a recommended method to analyze each element contribution in a bearing system. FBM analysis is a useful method to analyze the bridge under the seismic ground motion, in order to prevent the bridge falling during the earthquake.

In this study found that the behavior of the system under the near fault and far fault earthquake ground motions are different, to make sure how far the differences, the functional bearing (FBM) analysis under the design spectra of the far fault ground motion need to be studied more.

This research analysis the bridge under Chi-Chi and El-Centro Earthquakes only. In the future more earthquake ground motion need to consider. In order to increase the accuracy and study the bridge behavior in another conditions.

The structure under the near fault earthquakes is more prone to failure due to the near fault effect. in the future, further study about the bridge crossing the fault with the variation of the near fault position need to be observed more. Bridge crossing the fault means that the fault laid between two column of a bridge, this special case mostly happened in the earthquakes prone area. Distance of the fault and columns influence the different earthquake force that received by each column, the different force that received means that each column need to construct in different capacity to overcome the external force. Since this research assume that both column receive the same external force, then here assume that the fault placed right in the middle of two columns. In the future, variation of the fault distance toward the column need to study in further.

Under more complex and larger earthquakes ground motion, rubber bearing's properties need to improve in its capacity, in order to avoid the rubber bearing failure during the earthquakes.

REFERENCES

AASHTO LRFD, (2003). LRFD Bridge Design Manual. Minnesota: Minnesota Department of Transportation.

Ambrose, J. andVergun D., (1995). *Simplified Building Design for Wind and Earthquakes ForcesThird Edition*. Canada: John Wiley & Sons.

Borkowski, A. andJendo, S., (1990). *Structural Optimization Volume 2*. New York: Plenum Press.

CALTRANS, (1994). *Memo to Designers – Bridge Bearings*. California: The California Department of Transportation.

Chang, K. C., Lu, C. H., and Liu, K. Y., (2011). *Displacement-based Design for Highway Bridges with Functional Bearing System*. NCREE. Taiwan.

Chopra, Anil K., (2013). *Dynamics of Structures Theory and Applications to Earthquakes Engineering Fourth Edition*. USA: Pearson Education.

Constantinou, M. C. &Tsopelas, P., (1995). *Experimental Study of Bridge Seismic Sliding Isolation Systems.* Elsevier. Page: 301-310.

CSiBridge, (2016). *Bridge Seismic Design*. USA: Computers & Structures, Inc.

Dowrick, D. J., (1977). *Earthquake Resistant Design*. New York: John Wiley & Sons.

Dowrick, D. J., (1987). *Earthquake Resistant Design Second Edition*. New York: John Wiley & Sons.

Ginsberg, Jerry H., (1988). *Advance Engineering Dynamics*. New York: Harper & Row.

Horton, C., (2018, February 7th). *Taiwan Earthquake Toll Rises to 9 Dead, With Dozens Missing.* Retrieved from https://www.nytimes.com.

Iemura, H., Taghikhany, T., Takahashi, Y., and Jain, S. K., (2005). Effect of Variation of Normal Force on Seismic Performance of Resilient Sliding Isolation System in Highway Bridges. *Earthquake Engineering and Structural Dynamics.* Page: 1777-1797.

Jangid, R. S., (2007). Optimum Lead Rubber Isolation Bearings for Near Fault Motions.*Elsevier*. Page: 2503-2513.

Jara, M. and Casas, Joan R., (2005). A Direct Displacement-Based Method for the Seismic Design of Bridges on Bi-linear Isolation Devices. *Elsevier*. Page: 869-879.

Kalpakidis, Ioannis V., andConstantinou, M. C., (2010). Principles of Scaling and Similarity for Testing of Lead-Rubber Bearings.*Earthquake Engineering and Structural Dynamics.* Page: 1551-1568.

Kikuchi, M., Aiken, and Ian, D., (1997). An Analytical Hysteresis Model for Elastomeric Seismic Isolation Bearings.*Earthquake Engineering and Structural Dynamics.* Page: 215-231.

Liu, K. Y., Chang, K. C., Chung, L. L., Tseng, T. C., Yang, C. Y., and Jang, C. L., (2013). *Analytic Solution and Shaking Table Test on the Study of Bridge Structure with Functional Bearing System*. National Center for Research on Earthquake Engineering, Taiwan.

Lu, L. Y. and Hsu, C. C., (2012). Experimental Study of Variable-frequency Rocking Bearing for Near Fault Seismic Isolation.*Elsevier.* Page: 116-129.

Schiff, A. J. and Tang, A. K. of American Society of Civil Engineers, (2000). *Chi-Chi Taiwan Earthquake of September 21, 1999 Lifeline Performance*. Virginia: ASCE.

SMS Tsunami Warning, (2011-2018). *Earthquakes: Seismic Waves*. Retrieved from http://www.sms-tsunami-warning.com.

Taghikhany, (2005). *Variation of Axial Force due to Vibration of Flexible Girder in RSI System.* Dissertation. Page: 49-147.

Takahashi, Y., Iemura, H., Yanagawa, S., and Hibi, M., (2004). Shaking Table Test for Frictional Isolated Bridges and Tribological Numerical Model of Frictional Isolator. *13 WCEE Canada*. Paper No. 1531.

University of Tokyo, (2001-2002). *Catalog of Earthquake Research Institute University of Tokyo: 7-1. The 1999 Chi-Chi, Taiwan, Earthquake*. Retrieved from http://www.eri.u-tokyo.ac.jp.

Yu, N. T., et. al., (2015, November). *Geological Record of Western Pacific Tsunamis in Northern Taiwan: AD 1867 and Earlier Event Deposits.* Retrieved from https://www.researchgate.net.

APPENDIX

FUNDAMENTAL THEORIES

Functional Bearing Model (FBM) Analysis under the Design Spectra of Near Fault Ground Motions.

- **Bridge Dynamic Modelling**

1 Spring Assumption
(Common Analysis)

3 Springs Assumption
(FBM Proposed Analysis)

- **Determine the Bridge Degree of Freedoms**

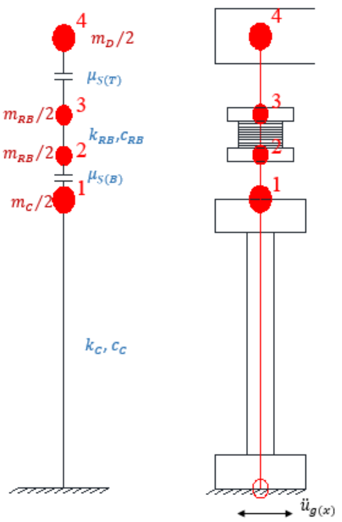

Lumped Mass Distributions

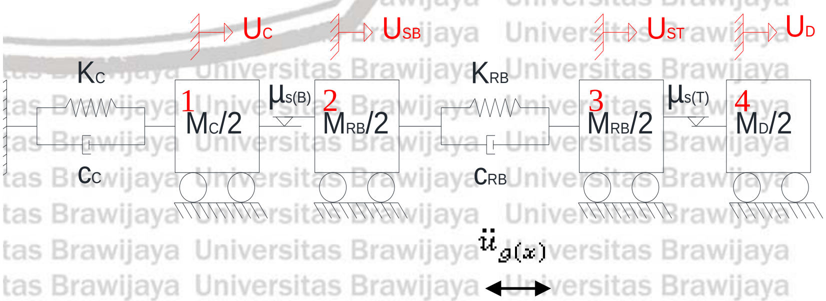

Simplify Bridge Model of Four Degree of Freedoms System

- **Force Equilibrium**

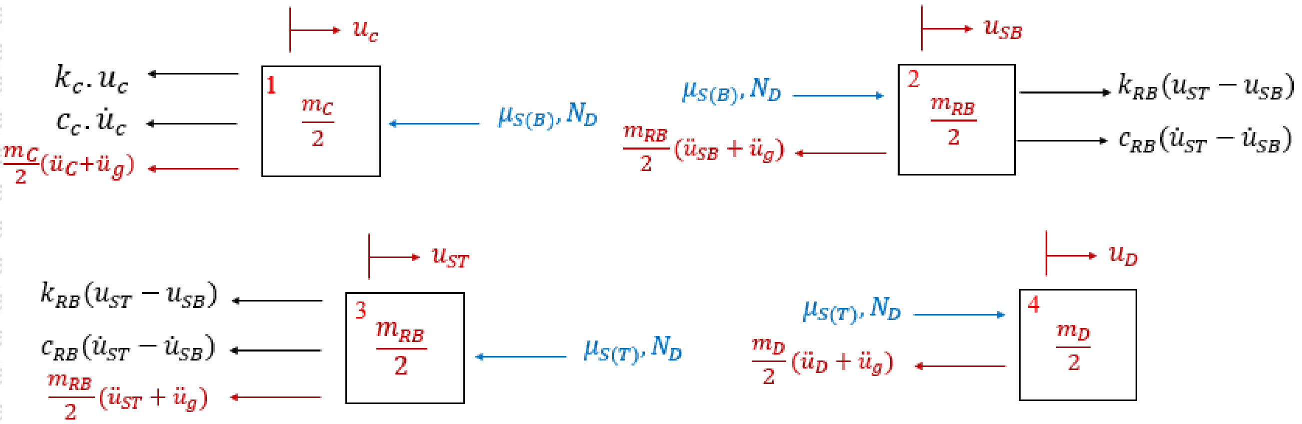

- **Assemble the Equation of Motions**

1. $-k_c u_c - c_c \dot{u}_c - {}^{m_c}/_{2}\,(\ddot{u}_c + \ddot{u}_g) - \mu_{SB} N_D = 0$

   $-{}^{m_c}/_{2}\,\ddot{u}_c - c_c\dot{u}_c - k_c u_c = {}^{m_c}/_{2}\,\ddot{u}_g + \mu_{SB} N_D$

2. $-{}^{m_{RB}}/_{2}\,(\ddot{u}_{SB} + \ddot{u}_g) + k_{RB}(u_{ST} - u_{SB}) + c_{RB}(\dot{u}_{ST} - \dot{u}_{SB}) + \mu_{SB} N_D = 0$

   $-{}^{m_{RB}}/_{2}\,\ddot{u}_{SB} + c_{RB}(\dot{u}_{ST} - \dot{u}_{SB}) + k_{RB}(u_{ST} - u_{SB}) = {}^{m_{RB}}/_{2}\,\ddot{u}_g - \mu_{SB} N_D$

3. $-{}^{m_{RB}}/_{2}\,(\ddot{u}_{ST} + \ddot{u}_g) - k_{RB}(u_{ST} - u_{SB}) - c_{RB}(\dot{u}_{ST} - \dot{u}_{SB}) - \mu_{ST} N_D = 0$

   $-{}^{m_{RB}}/_{2}\,\ddot{u}_{ST} - c_{RB}(\dot{u}_{ST} - \dot{u}_{SB}) - k_{RB}(u_{ST} - u_{SB}) = {}^{m_{RB}}/_{2}\,\ddot{u}_g + \mu_{ST} N_D$

4. $-{}^{m_D}/_{2}\,(\ddot{u}_D + \ddot{u}_g) + \mu_{ST} N_D = 0$

   $-{}^{m_D}/_{2}\,\ddot{u}_D = {}^{m_D}/_{2}\,\ddot{u}_g - \mu_{ST} N_D$

- **Assemble the Matrix of Motions**

$$\begin{bmatrix} -{}^{m_c}/_{2} & 0 & 0 & 0 \\ 0 & -{}^{m_{RB}}/_{2} & 0 & 0 \\ 0 & 0 & -{}^{m_{RB}}/_{2} & 0 \\ 0 & 0 & 0 & -{}^{m_D}/_{2} \end{bmatrix} \begin{bmatrix} \ddot{u}_c \\ \ddot{u}_{SB} \\ \ddot{u}_{ST} \\ \ddot{u}_D \end{bmatrix} + \begin{bmatrix} -c_C & 0 & 0 & 0 \\ 0 & -c_{RB} & c_{RB} & 0 \\ 0 & c_{RB} & -c_{RB} & 0 \\ 0 & 0 & 0 & 0 \end{bmatrix} \begin{bmatrix} \dot{u}_c \\ \dot{u}_{SB} \\ \dot{u}_{ST} \\ \dot{u}_D \end{bmatrix} + \begin{bmatrix} -k_C & 0 & 0 & 0 \\ 0 & -k_{RB} & k_{RB} & 0 \\ 0 & k_{RB} & -k_{RB} & 0 \\ 0 & 0 & 0 & 0 \end{bmatrix} \begin{bmatrix} u_C \\ u_{SB} \\ u_{ST} \\ u_D \end{bmatrix} = \begin{bmatrix} {}^{m_c}/_{2} \\ {}^{m_{RB}}/_{2} \\ {}^{m_{RB}}/_{2} \\ {}^{m_D}/_{2} \end{bmatrix} \ddot{u}_g + \begin{bmatrix} \mu_{SB} \\ -\mu_{SB} \\ \mu_{ST} \\ -\mu_{ST} \end{bmatrix}$$

- **Conditions**

Condition 1 :Sticking State

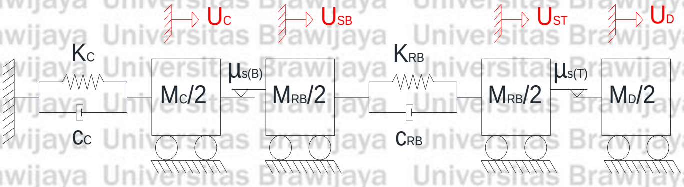

Condition 2 :Sliding State in the Top Interface Only

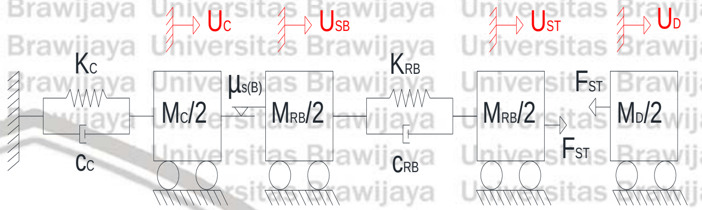

Condition 3 :Sliding State in the Bottom InterfaceOnly

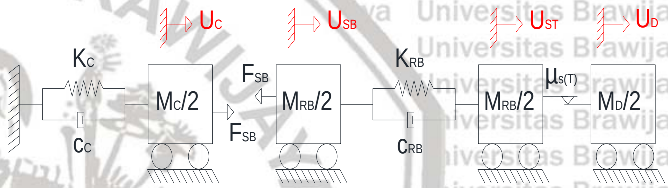

Condition 4 :Sliding State in the Top and BottomInterface

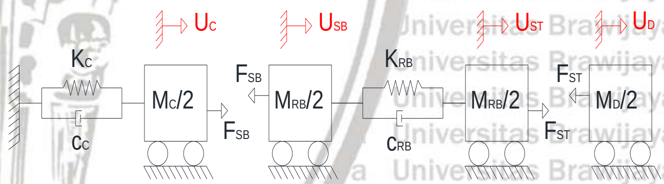

- **Boundary Conditions**

$$FSB = c_{RB}(\dot{u}_{ST} - \dot{u}_{SB}) + k_{RB}(u_{ST} - u_{SB})$$

$$FST = -c_{RB}(\dot{u}_{ST} - \dot{u}_{SB}) - k_{RB}(u_{ST} - u_{SB})$$

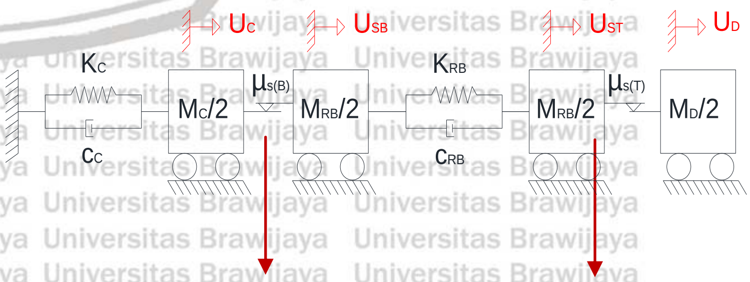

FSB = Shear Force in the Bottom

FST=Shear Force in the Top

1. Condition 1: Sticking State Condition

Requirements:

- Bottom Surface: No Sliding

$FSB < \mu_{SB(S)}.N_D$

- Top Surface: No Sliding

$FST < \mu_{ST(S)}.N_D$

2. Condition 2: Sliding State in the Top Interface Only

Requirements:

- Bottom Surface: No Sliding

$FSB < \mu_{SB(S)}.N_D$

- Top Interface: Sliding

$FST \geq \mu_{ST(S)}.N_D$

$Then, FST = \mu_{ST(k)}.N_D$

3. Condition 3: Sliding State in the Bottom Interface Only

Requirements:

- Bottom Surface: Sliding

$FSB \geq \mu_{SB(S)}.N_D$

$Then, FSB = \mu_{SB(k)}.N_D$

- Top Interface: No Sliding

$FST < \mu_{ST(S)}.N_D$

4. Condition 4: Sliding State in the Top and Bottom Surface

Requirements:

- Bottom Surface: Sliding

$FSB \geq \mu_{SB(S)}.N_D$

$Then, FSB = \mu_{SB(k)}.N_D$

- Top Interface: Sliding

$FST \geq \mu_{ST(S)}.N_D,$

$Then, FST = \mu_{ST(k)}.N_D$